UNIVERSITÀ DEGLI STUDI DI PADOVA

Dipartimento di Ingegneria Industriale

Corso di Laurea Magistrale di Ingegneria Chimica e dei Processi Industriali

Università degli Studi di Padova

Tesi di Laurea Magistrale in Ingegneria Chimica e dei Processi Industriali

Optimal design of experiments for the identification of kinetic models of HMF hydrogenation

Relatore: Prof. Fabrizio Bezzo

Correlatore: Prof. Federico Galvanin

Laureando: Andrea Bortoli

Anno Accademico 2017-2018

To my family, Monica, Paolo and Luca

To my grandmother, Maria

To my beloved Sara

Abstract

THE increasing issues about the use of fossil raw materials advocate for an increasing utilization of biomass-based fuels and chemicals. Among the bio-based furan compounds, the 5-hydroxymethylfurfural (HMF) has received considerable attention in the chemical industry since it can be hydrogenated to 2,5-dimethylfuran (DMF) that is a valuable alternative fuel. The identification of a suitable kinetic model, where all the non-measurable kinetic parameters are reliably estimated, is crucial to pursue the process optimisation.

In this work, the kinetic models currently available in literature for the HMF hydrogenation process are investigated to figure out their strengths and weaknesses using a sensitivity-based identifiability analysis. The application of identifiability analysis techniques allows to define a set of fully identifiable kinetic models to be used for statistically reliable predictions. Furthermore, the results lead to the characterization of the experimental design space regions that maximise the discriminating power between the different models.

Abstract esteso

Le crescenti problematiche relative all'uso delle materie prime di origine fossile, rendono l'impiego di combustibili e prodotti chimici derivanti dalle biomasse sempre più importante. Il vantaggio di questo tipo di derivati chimici è che essi non contribuiscono al surriscaldamento globale dato che vengono ottenuti da risorse rinnovabili. Per questa ragione, tra tutti i composti furanici ottenuti dalle biomasse, il 5-idrossimetilfurfurolo (HMF) sta ricevendo particolare attenzione, nel settore dell'indutria chimica, in quanto sembra uno dei più promettenti "building blocks" nell'immediato futuro: è considerato come il precursore di un'intera famiglia di composti chimici ad elevato valore aggiunto. In particolare, l'HMF può essere sottoposto ad un processo di idrogenazione in sistema trifasico nel quale viene convertito a 2,5-dimetilfurano (DMF), un combustibile alternativo particolarmente pregiato. Tra le ottime caratteristiche che lo contraddistinguono, le che più importanti sono sicuramente:

1. elevata densità di energia;
2. alto punto di ebollizione;
3. elevato numero di ottano;
4. marcate proprietà idrofobiche.

Per i vantaggi di cui sopra, si pensa che il DMF possa rappresentare un'alternativa migliore rispetto all'etanolo e ai combustibili fossili attualmente in uso. Questo lo rende una valida e sostenibile alternativa per la produzione di combustibili nel prossimo futuro.

L'identificazione di un modello cinetico adatto alla rappresentazione del processo di idrogenazione, che presenti la possibilità di ottenere accurate predizioni senza la necessità di condurre misurazioni sperimentali dirette, è essenziale per lo sviluppo

ed il miglioramento del processo stesso. In particolare, l'obiettivo è quello di trovare un modello cinetico la cui struttura matematica coinvolga variabili non misurabili (parametri) che possano essere stimate affidabilmente ed accuratamente mediante l'utilizzo di soli dati cinetici relativi alla concentrazione delle specie. Il raggiungimento di tale obiettivo può portare ad un incremento dell'efficienza ed una significativa riduzione del costo, in termini di tempo e risorse, per l'ottimizzazione del processo.

La capacità descrittiva di un modello cinetico e l'affidabilità delle previsioni derivanti da questo, dipendono dalla completezza delle leggi fisiche usate per sviluppare il modello stesso. Maggior complessità si riflette in maggior difficoltà nello stimare i parametri (attraverso l'impiego di dati sperimentali) con un elevato livello di accuratezza. Minor complessità si ripercuote sulla qualità delle predizioni ottenibili. In ogni caso, una caratteristica fondamentale che i modelli cinetici utilizzati devono possedere, è una completa identificabilità. A tal proposito, opportune tecniche sono state sviluppate per verificare l'identificabilità dei modelli e riconoscere in anticipo le debolezze strutturali (legate alla struttura matematica delle equazioni usate) e pratiche (relative alle condizioni di applicazione del modello). In particolare, la valutazione della correlazione tra i parametri cinetici che richiedono di essere stimati, in funzione del rango di quella che viene definita *matrice di stimabilità*, è un passaggio fondamentale per lo studio di un modello cinetico.

In questo lavoro, i modelli cinetici attualmente disponibili in letteratura (Gawade et al. (2016), Gyngazova et al. (2017), Jain and Vaidya (2016), Luo et al. (2015), Grilc et al. (2014)) sono stati raccolti, elencati e studiati. Un'analisi di identificabilità basata sulle sensitività è stata impiegata ed, in particolare, si è valutata con attenzione la correlazione tra i parametri cinetici di ogni modello in funzione delle condizioni sperimentali utilizzate e della tipologia di campionamento adottata. Si è scelto di considerare una campagna "in-silico" di 10 esperimenti, ognuno rappresentativo di un determinato set di variabili di design, distribuiti in modo omogeneo in tutto il dominio sperimentale. Si è impiegato il cosiddetto *Latin Hypercube Sampling* e le seguenti variabili di design sono state considerate:

1. concentrazione iniziale delle specie chimiche in comune tra i vari modelli cinetici;
2. temperatura;
3. pressione parziale dell'idrogeno.

Inoltre, le tipologie di campionamento sono state selezionate sulla base di vincoli pratici imposti dalle apparecchiature di laboratorio: per l'analisi della miscela di reazione, 5 minuti sono stati considerati come il tempo minimo necessario tra due campionamenti successivi. Fissata una durata nominale di 120 minuti per la reazione, sono quindi state adottate tre distribuzioni con punti di campionamento:

1. maggiormente concentrati all'inizio della reazione;
2. uniformemente distanziati;
3. maggiormente concentrati alla fine della reazione.

Successivamente all'analisi della correlazione, anche l'informazione attesa è stata studiata, in funzione della Matrice dell'Informazione di Fisher (FIM). La valutazione di questa metrica, per le diverse condizioni sperimentali, ha permesso di chiarire gli aspetti di identificabilità pratica per i vari modelli cinetici. Sono state cioè definite le condizioni sperimentali per cui l'informazione utile alla stima dei parametri è massima, e quelle per cui l'insufficienza di informazione comporta la non identificabilità dei modelli cinetici. Lo studio ha evidenziato, tuttavia, la presenza di errori numerici nello studio della covarianza: si è capito che la bassa sensitività mostrata dai coefficienti di adsorbimento rispetto ad esperimenti cinetici, comporta che la risultante FIM abbia una struttura che ne causa la non-invertibilità. A tal proposito, un'approssimazione può essere fornita ma l'affidabilità che la caratterizza è scarsa.

Per concludere, lo studio svolto ha permesso di definire un set di modelli cinetici completamente identificabili ed uno spazio di design che può essere utilizzato per ottenere affidabili predizioni sul processo di idrogenazione. I risultati hanno portato alla caratterizzazione delle regioni del dominio sperimentale in cui i parametri dei modelli cinetici strutturalmente identificabili, possono essere stimati con elevata accuratezza. Infine, sono state definite le condizioni sperimentali per le quali

l'utilizzo di modelli cinetici con una determinata struttura è maggiormente indicato.

Table of Contents

LIST OF SYMBOLS

General Symbols

A	=	Pre-exponential factor
C_{A}	=	Concentration of HMF
C_{B}	=	Concentration of BHMF
C_{D}	=	Concentration of DMF
C_{E}	=	Concentration of DMTHF
C_i	=	Concentration of the i-th species
$C_{\mathrm{H_2}}$	=	Concentration of hydrogen
C_{W}	=	Concentration of the water
CN	=	Condition number
D_{eff}	=	Effective diffusivity
E	=	Expectation
E_a	=	Activation energy
L	=	Likelihood function
k_i	=	Reaction kinetic constant of the i-th species
$k_{i,app}$	=	Reaction apparent kinetic constant of the i-th species
$\mathrm{K_A}$	=	Adsorption coefficient of HMF
$\mathrm{K_B}$	=	Adsorption coefficient of BHMF
$\mathrm{K_D}$	=	Adsorption coefficient of DMF
$\mathrm{K_E}$	=	Adsorption coefficient of DMTHF
$\mathrm{K_{H_2}}$	=	Adsorption coefficient of $\mathrm{H_2}$
$\mathrm{K_W}$	=	Adsorption coefficient of water
l	=	Characteristic particle size
M_{H2O}	=	Water molar mass
N_f	=	Number of model equations
N_m	=	Number of model outputs

N_θ	=	Number of model parameters
N_u	=	Number of model input variables time dependent
N_w	=	Number of model input variables time independent
N_x	=	Number of model differential variables
n_{sp}	=	Number of sampling points
n	=	Number of general variables
P	=	Generic statistical distribution
$p_{\mathrm{H_2}}$	=	Hydrogen partial pressure
P_{tot}	=	Total pressure
q_{ij}	=	ij-th element of local sensitivities
R	=	Universal gas constant
r_{eff}	=	Effective reaction rate
w	=	Catalyst loading
T	=	Temperature
t	=	Time
$\mathbf{V}_{\theta,ii}$	=	ii-th element of $\mathbf{V}_\theta$
$\mathbf{V}_{\theta,ij}$	=	ij-th element of $\mathbf{V}_\theta$
x_g	=	Mole fraction solubility
y_i	=	Measured value of the i-th output variable
$\hat{y}_i$	=	Expected value of the i-th output variable
y_i^*	=	Real value of the i-th output variable

Vectors and Matrices

$\mathbf{A}$	=	Singular matrix $[n \times n]$
$\mathbf{D}$	=	Singular value matrix $[n \times n]$
$\mathbf{f}$	=	Model equations $[\mathrm{N}_f]$
$\mathbf{H}$	=	Hessian $[n \times n]$
$\mathbf{I}$	=	Identity matrix $[n \times n]$
$\mathbf{P}_E$	=	Estimability matrix $[N_m n_{sp} \times N_\theta]$
$\mathbf{Q}_m$	=	m-th matrix of local sensitivities $[n_{sp} \times N_\theta]$

$\mathbf{Q}$	=	Global matrix of local sensitivities [$N_m \times N_\theta$]
$\mathbf{r}$	=	Correlation matrix [$N_\theta \times N_\theta$]
$\mathbf{U}$	=	Unitary matrix [$n \times n$]
$\mathbf{u}$	=	Input variables time dependent [N_u]
$\mathbf{V}$	=	Unitary matrix [$n \times n$]
$\mathbf{V}_\theta$	=	Variance-covariance matrix of the parameters [$N_\theta \times N_\theta$]
$\mathbf{w}$	=	Input variables time independent [N_w]
$\mathbf{x}$	=	State variables [N_x]
$\dot{\mathbf{x}}$	=	Differential variables [N_x]
$\hat{\mathbf{y}}$	=	Measurable output variables [N_m]
θ	=	Parameters to estimate [N_θ]
$\hat{\theta}$	=	Estimated value of the parameters [N_θ]
θ^*	=	Real value of the parameters [N_θ]

Greek Letters

α	=	Level of confidence
δ_i	=	i-th element of $\mathbf{D}$
ϵ	=	Measurement error
η	=	Effectiveness factor
θ_i	=	i-th model parameter to estimate
θ_i^*	=	Real value of the i-th model parameter
$\hat{\theta}_i$	=	Estimation of the i-th model parameter
λ_i	=	Matrix eigenvalue
ρ_{ij}	=	ij-th element of $\mathbf{r}$
ρ_{H2O}	=	Water density
σ_{ij}	=	ij-th element of $\mathbf{C}$
Φ	=	Thiele modulus
Ψ	=	Objective function
ω	=	Catalyst loading

Acronyms

2-MTHF	=	2-methyltetrahydrofuran
BDF	=	Backward differentiation formulae
BDNLSOL	=	Block decomposition non-linear solver
BHMF	=	bis-hydroxymethylfuran
CVP	=	Control vector parametrization
DAE	=	Differential-algebraic equation
DHMTHF	=	2,5-dihydroxymethyltetrahydrofuran
DMF	=	2,5-dimethylfuran
DMTHF	=	2,5-dimethyltetrahydrofuran
DoE	=	Design of experiments
FID	=	Flame ionization detector
FIM	=	Fisher information matrix
GC	=	Gas-chromatography
HDO	=	Hydrodeoxygenation
HMF	=	5-hydroxymethylfurfural
HPLC	=	High performance liquid chromatography
LHHW	=	Langmuir-Hinshelwood-Hougen-Watson
LHS	=	Latin hypercube sampling
LSS	=	Latin square sampling
MBDoE	=	Model-based design of experiments
MD	=	Model discrimination
MFA	=	5-methylfurfural
MLE	=	Maximum likelihood estimate
MS	=	Mass-spectrometry
ODE	=	Ordinary differential equation
OED	=	Optimal design of experiments
PDAE	=	Partial differential-algebraic equation
PTFE	=	Polytetrafluorethylene
PP	=	Parameter precision
SDV	=	Standard deviation

SP	=	Sampling point
THF	=	Tetrahydrofuran

INTRODUCTION

THE world has nowadays to face with the reality that fossil fuels are no longer a suitable alternative for the near future. Petroleum supplies are rapidly shrinking and the extraction companies are forced to drill always deeper with the consequence of making the process less profitable. Moreover, a lot of countries are trying to tackle the pollution problem by looking for more sustainable alternatives at the petroleum derivatives. The biomass-derived fuels currently used present some disadvantages that drove the researchers toward the investigation of better alternatives that now seem to be represented by furan-based compounds. Thus, especially for the non-well-established processes, a huge effort consists in the identification of a trustworthy kinetic model capable of giving accurate predictions both inside and outside the range of the already investigated experimental conditions. However, the model characterization always relies on the completion of specific studies which may involve the accomplishment of highly informative experiments. Since the number of possible mechanisms proposed can be high, a preliminary investigation of the model structure is crucial. Moreover, since the experiment execution may require considerable amounts of time and resources, a careful planning of the study represents a key aspect on the development of reliable chemical kinetic models. Many advanced techniques have been developed by researchers, following the initial work of Box and Lucas (1959), and applied in this Thesis. The purpose is to consider the existing kinetic models available in literature for the HMF hydrogenation process, and explore their strengths and lacks to end up with a set of identifiable kinetic models which non-measurable parameters can be estimated in a statistically reliable way. Both structural and practical identifiability are considered in the study.

To aid the orientation of the reader along the Thesis, the block diagram in Figure 1

Figure 1: *Block diagram representing thesis structure and connections between different chapters.*

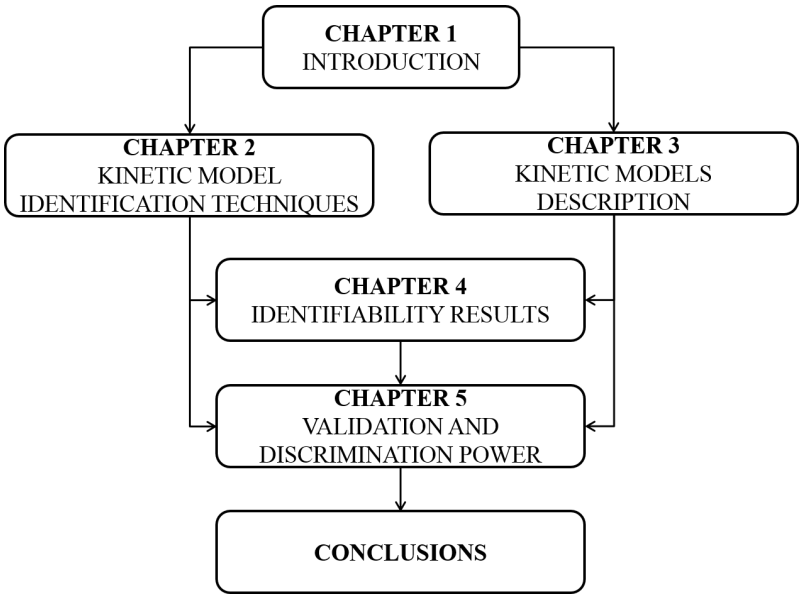

is proposed. It shows the connections between the different chapters and underlines the contribution of each part to the others. Chapter 1 reports the literature survey and the state of the art about the HMF hydrogenation process. The importance of the study is highlighted as well as the main general concepts and techniques employed are illustrated. Chapter 2 provides an in-depth analysis of the mathematical background for all the methodologies and techniques related to the model identifiability study, model-based design of experiments and parameter estimation. The statistical tests used to assess the parameters precision, as well as the meaning of the metrics used, are also discussed. Chapter 3 presents an overview of the most important aspects to be considered about the HMF hydrogenation process. Moreover, it focuses on the analysis of the kinetic models available in literature and their comparison in terms of complexity, variables involved and assumptions made. Finally, it addresses a summary of all the chemical, physical and structural uncertainties of the kinetic models, along with the proposals of possible solutions to overcome the problems. Chapter 4 shows the results of the identifiability analysis performed, with a particular focus on the discussion of the expected:

1. correlation between parameters;

2. information available for each parameter.

An efficient identifiability analysis leads to a great simplification of the design of experiments methodologies and allows to identify the cases in which a re-parametrization is required. Chapter 5 describes the application of validation and optimisation techniques to the final set of kinetic models. The results are discussed in details to identify the experimental domain regions that maximize the discriminating power and the parameter estimation quality. Furthermore, the validation allows confirming or rejecting the possibility of using in a general way the kinetic model previously defined. The conclusions section contains final remarks of the thesis project along with an explanation of the possible ways this work can be used as a starting point to pursue further studies aiming at the identification of more sophisticated kinetic models for the HMF hydrogenation process.

Chapter 1

Process introduction, scope of the work and techniques employed

Commonly, the mathematical description of a deterministic physical process goes beyond the simple fitting of data with known curves or functions. A well-established phenomenological model, founded on the study of the physical and chemical behaviour of a system, makes the extrapolation of the outcome of an experiment, not only a speculated forecast. When the system is studied outside the range of investigated experimental conditions, a trustworthy phenomenological model must be used to obtain reliable predictions of the result. At the purpose, the non-measurable quantities involved carry information about the meaningful physical reality that has to be exploited and understood for an efficient process improvement. When it turns to chemical processes, the identification of a suitable kinetic model for which all the non-measurable kinetic parameters can be reliably estimated, is crucial to improve the operations efficiency. The procedure is all but straightforward: the model descriptive capability and prediction reliability depend on the completeness of the physical laws used to develop the model itself. A high complexity in the phenomenological relations used ensures a good representation but reflects on the difficulty of estimating with a great level of accuracy the non-measurable kinetic parameters that are typically found by fitting experimental data. Model identifiability procedures are then used to recognise in advance structural and practical weaknesses related to models structure and application conditions. In this introductory chapter, the description of objectives and reasons that motivated this work is given. Moreover, it is given a brief presentation of the tools employed for performing the analysis exploited throughout the Thesis.

1.1 The problem of fossil fuels

During the last 150 years, crude oil has been largely exploited all around the world. It is, in its most basic form, mineral deposits formed deep in the earth or under the sea bed and it can be transformed into oil. That is, several million barrels a day are produced and refined into petrol and petroleum products such as plastics. Despite petrol-based fuels are often described as the energy of the world, used in power plants to convert their chemical energy into electricity, in domestic boilers to produce hot water and warm up the buildings and also in almost the entire transportation system, they have to face increasing issues related to pollutants emission and supplies abundance. As underlined by Roman-Leshkov et al. (2007), diminishing fossil fuel reserves and growing concerns about global warming indicate that sustainable sources of energy are needed in the near future. About that, the interest toward some *renewable fuels* is rapidly increasing. In particular, according to Demirbas (2010), biomass is the most important renewable energy source in the world. The new biomass-derived fuels seem indeed to be an alternative solution, clean and environmental safe, to the fossil and nuclear fuels that are liable to many of the environmental and social problems in the world. Moreover, they would be a cost-effective and sustainable supply of energy for the future as well as important contributors to the world's economy. Currently, as underlined by Chum and Overend (2001), about 60% of the needed process energy in pulp, paper and forest products is provided by biomass combustion. However, for fuels to be useful in transportation sector, they must have specific physical properties that allow for efficient distribution, storage and combustion. Unfortunately, while these properties are fulfilled by non-renewable petroleum-derived liquid fuels, the only renewable alternative produced nowadays, ethanol, suffers from several limitations. Indeed, low energy density, high volatility and tendency to absorb water are the reasons that bring the researchers to keep looking for a more efficient substitute. The catalytic production of 2,5-dimethylfuran (DMF) from 5-hydroxymethylfurfural (HMF) that can be derived from fructose – a carbohydrate obtained directly from biomass or by isomerization of glucose – could be the answer. In particular, advances in genetics, biotechnology, process chemistry and engineering are leading to a new manufactur-

ing concept for converting furan-based reactants to valuable fuels and products. In these terms, the use of a catalytic process leads to the identification of a route for transforming abundant carbon-neutral renewable biomass resources into a liquid fuel suitable for the transportation sector (Parikka (2004), Ragauskas et al. (2006)). For this reason, a study of the HMF characteristics allows to understand which are the best ways it can be efficiently converted to DMF. The final result will be a diminished reliance of world's economy on petroleum derivatives and an increased environmental safety.

1.2 The HMF as a possible solution

5-hydroxymethylfurfural is an organic compound consisting of a furan ring that contains both aldehyde and alcohol functional groups. In nature, HMF is a white solid with the very low melting temperature of 34 °C, and it is highly soluble either in water or in organic solvents. It is considered an important intermediate in biorefinery due to its rich chemistry and potential availability from carbohydrates: it is formed by dehydration of certain sugars such as fructose, glucose, sucrose, cellulose and inulin (van Putten et al. (2013)). Moreover, it represents a potential primary building block that might be employed to a wide range of applications in order to settle the current dependence on fossil-fuel resources. For this reason, as reported by Rosatella et al. (2011), in recent years considerable efforts have been made on the optimization and development of HMF transformation processes. Thus, over the

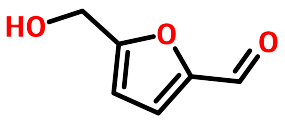

(a) *HMF: 5-hydroxymethylfurfural*

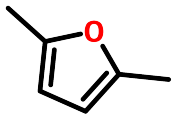

(b) *DMF: 2,5-dimethylfuran*

Figure 1.1: *Chemical structures of HMF and DMF.*

entire family of furan-based compounds that could be used, the importance of HMF is gaining impetus. As a precursor of an entire chemical tree of prominent value-added chemicals, the products of interest are many. However, 2,5-dimethylfuran (DMF) seems to be the most desired one in behalf of its high energy density, boiling point and research octane number (see Table 1.1). According to Roman-Leshkov

et al. (2007) and Lamia et al. (2012), DMF production reduces also the distillation costs from water – highly energy demanding – since it does not absorb moisture from the atmosphere. Eventually, for the reasons aforementioned, DMF represents a better substitute to ethanol or other fossil sources, and could provide a sustainable future for fuel production.

Table 1.1: *Comparison of the most important DMF characteristics in respect to petrol and ethanol.*

Fuel type	**Energy density [MJ/L]**	**RON**	**T_{eb} [K]**
DMF	30	119.0	~ 365
Petrol	34	95.0	~ 368
Ethanol	24	108.6	~ 351

At present, liquid DMF is obtained from the HMF hydration/hydrogenation process using a wide range of carbon-supported metals out of Pt, Pd and Ru as catalysts. Researchers are indeed putting a lot of efforts in the identification of the most efficient catalyst that maximizes yield and selectivity depending on the reaction conditions and desirable products. Moreover, many studies are oriented toward the definition of the best mathematical representation for the process, in order to allow the application of advanced model-based design of experiments techniques for process improvement.

1.3 State of art of HMF hydrogenation

One of the HMF hydrogenation first applications was introduced by Thananatthanachon and Rauchfuss (2010) who wanted to examine the use of new reagents to produce liquid fuels from biomass. In this case, the reactants are said to have three roles: to assist the isomerization/dehydration, to serve as an H_2 source for the hydrogenation and to help deoxygenate the alcohol functional groups. To the purpose, formic acid was used in suspension with tetrahydrofuran (THF), H_2SO_4 and Pd/C. Subsequently, Zhang et al. (2012) presented the results of an investigation aimed at identifying the optimal catalysts and solvents for the hydrogenation of glucose and xylose to HMF and DMF. Hu et al. (2014) considered the selective hydrogenation

of HMF to DMF in presence of THF as solvent, and carbon-supported ruthenium (Ru/C) as catalyst. The aim of the study was to identify the best conditions to run the process, and to propose a plausible reaction pathway. Grilc et al. (2014) developed a reaction kinetic model, based on group contributions, to determine the kinetic of hydrodeoxygenation (HDO), hydrogenolysis, decarboxylation, decarbonylation and hydrocracking of HMF and levulinic acid that are products of the low-temperature ultrasonic waste-wood biomass liquefaction. In that case, the activity of $NiMo/Al_2O_3$ bifunctional catalyst was investigated for three variants: oxide, reduced and sulphide form. A comparison with Pd/C catalyst was also presented. Furthermore, particular caution was taken on the minimization of mass transfer and heat transfer resistances. A study for the opimisation of the reaction parameters was conduced instead by Chatterjee et al. (2014) who investigated the use of supercritical carbon dioxide-water over a Pd/C catalyst. Eventually, the effect of CO_2 pressure on the product distribution was observed. Luo et al. (2015) investigated the three-phase HDO of HMF and hydrogenation of DMF over six carbon-supported metal catalysts: Pt, Pd, Ir, Ru, Ni and Co. The rate constants for the pseudo-first-order sequential reactions were obtained and, moreover, the catalysts were classified in terms of stability. In this case, a tubular flow reactor with 1-propanol solvent was used to study the reaction sequentiality by varying the space time. Finally, Gawade et al. (2016) studied the efficacy of a novel metal-acid palladium-cesium dodeca-tungsto-phosphoric catalyst supported on clay, and proposed a kinetic model based on the Langmuir-Hinshelwood-Hougen-Watson (LHHW) theory. In this research, the product DMF was reported to be used as a potential biofuel additive. Another approach was followed by Jain and Vaidya (2016) who studied the catalytic hydrogenation of HMF to BHMF (the less hydrogenated intermediate before DMF) using a 5% Ru/C aqueous phase as catalyst. Disappearance of HMF initial concentration was modeled using both power law and LHHW mechanisms: a model based on the competitive adsorption of the reactants was proposed. Eventually, the work of Gyngazova et al. (2017) represents possibly the most recent study that examines in details the reaction network, considering all the possible intermediates and by-products, and proposes a suitable kinetic model. Also in this case, particular attention to the mass transfer resistances and to the reaction rate determining step

has been taken.

A brief summary of the different contributions on the HMF hydrogenation process understanding is proposed in Table 1.2. Despite these findings, mostly oriented toward the identification of the best catalyst, conditions or solvents to be used, the study of identifiable kinetic models involving parameters that can be estimated in a statistically reliable way, has not been addressed yet.

Table 1.2: *Some researches regarding the HMF hydrogenation process.*

Main findings	**Catalyst**	**Reference**
Reaction screening	Pd/C	Thananatthanachon and Rauchfuss (2010)
Catalyst and solvents investigation	SO_4^{-2}/ZrO_2-TiO_2, Ru/C	Zhang et al. (2012)
Reaction parameters	Pd/C	Chatterjee et al. (2014)
Reaction mechanism	Ru/C	Hu et al. (2014)
Kinetic model, catalysts comparison	Ni/Al_2O_3-SiO_2, MoS_2, Pd/Al_2O_3-SiO_2, Pd/C	Grilc et al. (2014)
Catalysts comparison	(Pt, Pd, Ir, Ru, Ni, Co)/C	Luo et al. (2015)
Kinetic model	2Pd-20CsDTP/K-10	Gawade et al. (2016)
Kinetic model	5% Ru/C aq.	Jain and Vaidya (2016)
Kinetic model	Ni/C	Gyngazova et al. (2017)

1.4 Introduction to model identification

A first-principle mathematical model consists in a series of analytical expressions representing the phenomenological mechanism that links inputs with outputs: the cause-effect relationships. Since the purpose of a model is to provide insights into the dynamic response of a system, and to predict information to be used in substitution of real measurements, its structure is usually developed according to *a priori* knowledge given by the physical, chemical or biological laws that rule the system itself. In chemistry, the aim of many researchers is usually to enhance the reaction

efficiency by looking for the best combination of catalyst and experimental conditions which maximize the conversion of reactants and the selectivity of products. However, this method is all but straightforward: being mainly based on a trial-and-error procedure, it might lead to long and expensive studies. It is clear the need of representing the chemical systems differently, in order to describe complex processes and reaction mechanisms in a less resource-demanding way. Since any conclusion related to the process understanding must be proved by experimental evidences, that has to be somehow generated, the chemical industry can benefit of mathematical models by using them in substitution of real experiments, to make predictions through the generation of *in silico* data. Thus, the model identification is a procedure that aims at accomplishing two essential tasks:

1. defining the mathematical representation that better describe the reality among several different alternatives that can be postulated by the researchers;

2. estimating in a statistically reliable way the non-measurable parameters - physically meaningful or not - that are always included in the model structure.

It is clear that, in order to carry out the model selection, the mathematical structure proposed must be in possession of certain characteristics that makes it *identifiable*. For this reason, the heart of the kinetic modeling can be seen as the study of the model structure aimed at verifying the possibility of identifying each non-measurable parameter in a statistically reliable way. In this Thesis, the main objective is to select a set of identifiable kinetic models through the application of model identifiability techniques.

1.5 Identifiability analysis review

The importance of the identifiability analysis is given by the fact that the model identification problem does not always involve a solution. About that, the identifiability problems can be divided into two different categories: structural (also called *a priori*) and practical (also called *local*). Structural identifiability is, as the name suggests, a property of the model structure and depends on the shape of the differential equations used for the phenomenon description. Independently of the

measured data and of their intrinsic uncertainty, the structural identifiability determines the possibility of estimating the non-measurable model parameters. Practical identifiability, instead, depends on the specific experimental conditions considered: it may happen that the model parameters are identifiable, but the conditions required to gather enough information violate the practical constraints associated to constructive, safety and/or economical considerations. Many techniques have been proposed for the structural identification of both linear and nonlinear systems. Among them, Laplace transform and Lie derivatives (Walter and Pronzato (1996)), power series extension (Pohjanpalo (1978)) and differential algebra (Margaria et al. (2001)). Other recent systematic model-based procedures have been instead presented by Asprey and Macchietto (2000), Blau et al. (2008) and Kreutz and Timmer (2009) to support the development and statistical verification of dynamic process models described by DAEs.

It is anyway clear as the more complete the model is, in terms of physical and chemical laws involved, the better the phenomenon representation. However, each model has usually different strengths and weaknesses based on its complexity and its descriptive capability: a huge limit is usually given by the impossibility of measuring directly certain variables or coefficients. For instance, it would not be possible to detect some species if their concentration is below the precision of the instruments used. Furthermore, it might happen that the estimation of some parameters requires the execution of ad-hoc experiments for which specific equipment may not available. An example is given by the adsorption coefficients whose measurement usually require the application of High Performance Liquid Chromatography (HPLC). Finally, it may happen that it is even not possible to identify separately different mechanisms because their effects overlap. Imagine the case of two parallel reactions: their combined effect could be easily measured but the single contributions might be really difficult to discriminate. In this sense, a huge effort should be put on developing simple models:

1. capable of giving accurate predictions in a wide range of experimental conditions;

2. containing the lowest number of physically meaningful parameters.

Complex models, involving many parameters, could return very good results when used to fit the experimental data but their excessive complexity may require the accomplishment of costly (both in terms of time and resources) experiments. So far, it could also result in the identification of statistically unreliable parameters. Anyway, despite the big advantage represented by the mathematical modeling of reactive systems, the description of the reality is all but simple. To correctly represent the phenomenon under investigation, it is always required to perform some experiments that allow to develop a new model or to estimate the parameters of an already existing one. If these experiments are not properly designed, the information gathered could not be properly exploited because the data:

1. are affected by uncertainty;

2. have been gathered in poorly informative regions of the design space.

To solve this problem, optimal design of experiments techniques are born with the purpose of minimising the resources required to acquire the maximum information on the observed system.

1.6 Design of experiments: an overview

The DoE born from statistical considerations, based on the fact that the identification of a trustworthy model always relies on the conduction of highly informative experiments. Since the collection of data may require extensive amounts of time and resources, it is natural to wonder whether it is possible to plan carefully the experiments. Even the more sophisticated numerical techniques may be ineffective on extracting useful information from poorly informative experiments. For this reason, it is usually better to exploit mathematical techniques aimed at defining the conditions that maximise the amount of information and allow to get statistically satisfactory estimations and predictions from the minimum amount of data. These techniques represent a bridge between modeling and experimentation and they are useful tools for a rapid evaluation and development of kinetic - more generally mathematical - models, through the enhancement of the information content of each measure.

The merit for the DoE invention belongs to Ronald A. Fisher. As the first person to introduce this technique, in his celebrated book *The design of experiments* (Fisher (1935)) he defined the fundamental basis for the so called *factorial design*. The first objective was to analyse how the factors, or single design variables, must be modified to affect the system response in a certain way. Thus, in the factorial design, the main purpose was the identification of relationships between factors and measured variables - with the possibility of assessing also the interaction between factors - through a variance analysis. In the next years further methods were developed by Davies and van Dun En (1955), who applied the basic design techniques in fields like agriculture and industry where no mathematical models were available. Moreover, the study of DoE techniques on systems where the information is null, was extended by Box and Wilson (1992) who identified simple linear, parabolic, or at most polynomial relationships between factors and system response. Later, Ljung (1999) introduced the most common technique to pursue the identification of linear systems: it implies the perturbation of the process with the assessment of its response. For nonlinear systems, the choice of the experiments to be performed is less trivial although the rationale is still the same: each experiment must be as most informative as possible according to the amount of resources available. However, to better understand the concept of *information* it is possible to consider what underlined by Bard (1977). Transposed to chemical processes, the best experiment is not the one that gives the highest conversion or the best selectivity, the best experiment is the one that provides exactly the information required to reach a certain objective. Indeed, even though, virtually, any new measurement increase the total knowledge about a certain system, only the designed experiments allow with the lowest number of trials to collect the maximum amount of information needed to tackle a certain problem (usually the parameter estimation). For this reason, the DoE techniques have gained importance in all the research fields and all the industries interested in developing new processes and/or optimising the existent ones. Moreover, during the years people started to elaborate more advanced techniques to address also the systems with an high number of factors: since some of them could not play a significant role on the overall system response, if correctly identified they can be excluded from the design in order to reduce the resource and

computational expenditure.

1.6.1 Optimal Experimental Design (ODE)

This technique, which represents an evolution of the DoE, leads to the identification of the factors that are more suitable to be modified in order to obtain a certain response from the system. The rationale is that, for complex mathematical models that involve many measurable variables, it is better to discriminate the ones that affect heavily the model response from the others. This screening leads to a substantial decrease of the computation power and time required to perform the experimental design. Transposed to the chemical kinetics, the intuitions and the hypotheses on the ongoing phenomena can be many and the definition of a model is all but simple: different assumptions has to be investigated and their adequacy validated case by case. The different hypotheses may concern:

1. various *reaction pathways*, that represent the sequence of reactions leading to obtain the product, starting from the reactant, through a certain number of intermediate molecules;

2. peculiar *adsorption mechanisms*, that represent the way different molecules are physically adsorbed and desorbed, hence withheld or released, from and to the catalyst surface where the reactions usually take place.

In other words, through the optimal DoE it is possible to improve the information acquired from each experiment. As a consequence, the weight of the model identification task on the economy of the whole process development is remarkably lower. Eventually, since usually there are no information about the system, these techniques have been defined as *black-box design of experiments*. Along the years, however, they have been applied to a wide variety of fields, among which chemistry (Liang et al. (2001)), and they have been improved gradually to be used also when the preliminary information is not null.

1.7 Model-based design of experiments

The disadvantage on the application of black-box DoE techniques is that the amount of data required to build the model is usually high, especially if measurable and non-measurable variables are many. Moreover, even tough a relation between factors and response can be obtained, it is usually only locally reliable and it is not easy to determine the magnitude of the extrapolation error. However, the advantage of working with chemical and physical phenomena is that the preliminary knowledge is not null. It is indeed possible to describe the systems using basic principles and largely validated laws. The resulting *deterministic* or *phenomenological* approach, implies the formulation of a model through which any measurement can be associated to a precise value of variables and parameters. In these terms, the DoE previously defined must be recast in order to consider also the information intrinsically included on the model structure which reflects the knowledge on the system and can be used to predict the information content of an experiment. The resulting *model-based design of experiments* techniques (MBDoE) have been firstly applied to steady-state models, both linear and nonlinear, and a large number of studies, in a wide range of disciplines, are available in literature.

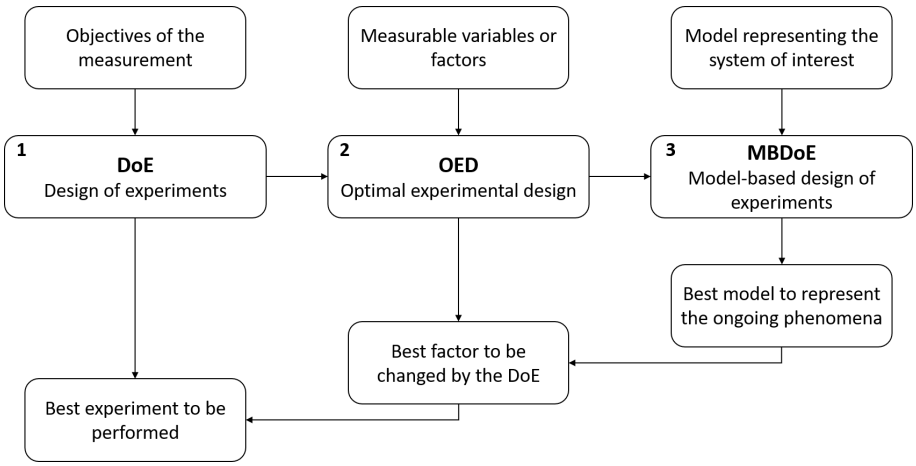

Figure 1.2: *Block diagram representing the evolution of the design techniques starting from the standard DoE (1) to end with the more advanced MBDoE (3)*

In Figure 1.2 it is reported the evolution of the DoE techniques. For each numbered block at the center, the inputs are reported above while the outcomes below.

MBDoE has been introduced by Box and Lucas (1959) who studied this strategy to reacting systems in order to estimate the kinetic parameters of simple reactions. Kiefer (1959) introduced the design criteria that defined the objective functions of the deterministic optimisation framework, in which the differential and algebraic equations that describe the underlying system are embedded. This so called "alphabetic criteria" represents the overall uncertainty of the system and have to be minimised. Other authors such as Hunter and Reiner (1965) and Atkinson and Fedorov (1975) followed the seminal work of Kiefer (1959) refining the model discrimination criteria to select the best model among a set of candidates. In particular, they have been the first to develop model-based experimental design criteria for model discrimination based on the distinct predictions between candidate models. Furthermore, some years later, Buzzi-Ferraris and Forzatti (1983) developed a MBDoE criterion for the model discrimination based on the relative variability on the predicted models responses. The same authors refined subsequently the criterion to consider also multi-response systems (Buzzi-Ferraris et al. (1990)). Eventually, among the most important contributions to the study conduced in this Thesis, Bard (1974) described how to apply to nonlinear parameter estimation problem the optimal design criteria based on the maximisation of scalar value related to information metrics: the most used, and further discussed in the next Chapter, is the *Fisher Information Matrix* (FIM). The use of the FIM and other metrics, leads to the possibility of exploiting the MBDoE to:

1. discriminate among a set of possible models (MBDoE for model discrimination or MD);

2. estimate the unknown parameters with the desired accuracy (MBDoE for parameter precision or PP).

MBDoE for MD was introduced by Espie and Macchietto (1989) and it is, as annunciated, the technique that allows the selection of the best model among a set of candidates. It is based on the design of highly discriminative experiments through which the difference between two, or more models, is enhanced. When the best model is selected, the quality of the estimates associated to the non-measurable parameters is assessed with specific statistical tests. Then, if the information is

not enough, through the MBDoE for PP new experiments are specifically designed to improve the unsatisfactory statistics to the desired level of precision (Galvanin et al. (2007)). Thus, MBDoE techniques lead to save time and money collecting from few targeted experiments more information of what it would be obtainable with numerous experiments at the wrong conditions. Eventually, some applications of the MBDoE have been proposed for biological systems by Espie and Macchietto (1989), who were the firsts to formulate the MBDoE as an optimal control problem, and Chen et al. (2004) for the accurate estimation of the model parameters. Some of the more recent examples of MBDoE application are reported by:

1. Donckels et al. (2009) for the study of nine rival models that describe the kinetics of an enzymatic reaction (glucokinase). A kernel-based method is presented to determine optimal sampling times to simultaneously estimate the parameters of rival models in a single experiment;

2. Schöneberger et al. (2009) for the catalytic SO_2 oxidation, in order to define a systematic approach based on nonlinear experimental design as an efficient tool for the validation of kinetic models. In this case, since the optimization problem contained a highly nonlinear objective function, a hybrid optimization framework is proposed to overcome the problem of local minima;

3. Zhang et al. (2012) for the protein ion-exchange equilibrium, to develop an efficient parallel/sequential design approach for the inclusion of practical restrictions in the optimization problem formulation such as maximal protein amount available, maximal solubility of protein and salt, or special characteristics of peak area determination during the measurement of protein concentrations using an analytical HPLC;

4. Galvanin et al. (2011) for the development of algorithms capable of tackling complex nonlinear dynamic systems in a continuous way. The study claims that current measurement technologies allow to perform measurements with a frequency so high that can almost be assumed as continuous.

To conclude, MBDoE represent the final step of the design of experiment evolution. It started from the intuition that designed experiments could have been more useful

to pursue a certain objective, it has been refined with the introduction of the optimal design to discriminate the best factors to consider as design variables, and it has evolved into the model-based design of experiments to account the phenomenological nature of many systems.

1.7.1 Model discrimination and parameter precision procedures

The way a phenomenological model can be identified is really important. If no prior information is available, preliminary experiments must be performed with the aim of understanding the mechanisms embroiled in the phenomenon of interest. Thus, especially when there are nonlinear phenomena involved, the number of alternatives proposed to describe the system could be high: a selection must be performed. The general procedure to follow is reported in Figure 1.3. It begins by defining a set of candidate models that are retrieved from the literature or obtained through the observation of the physical reality. On them, an identifiability analysis is conducted to obtain a set of identifiable models and the MBDoE for MD is applied to generate the optimal experimental conditions to be used for the parameter estimation. The assessment of certain statistics, that will be discussed on the next Chapter, allows to understand if the model is satisfactory from both structural and practical point of view. When the statistics of some parameters are unsatisfactory, the MBDoE for PP is applied until a positive result is obtained. Since the study presented in this Thesis is more linked to the models identifiability, this aspect is further refined introducing the more detailed procedure in Figure 1.4.

Since the model inadequacy may affect the MBDoE procedure, the importance of the model identifiability study must not be underestimated. It can prevent the execution of experiments that will never lead to a positive result, and can be largely helpful when the rejection of a model wants to be further investigated either because the set of models available is not particularly large or because a mechanism seems promising (perhaps it is effective in similar cases). Typically, starting from the identification of all the variables that can be manipulated, some estimability metrics are calculated. In this Thesis, the most used metrics are based on the cor-

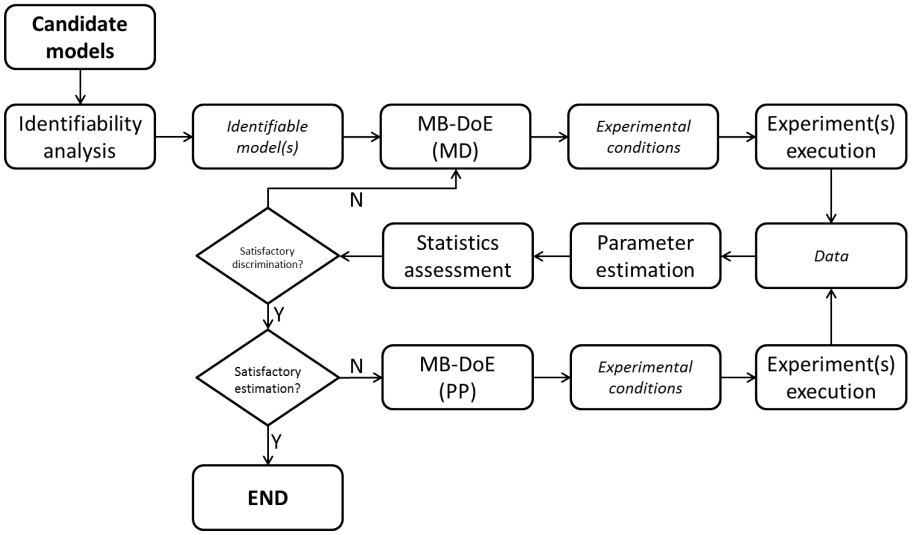

Figure 1.3: *General procedure for the model identification and parameter estimation staring from a set of candidate models.*

relation between parameters. If this assessment is satisfied, the model is hold and the analysis is repeated with another model of the available set. If it is not satisfied for any value of the design variables, the model is discarded.

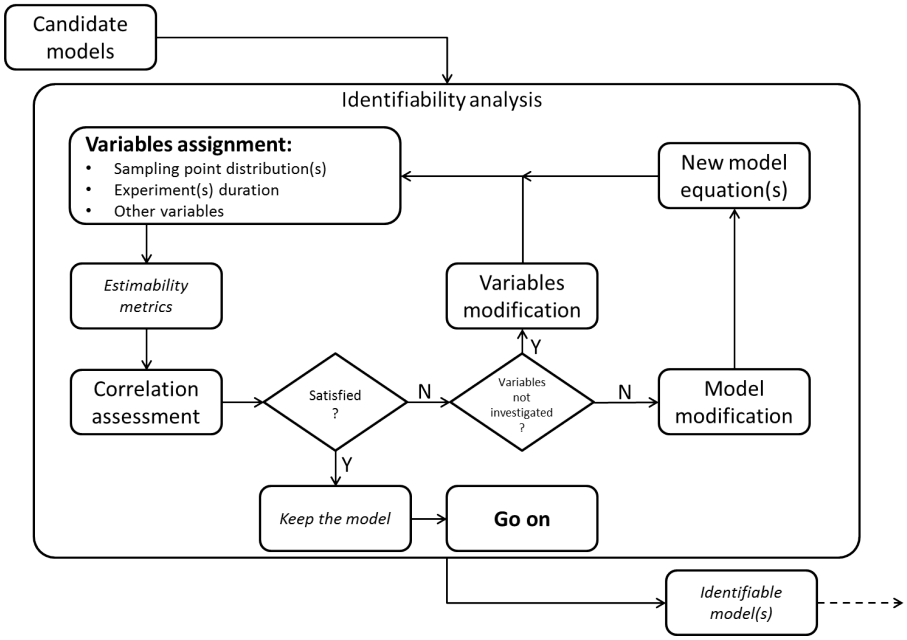

Figure 1.4: *Detailed procedure for assessment of the model identifiability staring from a set of candidate models.*

CHAPTER 2

KINETIC MODEL IDENTIFICATION TECHNIQUES

ONCE a kinetic model is available, experimental data have to be used to estimate its non-measurable parameters. It is clear as the accuracy of these estimates increases with the quality of the data gathered. Not only precision and repeatability should be achieved, the experiments should also be performed at the conditions that maximize the information they carry for the parameter estimation purpose. In other words, within the entire experimental domain – the space of all the possible experimental conditions that can be experienced – an optimal region has to be found. This Chapter illustrates the most important statistical analyses that can be used to determine whether the structure of a kinetic model is identifiable and if it is possible to get satisfactory estimates for its non-measurable parameters.

2.1 Parameter estimation problem

Considering a generic system, a model represents the phenomenological mechanism through which the different inputs affect the outputs. According to Bard (1974), a standard reduced model can be defined as:

$$\hat{\mathbf{y}}(t) = \mathbf{f}(\mathbf{x}(t), \mathbf{u}(t), \theta) \tag{2.1}$$

where $\mathbf{f}$ is a vector of N_f model equations, $\hat{\mathbf{y}}(t)$ is a vector of N_m measurable output variables, $\mathbf{x}$ is a vector of N_x state variables, $\mathbf{u}$ is a vector of N_u input variables that can be manipulated, θ is a vector of N_θ parameters that require estimation and t is the time. The kinetic models belong to a large class of nonlinear deterministic

dynamic structures that are described by a set of differential-algebraic equations (DAEs). Thus, (2.1) can be recast in vectorial and differential form as suggested by Asprey and Macchietto (2000) and Franceschini and Macchietto (2008) for the general model **M**:

$$\mathbf{M}: \begin{cases} \mathbf{f}(\dot{\mathbf{x}}(t), \mathbf{x}(t), \mathbf{u}(t), \mathbf{w}, \theta, t) = 0 \\ \hat{\mathbf{y}}(t) = \mathbf{h}(\mathbf{x}(t)) \end{cases} \tag{2.2}$$

where, regarding the new variables introduced, $\dot{\mathbf{x}}(t)$ is the vector of N_x differential variables, $\mathbf{w}$ is the vector of N_w input variables time independent that can be manipulated, $\mathbf{h}$ is a function of the state variables and represents the set of relations between the variables $\hat{\mathbf{y}}(t)$ and the state variables. Moreover, the system (2.2) undergo a set of initial conditions that, in the general form, are:

$$\mathbf{M}: \begin{cases} \mathbf{f}\left(\dot{\mathbf{x}}(t_0), \mathbf{x}(t_0), \mathbf{u}(t_0), \mathbf{w}, \theta^0, t_0\right) = 0 \\ \hat{\mathbf{y}}(t_0) = \mathbf{h}(\mathbf{x}(t_0)) \end{cases} \tag{2.3}$$

On the one hand, by assigning a certain time-window, the simulation of the system through the model requires the solution of (2.2), given initial conditions (2.3), time-invariant inputs, manipulated inputs profiles and values for the model parameters. On the other hand, under the assumption that the measured inputs are not affected by significant errors, the parameter estimation problem can be represented as:

$$\hat{y}_i(t) - \mathbf{f}(\dot{\mathbf{x}}(t), \mathbf{x}(t), \mathbf{u}_i(t), \mathbf{w}, \theta, t) = \mathbf{0} \quad \forall \quad i = 1, ..., N_{exp} \tag{2.4}$$

with $\mathbf{0}$ as a null vector consistent with the dimensionality of the system. In other words, the parameter estimation problem consists in the identification of the parameters set θ satisfying (2.4) for all the N_{exp} experiments performed. However, considering the uncertainty intrinsically associated with the measurements, the estimation problem becomes usually over-specified and a residual function must be defined. In reality, satisfying (2.4) is indeed practically impossible because:

1. the measurable variables are affected by a certain error ϵ such that $\hat{y}_i(t) = y_i^*(t) + \epsilon$;
2. the set of equations $\mathbf{f}$ is wrong or incomplete such that $\hat{\mathbf{y}}_i(t) - \mathbf{f}(\dot{\mathbf{x}}(t), \mathbf{x}(t), \mathbf{u}(t), \mathbf{w}, \theta, t) \neq \mathbf{0}$ for every choice of θ.

Then, in order to find an approximate solution, it is first required to define the so called *residual function* for each variable and each data collected. At the purpose, ρ_{ij} represents the difference between measured and predicted values for each of the j-th measurable outputs of the i-th experiment:

$$\rho_{ij}(\theta) = y_{ij} - \mathbf{f}(\dot{\mathbf{x}}(t), \mathbf{x}(t), \mathbf{u}_i(t), \mathbf{w}, \theta, t) = y_{ij} - \hat{y}_{ij}(\theta) \tag{2.5}$$

The parameter estimation problem can be recast in terms of finding the set of parameters θ that minimises a certain objective function related to the just defined (2.5). Moreover, to account the casual nature of the measurements, both measured outputs and parameter estimations must be treated as random variables. Thus, statistical concepts and derivations are used to describe properly the nature of the parameter estimation problem.

2.2 Least squares method for non linear problem

Especially in data fitting, that represents its most important application, the least squares method is used to approximate the solution of overdetermined systems. It means that, by defining the residual as the difference between the observed value and the value estimated through the model, the best fitting is the one that minimise the sum of the squared residuals. Moreover, as a function of the residuals in all the unknowns, two categories of least-square problems can be defined: linear and nonlinear. While the linear case has a closed-form solution, the nonlinear problem is solved approximating the system by a linear one for each iteration. It is called *iterative refinement*.

Applied to the parameter estimation problem, the least squares method is recast in terms of finding the best set of parameters that minimise the objective function Ψ such that:

$$\min_{\theta}\{\Psi\} = \min_{\theta}\left\{\sum_{i=1}^{N_{exp}}\sum_{j=1}^{N_m}\left[\rho_{ij}(\theta)\right]^2\right\} \tag{2.6}$$

Notice that, although the least squares method can be used also for the parameter estimation problem, it does not account for the uncertainty instrinsically related to the measurements. Beside it has been demonstrated that in some specific cases the results are identical (Charnes et al. (1976)), it is usually preferred to adopt other objective functions.

2.3 The likelihood function

The usefulness of the particular function defined in this section, becomes clear considering that a mathematical model should always consider the casual nature of the measurements used for the identification, validation and estimation purposes. Indeed, tools and equipment used to gather the data are always characterized by some degree of accuracy that leads to the necessity of treating the resulting measurements as random variables. A good model must then address the casual nature of the measurements starting from the fact that the different data cannot be assumed to have the same level of reliability. In other words, the disturbances must be accounted as an integral part of the physical phenomenon under investigation.
To describe appropriately the events related to this kind of variables, the concept of probability must be introduced. Specifically for the parameter estimation case, this is the probability of getting certain data from an assigned model or theory, in order to answer the question: when measurements are made, how likely is it to get the same value through the specific model that involves the parameters to be estimated? The answer is given by a joint probability density function called *likelihood function*:

$$L(\theta) \equiv P[\text{data}|\text{model}]. \tag{2.7}$$

Considering the most common case in which the measurement errors ($\mathbf{y} = \hat{\mathbf{y}} + \boldsymbol{\epsilon}$) are normally distributed random variables with zero mean and a certain standard deviation σ_{ij}, the shape of the likelihood function is a Gaussian more or less broad (see Figure 2.3).
If the model is exact, there is a value for the set of parameters ($\hat{\theta}$) for which the prediction of the measurable outputs satisfy (2.4). The residuals follow the same distribution of the measurement errors such that:

$$\rho_{ij}(\theta^*) = y_{ij} - \hat{y}_{ij}(\theta^*) = y_{ij} - y^*_{ij} \ . \tag{2.8}$$

Under the assumption that the model is exact and through (2.8), the residuals $\rho_{ij}(\theta^*)$ can be assumed as random variables completely uncorrelated and normally distributed with zero mean and the same standard deviation σ_{ij} of the measure-

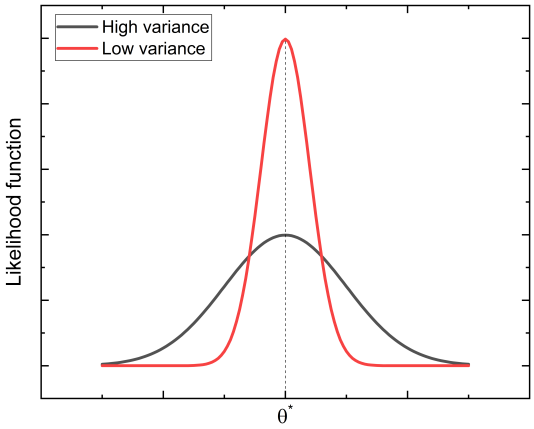

Figure 2.1: *Comparison of the shape the Likelihood function can assume as a function of the variance associated with the parameter estimation.*

ments. Thus, (2.7) can be written in explicit form as:

$$L(\theta) \equiv \prod_{i=1}^{N_{exp}} \prod_{j=1}^{N_m} \frac{1}{\sqrt{2\pi\sigma_{ij}^2}} \exp^{-\frac{1}{2}\left(\frac{\rho_{ij}(\theta)}{\sigma_{ij}}\right)^2} \tag{2.9}$$

that is the joint probability density function of the residuals, named likelihood function.

At this point, to address the parameter estimation problem, it is possible to consider the two distributions in Figure 2.1. First, assuming to look for the set of parameters that gives a certain value of the measurable outputs $\hat{y}_{ij}(\theta)$, it is clear as the red curve leads to a more accurate result: even small variations around the exact value of the parameters θ^* make the model outcome inconsistent. In the other case instead, when the distribution is very broad, a peak still exists at θ^* but there is also a good deal of likelihood at some distance away from it. That is, with the black distribution, consistent data can also be obtained when the values of the model parameters are significantly different from θ^*. Thus, the likelihood function can be used to understand how the data are constrained to the assigned theory, or model, and the narrower the range of values that satisfies the data, the more accurate the estimation itself. Giving a set of measurements, the parameter estimation problem reduces to the identification of the parameter values $\hat{\theta}$ that maximise the objective function $L(\theta)$ and lead to final residuals distributed like the corresponding mea-

surement errors. The technique is called maximum likelihood estimate (MLE):

$$\max_{\theta}\{L(\theta)\} = \max_{\theta}\left\{\prod_{i=1}^{N_{exp}}\prod_{j=1}^{N_m}\frac{1}{\sqrt{2\pi\sigma_{ij}^2}}\exp^{-\frac{1}{2}\left(\frac{\rho_{ij}(\theta)}{\sigma_{ij}}\right)^2}\right\}. \tag{2.10}$$

To reduce the probability of occurring in numerical errors due to the complexity of the problem, it is usually better to adopt the natural logarithm. Since it represents a monotonic increasing function of its argument, the solution that maximises $L(\theta)$, maximises also $\ln(L(\theta))$. The corresponding objective function (Bard (1974)) is:

$$\max_{\theta}\{\ln(L(\theta))\} = \max_{\theta}\left\{\ln\left[\prod_{i=1}^{N_{exp}}\prod_{j=1}^{N_m}\frac{1}{\sqrt{2\pi\sigma_{ij}^2}}\exp^{-\frac{1}{2}\left(\frac{\rho_{ij}(\theta)}{\sigma_{ij}}\right)^2}\right]\right\}. \tag{2.11}$$

Eventually, although the assumption of having an exact model is necessary to assume residuals and measurement errors follow the same distribution, all the previous findings hold also when a model represents only a good approximation of the reality. With these so called *quasi-exact* models, the discrepancy between reality and predicted values is usually detected through specific analyses capable of identifying the lacks on the model descriptive capability. These tests, as the χ^2-test discussed later on, can be performed *a posteriori*. Nevertheless, the possibility of finding an optimal point always depends on the model structure: before starting any estimation procedure, it is extremely important to verify the model identifiability.

2.4 Model identifiability

Structural (or *a priori*) identifiability analysis must demonstrate the possibility of identifying the parameters as a property of the model, independently of the measured data and their uncertainty. Local identifiability is also performed *a priori* but it is valid only for a specific configuration of the system: it represents a weaker notion in respect to the structural identifiability. According to Saccomani P. et al. (2003), a model can be:

1. a priori globally (or uniquely) identifiable when

$$\mathbf{M}(\theta) = \mathbf{M}(\theta^*) \tag{2.12}$$

has the only solution $\theta = \theta^*$ for all the initial states $\mathbf{x}(t_0)$;

2. locally identifiable when (2.12) has a finite number of solutions;

3. unidentifiable when the number of solutions for (2.12) is not defined and, in particular, when it is satisfied for any value of θ_i.

Several authors tried to propose general guide lines to solve the identifiability problem. Unfortunately, the structural identifiability for a nonlinear model is usually tough to tackle and cannot be treated in a general way: the solution usually depends on the modeler experience. Thus, the impossibility of defining a standard way to test the global identifiability led to the development of numerical methods aimed at checking at least the local identifiability.

2.4.1 Sensitivity analysis

Among the several techniques available, the most simple and popular is the *sensitivity analysis*: it represents the study of the model response when the value of the parameters $\hat{\theta}$ is varied around their real value θ^*. It can be considered as the investigation of how the uncertainty in the measurable outputs of a model can be allocated to different sources of variation in the inputs (Saltelli (2002)). For the parameter estimation problem, it leads to assess how the model response $\hat{\mathbf{y}}$ is affected by a small variations on the parameter set $\hat{\theta}$. Thus, it practically consists on changing one factor at a time – in respect to a nominal case – and evaluating the partial derivative of each output with respect to each input. The goals are:

1. identifying the parameters that affect most the model response(s);

2. determining the amount of information available for certain experimental conditions;

3. obtaining advices about the correlation between model parameters.

Virtually, from the sensitivity analysis, it is possible to derive the most important metrics used for the model identifiability study and for the optimal design of experiments. Thus, the local sensitivities for any m-th measurable output are evaluated at each sampling time and the result is the $n_{sp} \times N_\theta$ matrix that follows:

$$\mathbf{Q}_m = \begin{bmatrix} \left.\frac{\partial \hat{y}_m}{\partial \theta_1}\right|_{t_1} & \cdots & \left.\frac{\partial \hat{y}_m}{\partial \theta_{N_\theta}}\right|_{t_1} \\ \vdots & \ddots & \vdots \\ \left.\frac{\partial \hat{y}_m}{\partial \theta_1}\right|_{t_{nsp}} & \cdots & \left.\frac{\partial \hat{y}_m}{\partial \theta_{N_\theta}}\right|_{t_{nsp}} \end{bmatrix} \quad \forall\ m = 1,...,N_m \tag{2.13}$$

These outputs can be converted to a 3D matrix (see Figure 2.2) containing all the sensitivities for each output, in respect to each parameter, at any time. In particular, while the third dimension of this 3D matrix represent the sampling time, the first two dimensions consist of a $N_m \times N_\theta$ matrix of local sensitivities:

$$\mathbf{Q}(t) = \begin{bmatrix} q_{1,1}(t) & \cdots & q_{1,N_\theta}(t) \\ \vdots & \ddots & \vdots \\ q_{N_m,1}(t) & \cdots & q_{N_m,N_\theta}(t) \end{bmatrix} = \begin{bmatrix} \frac{\partial \hat{y}_1(t)}{\partial \theta_1} & \cdots & \frac{\partial \hat{y}_1(t)}{\partial \theta_{N_\theta}} \\ \vdots & \ddots & \vdots \\ \frac{\partial \hat{y}_{N_m}(t)}{\partial \theta_1} & \cdots & \frac{\partial \hat{y}_{N_m}(t)}{\partial \theta_{N_\theta}} \end{bmatrix} \tag{2.14}$$

where $q_{ij}(t)$ represents the local sensitivity of the i-th output $\hat{y}_i$ in respect to the j-th parameter θ_j at any time t. Repeating the matrix above for each sampling time, it is so possible to build layer by layer the 3D matrix reported in Figure 2.2. The convenience of computing a matrix like this, is that with simple permutations it is possible to obtain a wide range of information.

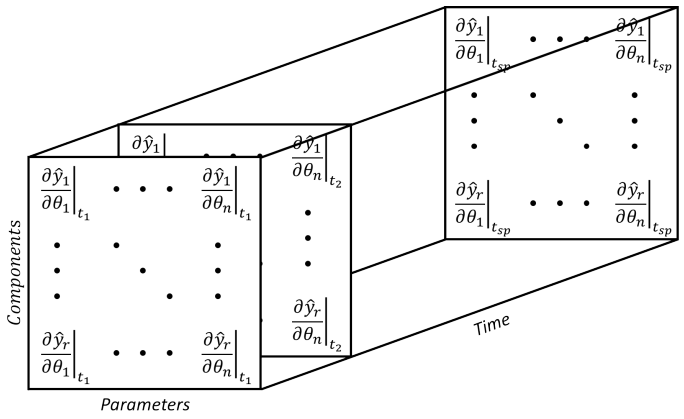

Figure 2.2: *Schematic representation of the 3D sensitivity matrix.*

At this point, in order to understand if a model is identifiable, the estimability matrix can also be assembled. It is a $N_m n_{sp} \times N_\theta$ matrix, based on the local sensi-

tivities, such that:

$$\mathbf{P}_E = \begin{bmatrix} \mathbf{Q}(t_1) \\ \vdots \\ \mathbf{Q}(t_{n_{sp}}) \end{bmatrix} = \begin{bmatrix} \frac{\partial \hat{y}_1}{\partial \theta_1}\Big|_{t_1} & \cdots & \frac{\partial \hat{y}_1}{\partial \theta_{N_\theta}}\Big|_{t_1} \\ \vdots & \ddots & \vdots \\ \frac{\partial \hat{y}_{N_m}}{\partial \theta_1}\Big|_{t_1} & \cdots & \frac{\partial \hat{y}_{N_m}}{\partial \theta_{N_\theta}}\Big|_{t_1} \\ \vdots & \vdots & \vdots \\ \frac{\partial \hat{y}_1}{\partial \theta_1}\Big|_{t_{nsp}} & \cdots & \frac{\partial \hat{y}_1}{\partial \theta_{N_\theta}}\Big|_{t_{nsp}} \\ \vdots & \ddots & \vdots \\ \frac{\partial \hat{y}_{N_m}}{\partial \theta_1}\Big|_{t_{nsp}} & \cdots & \frac{\partial \hat{y}_{N_m}}{\partial \theta_{N_\theta}}\Big|_{t_{nsp}} \end{bmatrix} \tag{2.15}$$

where $\mathbf{Q}(t_s)$ are the $N_m \times N_\theta$ matrices of local sensitivities for each n_{sp}-th sampling time. Shaw (1999) underlines that a model can be classified as identifiable if $rank(\mathbf{P}_E) < N_\theta$, that is satisfied when each column of the matrix is independent on the others. Besides, although the sensitivity analysis is a really versatile tool, it could result very complex to represent even when the number of parameters or outputs is not really high: it always involves $N_m \times N_\theta \times N_{sp} \times N_{exp}$ sensitivity terms. For this reason, it is usually more convenient to define other metrics capable of giving a suitable scalar measure of the correlation and the information available.

2.5 Information metric

In order to mathematically define the concept of information, it is firstly required to introduce the Hessian matrix. Given a scalar-valued function Φ in n variables, the Hessian is a square matrix $n \times n$ of its second-order partial derivatives:

$$\mathbf{H} = \frac{\partial^2 \Phi}{\partial \mathbf{u} \partial \mathbf{u}} \tag{2.16}$$

Since it describes the local curvature of a function, it can be usefully applied to the parameter estimation problem. In particular, when the scalar-valued function Φ is the logarithm of the likelihood function, the resulting Hessian is called *Fisher information matrix* (FIM). It allows to quantify the amount of information available for each parameter that requires estimation. There are indeed two aspects to consider:

1. the ease of reaching the desired accuracy on the estimation depends on the information available for each parameter;

2. the information carried by different measurable variable may vary considerably.

On the one hand, the Fisher information matrix analysis can help to identify in advance the parameters that require more attention – meaning that more experiments will be probably required for them – while, on the other hand, it allows to figure out the contribution of each measurable variable to the overall information content. The rationale is that it does not make sense to spend effort and resources to measure something that does not substantially contribute to improve the estimation quality.
However, to finally find the mathematical link between Fisher matrix and sensitivity analysis, it is required first to consider totally uncorrelated measurable variables. As already specified, the function Φ must be the log-likelihood such that:

$$\Phi = \ln\left(L(\hat{\theta})\right) = -\frac{1}{2}\sum_{i=1}^{N_{exp}}\sum_{j=1}^{N_m}\left[\ln\left(2\pi\sigma_{ij}^2\right) + \left(\frac{\rho_{ij}(\hat{\theta})}{\sigma_{ij}}\right)^2\right] \tag{2.17}$$

Thus, the Hessian turns out to be a matrix containing the second-order partial derivatives of the measurable outputs $\mathbf{y}$ in the unknown parameters θ and (2.16) can be re-formulated as:

$$\mathbf{H} = -\frac{\partial^2 \ln\left(L(\hat{\theta})\right)}{\partial\theta\partial\theta} = \sum_{i=1}^{N_{exp}}\sum_{j=1}^{N_m}\left[\frac{1}{\sigma_{ij}^2}\nabla y_{ij}\cdot\nabla y_{ij}^T\right] \tag{2.18}$$

From (2.18) it is possible to calculate the N_θ elements of the FIM as the elements of the Hessian associated to the function Φ, such that the kl-th element can be calculated as:

$$[\mathbf{H}]_{kl} = -\left[\frac{\partial^2 \ln\left(L(\hat{\theta})\right)}{\partial\theta\partial\theta}\right] = \sum_{i=1}^{N_{exp}}\sum_{j=1}^{N_m}\left[\frac{1}{\sigma_{ij}^2}\left(\frac{\partial\hat{y}_{ij}}{\partial\theta_k}\frac{\partial\hat{y}_{ij}}{\partial\theta_l}\right) + \frac{1}{\sigma_{ij}^2}(\hat{y}_{ij}-y_{ij})\frac{\partial^2\hat{y}_{ij}}{\partial\theta_k\partial\theta_l}\right] \tag{2.19}$$

which can be greatly simplified under the assumption that the residuals $\rho_{ij} = \hat{y}_{ij} - y_{ij}$ are small enough:

$$[\mathbf{H}]_{kl} \approxeq \sum_{i=1}^{N_{exp}}\sum_{j=1}^{N_m}\left[\frac{1}{\sigma_{ij}^2}\left(\frac{\partial\hat{y}_{ij}}{\partial\theta_k}\frac{\partial\hat{y}_{ij}}{\partial\theta_l}\right)\right] \tag{2.20}$$

where the partial derivatives of the estimated outputs in respect to the non-measurable parameters are the previously defined sensitivities.

2.5.1 Information content representation

In most of the cases where the aim is only to collect preliminary information about the problem to be tackled, it is less time expensive to calculate only the FIM trace:

$$\mathbf{T}[\mathbf{H}]_{kl} = \sum_{k=1}^{N_\theta} \sum_{i=1}^{N_{exp}} \sum_{j=1}^{N_m} \left[\frac{1}{\sigma_{ij}^2} \left(\frac{\partial \hat{y}_{ij}}{\partial \theta_k} \frac{\partial \hat{y}_{ij}}{\partial \theta_l} \right) \right]. \tag{2.21}$$

When its elements are close or equal to zero for any experimental condition, the associated parameters are tough to identify. Notice anyway that the information content, hence the possibility of estimating a parameter in a statistically reliable way, strongly depends on the sampling procedure adopted. Different procedures differ for:

1. abundance of samples;
2. distribution of the samples in the time interval considered.

The ideal case is represented by a continuous sampling that leads to the identification of the full information profile along the experiment time. Trivially, the more abundant the samplings, the higher the knowledge about the phenomenon of interest but unfortunately, in reality there are several constraints that prevent a frequent sampling. Furthermore, there is no reason on having all the samplings concentrated in a time-window where they cannot catch the most from the experiment because the information at that moment is low. Thank to these features, the FIM and its trace have been largely adopted in this Thesis. Notice however that, in any case, the analysis of the trace is not enough to declare a model as unidentifiable: it considers neither the correlation between parameters nor the region of the experimental domain explored.

An example of Fisher trace profiles is illustrated in Figure 2.3. In the first plot (a) it is reported the overall profile given by the sum of the information available for each parameter at any time. The area under the curve is filled because through integration over the time, it is possible to obtain the total amount of information collectable. Besides, (b), (c) and (d) shows how the information can be decomposed for the single parameters. Eventually, (e) gives an idea of the best way to summarise the differences in the information content available for the single parameters, against the total.

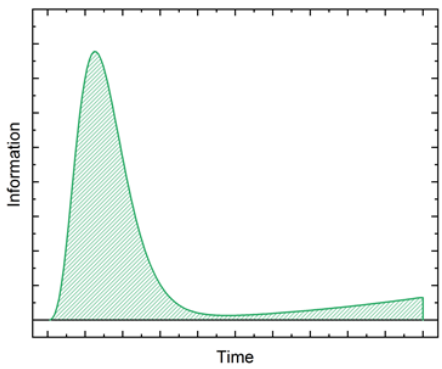

(a) *Total information available*

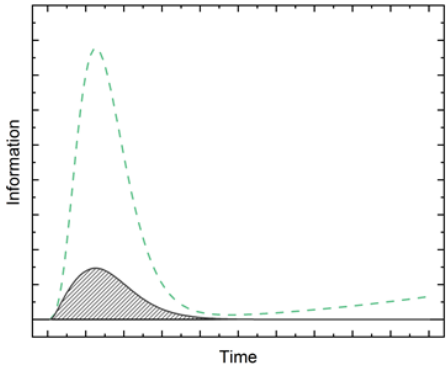

(b) *Information available for* θ_1

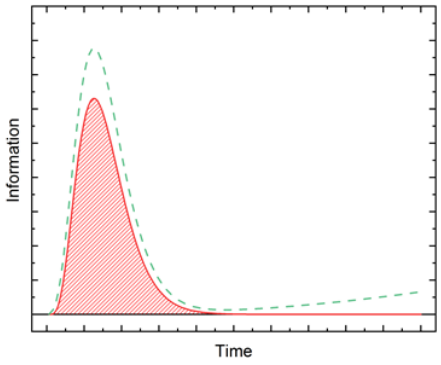

(c) *Information available for* θ_2

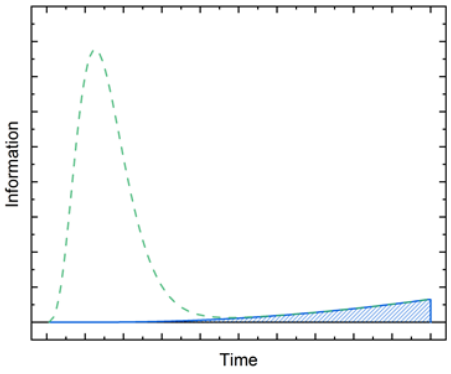

(d) *Information available for* θ_3

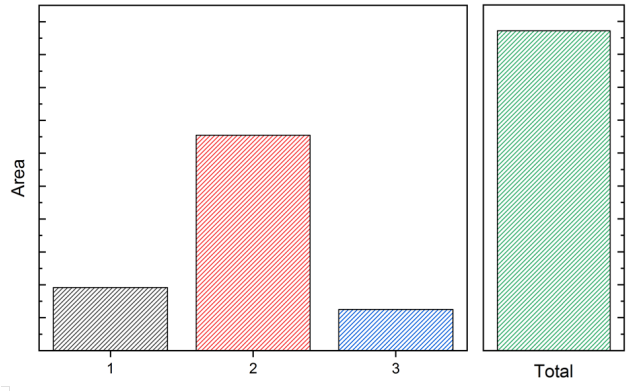

(e) *Bar plot for comparison of the total information available*

Figure 2.3: *Illustration of the Fisher trace decomposition in the single parameter contributions for a general model involving 3 parameters. Information profiles and comparison of the area below each curve through the use of a bar plot.*

2.6 The Variance-Covariance Matrix

The understand how to exploit the covariance in terms of variance-covariance matrix, the parameter estimation problem has to be addressed directly. It has been

already demonstrated how to estimate a set of parameters, the maximum of the likelihood function must be determined. However, since the measurements are always affected by uncertainty – reason for which the variables are assumed to be random and normally distributed – it is not possible to consider the parameter estimation $\hat{\theta}$ as true. Indeed, any estimate must always be related to a certain level of confidence that depends on the reliability of the data gathered. To understand the effect of a certain variability, the impact of a measurements variation on the estimation result, must be assessed. The purpose is to determine how the location of the likelihood function optimal point is affected by the intrinsic uncertainty of the measured values, used to perform the estimation. First, considering all the measurable variables $\mathbf{y}$ for all the sampling points and all the experiments, the optimal point of the log-likelihood function represents the place where the following must hold:

$$\frac{\partial \ln\left(L(\hat{\theta},\mathbf{y})\right)}{\partial \theta} = \mathbf{0} \tag{2.22}$$

with the left-hand side term that represents all the partial derivatives of the logarithmic likelihood function with respect to all the parameters. At this point, looking for the curvature of the objective function means looking for an indication of how fast the log-likelihood function itself falls off from the optimal point. Hence, if it falls off very quickly, the data are relatively constrained to the model. However, if it falls off very slowly, the data do not feel this constraint and the optimal region turns out to be wider. Translated in terms of information, if the likelihood function is sharply peaked with respect to $\hat{\theta}$, the data provide a lot of information and only few measurements are required to reach the desired accuracy. Contrarily, when the likelihood is flat and spread-out, the estimation takes many experiments to be satisfactory. Assuming now the $\ln(L(\theta))$ function as continuous, a small variation of the measurable variables determines a small shift of the optimal point, such that:

$$\frac{\partial \ln\left(L(\hat{\theta}+\partial\hat{\theta},\mathbf{y}+\partial\mathbf{y})\right)}{\partial \theta} = \mathbf{0} \tag{2.23}$$

Thus, the Taylor expansion of (2.23) gives:

$$\frac{\partial \ln\left(L(\hat{\theta}+\partial\hat{\theta},\mathbf{y}+\partial\mathbf{y})\right)}{\partial \theta} \approxeq \frac{\partial \ln\left(L(\hat{\theta},\mathbf{y})\right)}{\partial \theta} + \frac{\partial^2 \ln\left(L(\hat{\theta},\mathbf{y})\right)}{\partial \theta \partial \theta}\partial\hat{\theta} + \frac{\partial^2 \ln\left(L(\hat{\theta},\mathbf{y})\right)}{\partial \theta \partial \mathbf{y}}\partial\hat{\mathbf{y}} \tag{2.24}$$

Considering (2.22) and (2.16), by simple substitutions and rearrangements the vari-

ation of the estimated value for the parameters shift $\partial\hat{\theta}$ can be obtained.

$$\partial\hat{\theta} \approxeq -\mathbf{H}^{-1}\left(\frac{\partial^2 \ln\left(L(\hat{\theta},\mathbf{y})\right)}{\partial\theta\partial\mathbf{y}}\partial\hat{\mathbf{y}}\right)\partial\mathbf{y} \approxeq -\mathbf{FIM}^{-1}\left(\frac{\partial^2 \ln\left(L(\hat{\theta},\mathbf{y})\right)}{\partial\theta\partial\mathbf{y}}\partial\hat{\mathbf{y}}\right)\partial\mathbf{y} \tag{2.25}$$

From (2.25), it is possible to introduce the covariance matrix that represents the expected value for the squared residuals of the parameters or, in other words, the difference $\partial\hat{\theta}$ between the parameters before the shift and their expected value $E(\theta)$ such that:

$$\mathbf{V}_\theta \equiv E\left\{[\theta - E(\theta)][\theta - E(\theta)]^T\right\} \tag{2.26}$$

Assuming then $E(\theta) = \hat{\theta}$, and replacing (2.25) into (2.26), the variance-covariance matrix turns to be:

$$\mathbf{V}_\theta \equiv E\left\{\left[-\mathbf{H}^{-1}\left(\frac{\partial^2 \ln\left(L(\hat{\theta},\mathbf{y})\right)}{\partial\theta\partial\mathbf{y}}\partial\hat{\mathbf{y}}\right)\partial\mathbf{y}\right]\left[-\mathbf{H}^{-1}\left(\frac{\partial^2 \ln\left(L(\hat{\theta},\mathbf{y})\right)}{\partial\theta\partial\mathbf{y}}\partial\hat{\mathbf{y}}\right)\partial\mathbf{y}\right]^T\right\} \tag{2.27}$$

$$\mathbf{V}_\theta \equiv E\left\{-\mathbf{H}^{-1}\left(\frac{\partial^2 \ln\left(L(\hat{\theta},\mathbf{y})\right)}{\partial\theta\partial\mathbf{y}}\partial\hat{\mathbf{y}}\right)\partial\mathbf{y}\partial\mathbf{y}^T\left(\frac{\partial^2 \ln\left(L(\hat{\theta},\mathbf{y})\right)}{\partial\theta\partial\mathbf{y}}\partial\hat{\mathbf{y}}\right)^T\mathbf{H}^{-1}\right\} \tag{2.28}$$

where $\partial\mathbf{y}\partial\mathbf{y}^T$ represents the variance-covariance matrix $\mathbf{V_Z}$ of the measurements. This derivation brings, eventually, to the formulation of Bard (1974). He demonstrated the validity of the following approximation specifying that, by increasing the measurements variance, hence improving the fitting of the model, the approximation quality improves as well.

$$\mathbf{V}_\theta \approxeq \mathbf{H^{-1}} \tag{2.29}$$

In (2.29), the Hessian matrix can be referred to any type of objective function: in this work it is assumed to be the FIM. Furthermore, the implication of the just derived formulation is in agreement with the Hessian definition and represents the link between the likelihood function and the reverse of the variance-covariance matrix. Specifically, it tells how curved is the $\ln(L(\theta))$ around the optimal point: the higher the values of the FIM elements, the more curved and peaked the likelihood function and, eventually, the greater the covariance reduction.

To conclude, the representation of the covariance trend along a hypothetical campaign of experiments, underlines the different contribution of each experiment on the covariance reduction and permit to figure out which are the best conditions to ensure a statistically reliable estimation.

2.7 The matrix inversion problem

The study of the covariance trend, hence the evolution of the variance-covariance matrix during a theoretical campaign of experiments, leads to identify the best experimental conditions to be used for the estimation purposes. However, considering (2.29), it is extremely important to underline as the computation of a matrix inverse requires some caution. In particular, for a matrix to be invertible, its determinant cannot be zero or even close to. Often, especially in the study of complex kinetic models, this condition does not occur and the reasons for that are essentially two:

1. the FIM is singular;

2. the FIM is ill-conditioned or bad-scaled.

In general, if the sensitivities of some parameters are really low, the elements of the FIM are small and the matrix turns out to be singular. The same problem of ill-condition comes out by the eigenvalues analysis: they should be positive for definition of the variance-covariance matrix itself – such that it results to be positive semidefinite – but instead some negative values appears because numerical errors arise when the sensitivities are extremely low. To counteract that, several methods for modifying symmetric indefinite matrices have been developed (e.g. Nocedal and Wright (1999)). These methods include eigenvalues modification by flipping the sign of the negative ones, addition of a multiple of the identity and Modified Cholesky Factorization in its many variants (Dereniowski and Kubale (2004)). Unfortunately, once these modifications are done, it is still not well clear how to come back with a well-posed FIM and, for this reason, they represent a risk that researchers usually prefer to avoid: it would compromise the statistical significance of the results.

2.7.1 Condition number

The condition number is an index used in numerical analysis to assess how much the outputs of a function can change for a variation on its inputs. It represents, in other words, the sensitivity of a function to inputs variations.

$$\mathbf{A}\vec{x} = \vec{b} \tag{2.30}$$

Considering (2.30), the main issue is that very small changes in $\vec{b}$ can lead to huge changes in $\vec{x}$. This is very critical in the case $\vec{b}$ represents any kind of measurement affected by any sort of errors. From a formal point of view, when this index is used to assess the condition of a matrix, the way in which it can be calculated depends on the matrix norm used: norm-1, norm-2, Frobenius or Infinite. However, assuming to have a symmetric and diagonalizable matrix and to use the norm-2, the condition number is given by the ratio between the highest and the lowest eigenvalue of the matrix itself (see Appendix A).

$$\mathrm{CN}(\mathbf{A}) = \frac{\max(\lambda_i)}{\min(\lambda_i)} \tag{2.31}$$

The larger CN, the worst the condition of matrix and system. Specifically, a matrix is defined *well-conditioned* when this number is small or *ill-conditioned* when the number is large.

2.7.2 Singular Value Decomposition

The Singular Value Decomposition is a factorization technique for matrices, based on eigenvalues and eigenvectors, that is particularly suitable to define an approximation for the matrix inverse (also called pseudo-inverse) of a rectangular matrix. In the modeling environment, it can be used to provide an approximation of the variance-covariance matrix when the FIM turns out to be non-invertible. Considering a generic matrix $\mathbf{A}$, it can be decomposed as:

$$\mathbf{A} = \mathbf{U}\mathbf{D}\mathbf{V}^{\mathbf{T}} \tag{2.32}$$

where $\mathbf{D}$ is a singular values matrix of non-negative diagonal elements in decreasing order and $\mathbf{U}$ and $\mathbf{V}$ are two unitary matrices. According to Trucco and Verri (1998), if $\mathbf{A}$ is singular or ill-conditioned, an approximation for its inverse is:

$$\mathbf{A}^{-\mathbf{1}} = (\mathbf{U}\mathbf{D}\mathbf{V}^{\mathbf{T}})^{-1} \approx \mathbf{V}\mathbf{D}_{\mathbf{0}}^{-\mathbf{1}}\mathbf{U}^{\mathbf{T}} \tag{2.33}$$

$$\mathbf{D}_0^{-1} = \begin{cases} 1/\delta_i & \text{if } \delta_i > \varepsilon; \\ 0 & \text{if } \delta_i \leq \varepsilon \end{cases} \tag{2.34}$$

where ε is a small threshold that is usually around 10^{-10}.

Notice that, although the technique allows to compute the matrix inverse, the result

represents still an approximation and the product between $\mathbf{A}^{-1}$, estimated via (2.34) and the original matrix $\mathbf{A}$ does not give back the identity matrix $\mathbf{I}$.

2.8 Analysis of parameter estimation results

The assessment of the diagonal values of the variance-covariance matrix, hence the variances associated to the parameter estimates $\hat{\theta}$, is essential to acquire preliminary information about the most critical parameters. Moreover, the same metrics allows also to understand whether a model is structurally weak or not. As highlighted by Emery (2001), to establish the statistical quality of the estimated parameters, two main aspects must be satisfied:

1. accuracy, that represents the proximity of the estimate to the true unknown real value;
2. precision, that is given by the definition of the smallest uncertainty region.

When the parameter estimation is performed, the objective is then to identify a set of parameters whose values are confined within a restricted confidence region, thank to the information gathered through the measurements.

2.8.1 The t-test

Any statistical test whose aim is to assess the validity of an hypothesis, and in which the test statistic follows a Student's t-distribution under the null hypothesis, is referred as a t-test. First, the concept of hypothesis verification must be introduced: it is an inferential procedure consisting on the formulation of a hypothesis regarding an unknown parameter of the population which then, on the basis of a random sample, involves the decision of whether the parameter is reliable or not. According to Neyman and Pearson (1933), the hypothesis system is composed by:

1. a null-hypothesis (H_0) that must be verified. It has been formulated before the collection of the sample and represents the actual knowledge about a phenomenon;
2. an alternative-hypothesis (H_1) that represents the new hypothesis formulated on the basis of a new knowledge or a new belief of the researchers.

The null-hypothesis is the one to be verified: it represents a conservative behaviour that allows to reject the previous knowledge only in presence of strong adverse evidences. Commonly, the t-test is applied when the test statistics can be normalized to a Student's t-distribution with a certain degree of freedom and it can be used, for instance, to determine if two datasets are significantly different from each other. However, dealing with parameter estimates, the aim is to assess the statistical quality of the parameters and, in order to do that, it is required to assess how large the confidence region of a parameter is, compared with its absolute value. In other words, the purpose is to analyse the value of each estimated parameter in respect to its confidence range. For this reason, it is usually preferred a one-tailed t-test with 95% of confidence, in which the alternative hypothesis is that the true value of a parameter lays in a range of approximately 2 standard deviations (SDVs) of a Student's t-distribution estimated from the available samples.
Assuming the experimental data are gathered through a campaign of N_{exp}, each characterized by N_{sp} measurements, and N_θ is the number of parameters to estimate, the reference distribution has $N_{exp} \times N_m - N_\theta$ degrees of freedom and mean of $\hat{\theta}_i$ for each parameter that requires estimation. In these terms, the t-test for a generic α level of confidence turns to be:

$$\frac{\hat{\theta}_i}{t\left(\frac{1-\alpha}{2} N_{exp} N_m - N_\theta\right) \cdot \sqrt{V_{\theta,ii}}} > t\left(\frac{1-\alpha}{2} N_{exp} N_m - N_\theta\right) \quad \forall i = 1,...,N_\theta \tag{2.35}$$

where the t-values in both left-hand side and right-hand side terms of (2.35) are usually evaluated from the reference Student's t-distribution at the cumulated probability of 0.975 and 0.950 respectively. Eventually, the parameter estimation is statistically satisfactory when (2.35) is satisfied and, moreover, the higher the t-value, the higher the estimates accuracy. Unfortunately, the t-test does not give information about the covariance of the system, hence the possible correlation between parameters: if high correlation is present, a multivariate normal analysis is a better choice and, for instance, a Hotelling t^2-test can be performed.

2.8.2 The χ^2-test

Since in the conventional parameter estimation problem the model is used to fit a set of data, a measure of the fitting quality is required. Thus, as for the t-test, the

χ^2-test is a statistical tool that exploits a χ^2-distribution to verify a null-hypothesis. It is widely adopted to verify if the differences between observed and attended events are statistically meaningful or just related to the random nature of a variable. Indeed, the model proposed might not be suitable for representing exactly the physical phenomenon and this can affect the experimental data fitting. Perhaps, the parameter estimates could be obtained with acceptable accuracy but if the fitting quality is poor, the model cannot be used to make accurate predictions. For this reason, the χ^2-test allows to understand if the residuals computed at the end of the parameter estimation are due to measurement errors or lack in the model descriptive capability.

Let us assume that the reference distribution has again $N_{exp} \times N_m - N_\theta$ degrees of freedom. Since the measurable variables have been assumed to be random and normally distributed, if the sum of the $N_{exp} \times N_m - N_\theta$ random variables is smaller than the reference value χ^2_{ref}, with a 95% of confidence the residuals are only due to measurements errors. At this purpose, the sample statistic is given by the sum of weighted residuals squared:

$$\chi^2 = \sum_{i=1}^{N_{exp}} \sum_{j=1}^{N_m} \left[\frac{\rho_{ij}(\hat{\theta})}{\sigma_{ij}} \right]^2 \tag{2.36}$$

When a model is capable of characterizing a phenomenon, and when the sample is sufficiently representative of the entire population, the estimates are expected to be very close to their true value as well as the predicted profiles for the variables involved. As a consequence, the residuals would be errors normally distributed such that $\chi^2 \leq \chi^2_{ref}$ or, in the opposite case, either the assumption of having normally distributed errors with a certain SDV is wrong or the model is not suitable to represent the data.

2.8.3 Ellipsoids of confidence

The variance-covariance matrix $\mathbf{V}_\theta$ defines an uncertainty region that is strongly related to the estimates precision. The graphical representation of this confidence interval is significantly helpful to understand whether the estimated parameters statistically satisfactory or not. The so called *ellipsoids of confidence* are 2D representations in the N_θ-dimensional parameters domain that enclose the region of

all the possible values the parameters can assume within a fixed level of confidence. In this sense, they allow to consider the intrinsic uncertainty on the estimates as a consequence of the data variability. Three distinctive features, given by the fact that these ellipsoids are obtained from the variance-covariance matrix, are acknowledged:

1. the ellipse major axis is determined by the highest value of variance - the direction of highest variability - while the minor axis by the lowest one;
2. when the co-variance terms are null, Cartesian and ellipse axes are parallel and it is possible to step change the value of a parameter without affecting the others (no correlation is present);
3. when the co-variance terms are not null, the ellipse is oblique and the inclination is positive or negative as a function of the correlation.

2.8.4 MBDoE criteria based on the ellipsoids of confidence

By improving the estimates quality through the enhancement of the information available, the size of the region of confidence is expected to shrink. Formally, the objective is to minimise some scalar measure ϕ of the variance-covariance matrix and, in order to do that, several real-valued functions can be suggested: each of them tries to represent a measure of *smallness* for the magnitude of the variance-covariance matrix. Thus, the most commonly used design criteria are the so defined "alphabetic criteria" by Kiefer (1959).

1. A-optimality: minimise the $\mathbf{V}_\theta$ trace and corresponds to minimising the sum of the variances for the individual parameter estimated or, in other words, the dimensions of the smallest polyhedron in the N_θ-dimensional hyperspace within which the confidence ellipsoid can be inscribed: $\phi_A(\mathbf{V}_\theta) = \frac{1}{N_\theta} \sum_{k=1}^{N_\theta} (\mathbf{V}_\theta)_{k,k}$;
2. D-optimality: minimise the $\mathbf{V}_\theta$ determinant and corresponds to minimising the volume of the confidence ellipsoid itself: $\phi_D(\mathbf{V}_\theta) = \det(\mathbf{V}_\theta)^{\frac{1}{N_\theta}}$;
3. E-optimality: minimise the largest eigenvalue of $\mathbf{V}_\theta$ hence the length of the confidence ellipsoid longest axis with the aim of rendering the confidence region as spherical as possible: $\phi_E(\mathbf{V}_\theta) = \lambda_{\max}(\mathbf{V}_\theta)$

The previous design criteria can be geometrically interpreted as shown in Figure

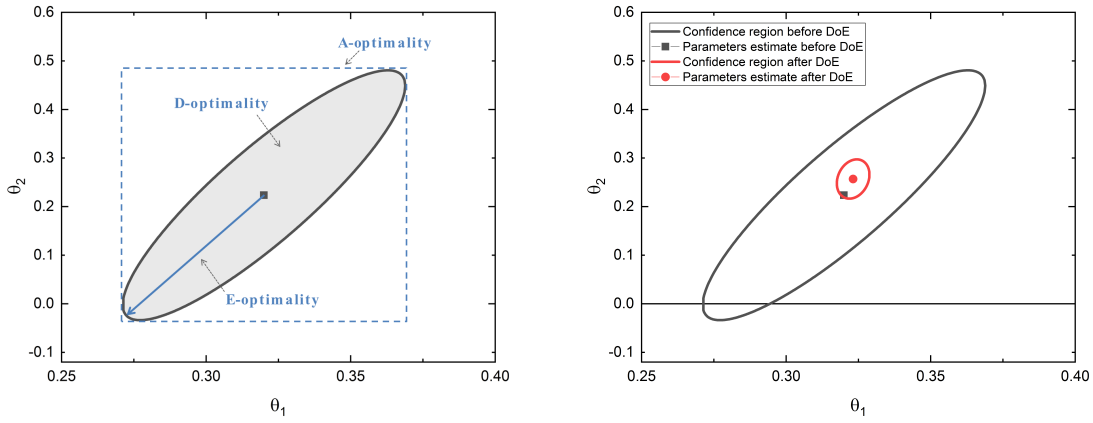

(a) *Geometrical representation of the design criteria.*

(b) *Shrinking of the confidence region thanks to DoE application.*

Figure 2.4: *Geometrical representations of the ellipsoids of confidence criteria and confidence region shrinking due to the application of DoE techniques.*

2.4a while in Figure 2.4b it is illustrated an example referring to the confidence region reduction for the estimation of a couple of parameters, before and after the application of MBDoE techniques. It is interesting that, even in the case the parameter values do not change, the reduction of the ellipsoid size makes the parameter more reliable.

2.9 Parameters correlation metrics

The importance of the correlation metrics is related to the need of verifying the existence of structural identifiability issues that prevent from obtaining reliable predictions from the model. To the purpose of illustrating the correlation effect in a comprehensive manner, let us consider the following model:

$$y = (\theta_1 - \theta_2)u \tag{2.37}$$

Assuming that y and u are measurable without uncertainty, two experiments are performed to collect the following (u,y) data points: (1,1) and (2,2). Using the least squares method introduced in a previous section, the parameter estimation problem

reduces to the solution of the following system:

$$\begin{cases} \dfrac{\partial S}{\partial \theta_1} = 0 = \theta_1 - \theta_2 - 1 \\ \dfrac{\partial S}{\partial \theta_2} = 0 = \theta_2 - \theta_1 - 1 \end{cases} \tag{2.38}$$

Unfortunately, it represents an undetermined system that admits infinite solutions. The consequence of this intrinsic weakness of the model, related to the structure of (2.37), is that the parameters cannot be identified separately. Specifically, given a value for $(\theta_1 - \theta_2)$ there are infinite combination of θ_1 and θ_2 that satisfy (2.37).
While for a simple model a careful analyst can easily detect the correlation problem, in chemical kinetic models the structure of the equations and the number of parameters involved, make the analysis not straightforward. For this reason, to assess the presence of critical correlations between non-measurable parameters, a comprehensive metric must be used. There are different ways in which the correlation matrix can be calculated, the following techniques are considered in this Thesis:

1. the estimability matrix $\mathbf{P}_E$ built on the sensitivities;

2. the Fisher information matrix.

It is also important to acknowledge that the correlation matrix depends on the experimental conditions considered. It could happen that in some regions of the experimental design space couples of parameters show a certain correlation while, in other regions, this correlation is different.

2.10 gPROMS *ModelBuilder*®

gPROMS *ModelBuiler*® 5.0.2 is an advanced process modeling environment developed by Process System Enterprise (PSE), that has been used to accomplish most of the analyses presented in this Thesis. It allows to build, validate and execute custom process models of virtually any level of complexity. It includes also a powerful optimisation environment that allows to determine the optimal solution in a more direct way rather than the standard trial-and-error procedure. Moreover, its computational framework lets the user to deal with advanced nonlinear dynamic

model simulations and leads to the possibility of validating the models against experimental data, using built-in advanced parameter estimation techniques.
For the solution of nonlinear algebraic sets of equations there are two standard mathematical solvers named BDNLSOL and SPARSE. They are especially designed to deal with models characterized by large and sparse systems of equations in which the variable values must stay within specified lower and upper bounds. Thus, simulation, optimisation and parameter estimation activities make use of these solvers especially because they can handle situations in which some of the partial derivatives of the equations, with respect to the variables, are available analytically while the rest have to be approximated.
To solve the differential-algebraic systems instead, gPROMS implements other two advanced solvers named DASOLV and SRADAU. These are standard mathematical solvers for the solution of mixed sets of differential and algebraic equations, that are designed to work with large and sparse systems characterized by bounded variable values. Moreover, they are capable of dealing with situations in which some of the partial derivatives of the equations with respect to the variables are analytically available while the rest have to be numerically approximated. Finally, their peculiarity is that they automatically adjust each time step in a way the error incurred in a particular variable, over a single time step, must not exceed a certain limit that is function of the absolute tolerance, relative tolerance, and variable absolute value.
Eventually, for the optimisation purposes, there is one standard solver based on a control vector parametrization (CVP) approach that assumes, over a specified number of control intervals, that the time-varying control variables are piecewise-constant or piecewise-linear. It is applicable to large problems: the number of control variables is usually a small fraction of the total and then the algorithm has to deal only with a relatively small number of decisions. The name of this solver is is CVP_SS.
The characteristics of the five solvers aforementioned are briefly resumed below:

1. BDNLSOL is the acronyms of Block Decomposition Non-linear SOLver. It is a modular solver based on a novel algorithm which is particularly suitable when the model involve "if" conditions that, mathematically, represent sym-

metric discontinuities. The reduction of the nonlinear equation sets to a block triangular form, permit the use of any other nonlinear solver to compute the individual blocks;

2. SPARSE solver is designed to solve nonlinear algebraic systems using a sophisticated implementation of a Newton-type method. It is a true solver component that does not use the block decomposition;

3. DASOLV is a solver that has been proved to be efficient in several situations and it is based on the variable time step method called Backward Differentiation Formulae (BDF). Notice that for highly oscillatory problems, with frequent discontinuities, it suffers from loss of stability;

4. SRADAU solver is particularly useful when the models involve transport phenomena or frequent discontinuities. Based on a variable time step fully-implicit Runge-Kutta method, it is suitable to solve problems arising from the discretisation of partial differential algebraic equations (PDAEs). Contrarily to DASOLV, it can address highly oscillatory ODE systems;

5. CVP_SS is used to solve steady-state and dynamic optimisation problems involving both discrete and continuous variables. It implements a "single-shooting" dynamic optimisation algorithm based on a single integration of the dynamic model over the entire time horizon.

Among these five, SPARSE, DASOLVE and CVP_SS have been largely used for the analyses performed in this study. Other features of the software, including the tools for model validation, have been largely exploited too.

CHAPTER 3

KINETIC MODELS OF HMF HYDROGENATION AND PROCESS DESCRIPTION

SINCE HMF hydrogenation can be considered as a relatively new process - one of the first studies has been published by Thananatthanachon and Rauchfuss (2010) - a well established route to obtain the DMF has not been defined yet. The purpose of this Chapter is to introduce the HMF hydrogenation process and to discuss the different conditions that can be used to perform the reaction. Furthermore, the kinetic models derived by some authors are reported and compared in terms of assumptions, equations involved and overall complexity. State variables and non-measurable model parameters are listed as well. The last part of the Chapter is finally dedicated to the discussion of practical and theoretical uncertainties and limitations related to the structures of the kinetic models presented.

3.1 Overview of the HMF hydrogenation process

The reaction pathway, consisting in the sequence of reactions that characterize the HMF hydrogenation process, varies as a function of the catalyst employed. In most of the cases, the reaction shows two-steps in which HMF is converted first to bis-hydroxymethyl furan (BHMF) and then it is further hydrogenated to the highly reactive 5-methyl furfuryl alcohol (MFA). This intermediate rapidly undergoes hydrogenolysis to finally give DMF and small amounts of 2,5-dimethyltetrahydro furan (DMTHF) as main by-product. The formation of DMF is always presented as the rate determining step. Some of the most important reaction pathways, identified using several catalysts, are reported in Figure 3.1.

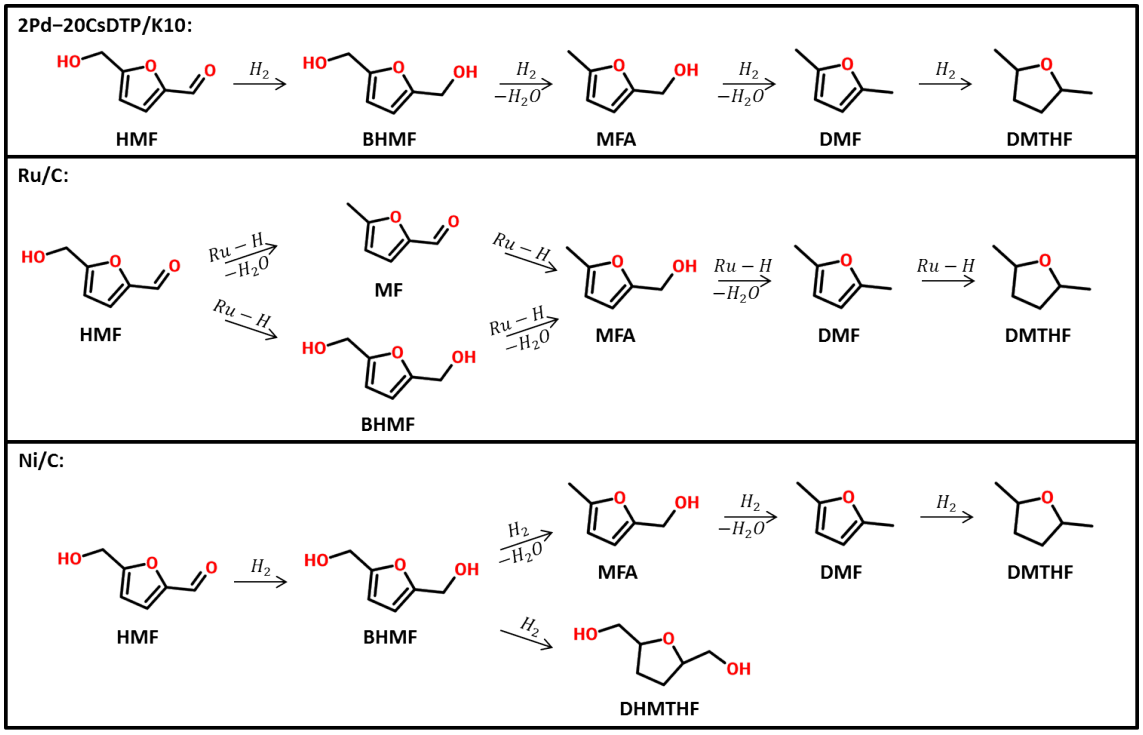

Figure 3.1: *Comparison of reaction pathways for some of the most important catalysts reported in literature.*

From the industrial point of view, the reaction is usually carried out in stainless steel reactors – the conventional equipment to obtain time course data (Nauman (2008)) – which volume goes from 50 mL to 300 mL. The conditions, such as temperature, pressure and reactants initial concentrations, may change significantly according to the products of interest. In Table 3.1 it is possible to find the nominal conditions at which the most important catalysts currently investigated have found to give the best outcome.

3.1.1 Solvent influence

Apart from the liquid phase, consisting in HMF, products, by-products and intermediates, the other two phases of the reactive system – the ensemble of all the species and phases which characterise a chemical transformation – are solid catalyst and gaseous hydrogen. Thus, as a three-phase system, the solvent choice is very important as well as very complex: it must account for many different factors that affect rate of reaction and selectivity of the products. In particular, the HMF hydrogenation can be carried out using both alcoholic or non-alcoholic solvents: water,

Table 3.1: *Comparison of conditions and reaction parameters for the most important catalysts reported in literature. Table proposed by Gawade et al. (2016).*

Catalyst	Hydrogen source	Solvent	T [°C]	t [h]	Conversion [%]	Yield [%]
CuRu/C	H_2	*n*-butanol	220	10	100	61
Ru/C	H_2	THF	200	2	100	95
PtCo@HCS	H_2	*n*-butanol	180	2	100	98
PdAu/C + HCl	H_2	THF	60	6	100	96
Ru/Co_3O_4	H_2	THF	130	24	100	93
Ru-NaY	H_2	THF	220	1	100	78
$Pd/C/H_2SO_4$	HCOOH	THF	70	15	100	95
Ni/Co_3O_4	H_2	THF	130	24	99	76
Pd/Zn/C	H_2	THF	150	6	99	85
NiSi-PS	H_2	1,4-dioxane	130	3	100	72.9
Ru-HT	H_2	2-propanol	220	4	100	58
2Pd-20CsDTP/K-10	H_2	THF	90	2	98	81

tetrahydrofuran (THF), 2-methyl tetrahydrofuran (2-MTHF), *n*-butanol, 1-butanol, 2-propanol, secondary phenyl alcohols and 1,4-dioxane are among the most employed. However, not all of them are suitable to be used with every catalyst: Nickel, for instance, is capable of hydrogenating alcohols and this makes its pairing with alcoholic solvents incompatible. Moreover, even though the HMF conversion is total with a certain solvent, the selectivity may be extremely low. To explain this dependency, different theories have been proposed and the main contributions are thought to be three:

1. Hildebrand solubility parameter, or δ-value, that is a measure of the cohesive energy density and provides an estimation of the interaction between different materials. Particularly suitable for nonpolar substances, such as many polymers, it is a good indication of solubility: components with similar δ-values are likely to be miscible.
2. Dielectric constant, or relative static permittivity, that represents a measure of the chemical polarity of a solvent.
3. Solvation effect, that describes the interaction between the molecules of a dissolved material in a solvent and represents the reorganization of solvent and solute molecules into solvation complexes involving bond formation, hydrogen

bounding and Van der Waals forces.

The cohesive energy density from which the δ-value is based, represents the amount of energy needed to remove completely unit volume of molecules from their neighbours to infinite separation. It has been discovered by Burke (1984) to be an indication of the solvency power because, in order to dissolve, the molecules of a material must be separated from each other and surrounded by solvent. For the same reason, the substances with similar solubility parameters can easily interact with each other and give solvatation, miscibility or swelling phenomena. Regarding the HMF hydrogenation process, on the one hand it has been found by Chatterjee et al. (2014) as increasing the δ-value, the HMF rate of conversion oppositely decreases because of the competitive adsorption of its molecules on the metal surface of the catalyst. Indeed, the solvents with very low δ-value show weak interactions with metal catalysts while for the solvents characterized by a greater δ-value the interactions are much stronger. On the other hand, Toukoniitty et al. (2003) correlated through a proportional dependency the solubility of hydrogen with the dielectric constant value. Although the difference between the dielectric constants of two solvents could be in principle used to determine their miscibility, other phenomena must be considered: water and THF are indeed miscible even though their dielectric constants are remarkably different (respectively 80.10 at 20°C and 7.52 at 22°C) because the oxygen atom of THF can act as hydrogen bond acceptor. Thus, the hydrogen solubility in the solvent used to carry on the reaction, is significative higher in organic solvents rather than in water. Furthermore, Augustine and Techasauvapak (1994) studied that the adsorption of components on the catalyst surface is easier when these components are affine. Thus, in a polar medium the polar compounds remain more strongly solvated and the same happens also for non-polar medium with non-polar compounds. That is why, using polar solvents, the reaction intermediates are found to be more disperse and toughly find access to the catalyst metal surface. Considering all these effects and characteristics briefly resumed in Table 3.2, Gawade et al. (2016) gave a comparison on the basis of yield and selectivity measurements:

1. water usually shows a high rate of conversion for the poor interactions with the metal catalyst surface, but a very low selectivity of DMF cause the poor

hydrogen solubility;

2. 1,4-dioxane leads to a very low conversion due to the δ-value – even though the solvatation effect partially helps to increase the interaction between BHMF and catalyst – and also a low selectivity due to the high solubility of hydrogen that leads to further hydrogenation of DMF in to DMTHF;

3. *n*-butanol and 1-butanol give a good conversion but a low selectivity because of the polar nature of BHMF that tends to solubilize in the solvents and does not undergo further hydrogenations;

4. THF and 2-MTHF are the best trade-off between the different effects: although they do not ensure the highest conversion in a short time window, they lead to the highest selectivity. Moreover, THF gives better results thanks to the lower water miscibility as water forms during the reaction and acts as a product inhibitor.

Table 3.2: *Summary of properties for some of the most commonly used solvents in the HMF hydrogenation process. All values were obtained at 20°C unless specified otherwise.*

Solvent	**δ-value [MPa$^{\frac{1}{2}}$]**	**Dielectic constant**	**Polarity**
Water	47.8	78.5	Polar
n-butanol	28.7	17.7	Polar
1-butanol	23.1	17.8	Polar
2-propanol	23.5	18.3 @25°C	Polar
THF	19.4	7.52	Non-polar
2-MTHF	18.2	7.00 @25°C	Non-polar
1,4-dioxane	20.5	2.21 @25°C	Non-polar

3.1.2 Mass transfer assumptions

Since the reaction system is three-phase, the problem of mass transfer relays on the choice of the stirring speed which ensure an optimum agitation such that any

external mass transfer resistance can be overcome. There are three critical regions where mass transfer limitations can arise: at the liquid-solid interface, at the gas-liquid interface and inside the catalyst pores. Through the use of an efficient stirrer, once a sufficient agitation is provided, it is possible to exclude any inerfacial mass-transfer resistance. At this point, no significant differences in HMF conversion or DMF selectivity are expected if the impeller speed is increased even more. On the other hand, Salmi et al. (2004) specified that to avoid the internal mass transfer resistance occurring inside the catalyst pores, particles with a size smaller than 50μm should be used. To verify this resistance, the Wagner-Weisz-Wheeler criterion in (3.1) can be used:

$$\phi^2\eta = \frac{l^2}{D_{\text{eff}} \cdot C_{\text{i}}} \cdot \omega r_{\text{eff}} \tag{3.1}$$

where ϕ is the Thiele Modulus, η is effectiveness factor, l is characteristic size of the particle (m), D_{eff} is effective diffusivity (m^2/s), r_{eff} is effective reaction rate (kmol/(kg s)), ω is the catalyst loading (kg/m^3) and C_i is concentration of i-th species (M). The value of C_{H_2} can be estimated using a correlation suggested by Pintar et al. (1998):

$$C_{\text{H}_2} = y_i P_{tot} \frac{x_g}{1 - x_g} \frac{\rho_{\text{H}_2\text{O}}}{M_{\text{H}_2\text{O}}} \tag{3.2}$$

where the dimensionless mole fraction solubility x_g is given by an empirical relation defined by Puhl (1991). Furthermore, Crezee et al. (2003) and Negahdar et al. (2014) found that no internal diffusion limitations are present when the value $\phi^2\eta$ of the criterion is in the order of magnitude of 10^{-3}-10^{-2}. These values are valid considering small catalyst particles (smaller than 50μm) if biomass based feed-stock and hydrogen are used as reactants. In such case, the investigated reaction system is under kinetically controlled conditions. Eventually, altough some authors (Gyngazova et al. (2017)) used the rigorous Wagner-Weisz-Wheeler criterion to assess the mass-transfer, in other cases (Gawade et al. (2016)) the appropriate impeller speed was chosen through trial-and-error procedure increasing the rotations-per-minute (rpm) until no significant improvements on the reaction parameters were registered.

3.1.3 Hydrogen partial pressure and temperature influence

As a series of hydrogenation reactions, the hydrogen pressure effect is expected to be greatly relevant for the conversion of HMF into the various intermediates, product and side products. In practise, the rate of hydrogenation of HMF increases when the pressure increases as well because the concentration of dissolved hydrogen in the reaction mixture becomes higher. In general, in the paper reviewed, the authors prefer to operate with a concentration at least three times higher for the hydrogen rather than for the HMF, in order to assume the hydrogen amount as constant during the whole reaction. Besides the models simplification, this ensures also a better pressure control. However, the enhancement due to the pressure increment tends to invert when it is increased above a certain level because it means reaching a superabundant amount of hydrogen which promotes the formation of overhydrogenated products. Thus, the opening and hydrogenation of the furan ring lead to a sharp decrease in DMF yield (Hu et al. (2014)). Furthermore, not only an excessive increase in the pressure determines an increment in the equipment and production cost but also increases the operational risk.

Almost the same considerations hold for the temperature. However, in this case the effect is mostly related to reaction kinetics. Since the reactions are supposed to be kinetically controlled – hence there is no influence of any mass transfer resistance on the reaction rates –, increasing the temperature makes the rate of hydrogenation higher. Obviously, for each different catalyst, different optimal temperatures have been identified according to the activity of the catalyst it-self. Moreover, being a sub-sequential ring of hydrogenations, there will always be a certain temperature above which the DMF selectivity will drop substantially. About that, each author reports the optimal hydrogen pressure and optimal temperature to maximize yield and selectivity, according to the specified reaction conditions.

3.1.4 Catalyst loading influence

The determination of the optimal catalyst loading is done on the basis of yield and selectivity measurements and often depends on the nature of the catalyst it-self because of the nature of its active sites. It represents usually a parameters which tends to be optimized through trial-and-error procedures which assess conversion and selectivity at different concentrations: the catalyst loading which corresponds to the best trade-off between these two is chosen. In any case, by increasing the catalyst amount a significant enhancement of both conversion and selectivity is expected due to the proportional increase in the number of active sites. The overall effect can be indeed assessed in terms of turn over frequency (TOF) so that the higher the amount of catalyst, the higher the number of reactants molecules that can be adsorbed and converted on the catalyst surface per unit time. However, up to a certain optimal quantity, the result of further increments can be undesired as well as unpredictable. For instance, Gyngazova et al. (2017) found that an excess of acid centres lead to an intensive polymerization which cause the product yield to drop critically. In general, when the number of active sites becomes too large, the DMF selectivity tends to drop because of the further hydrogenations which convert the product of interest into over-hydrogenated species.

3.1.5 Initial concentration influence

The effect of changing the initial HMF concentration or other species is strongly correlated to the other variables. In particular, when HMF concentration increase, the products rate of formation decreases because the ratio between substrate to catalyst decreases as well. Moreover, it has been previously underlined that the hydrogen must be in excess and an increase in the HMF concentration could lead to an unbalance between the two reactants along with detrimental effects for the DMF selectivity. For this reason, the initial concentrations are considered as bounded variables, which can be varied within a certain range. The rationale is that changing the initial concentration is possible to modify the reaction profiles hence the results of the identifiability and discrimination analysis. Eventually, initial concentration of the species (not only reactants) as well as the hydrogen partial pressure

will be used as optimisation variables for the model discrimination purposes.

3.2 Kinetic models of HMF hydrogenation state of the art

In this section, all the most significant kinetic models currently available in literature for the HMF hydrogenation process are reported. A brief introduction anticipate the system of constitutive equations that characterize each of them. The variety of alternatives, characterized by different strengths and complexities, underlines the usefulness of MBDoE and identifiability techniques. Moreover, Table 3.3 gives a first idea about the main characteristics of each model in terms of typology and number of parameters involved.

Table 3.3: *Summary of the main characteristics of the proposed kinetic models.*

Paper	**Model type**	$\mathbf{N}_\theta$	N_m
Gawade et al. (2016)	Dual-site LHHWs	9	6
Gyngazova et al. (2017)	Power law	5	5
Jain and Vaidya (2016)	Different LHHWs variants	3	2
Luo et al. (2015)	First-Order Power law	3	3
Grilc et al. (2014)	Power law	4	6

3.2.1 Gawade et al. (2016) kinetic model (M1)

This model has built by considering the non-competitive and dissociative hydrogen adsorption on the catalyst surface: a novel bifunctional metal-acid palladium-cesium dodeca-tungsto-phosphoric acid supported on K-10 acidic clay (2Pd-20CsDTP/K-10). This catalyst is said by the authors to be stable, active and selective with a good reusability over many operational cycles. Moreover, its bifunctionality causes hydrogen to interact with metallic sites while the other chemical species react with the acidic ones. The dual-site Langmuir-Hinshelwood-Hougen-Watson (LHHW) theory has been used to describe the adsorption and desorption mechanisms. The set-up used to collect the data was a 100 mL autoclave reactor in which the agitation was

provided by a pitched turbine impeller. The experiments were performed in 20 mL of THF with an impeller speed of 1000 rpm, velocity that is said to guarantee the overcoming of any mass transfer limitation. The rate determining step is assumed to be the conversion of BHMF, since the transformation of MFA to DMF – as well as their adsorption/desorption mechanisms – is neglected because really fast. The measurements of the reaction mixture was performed with a gas-chromatograph mass-spectrometer (GC-MS, *PerkinElmer Clarus 500*) equipped with a Flame Ionization Detector (FID). Finally, the reaction equations are shown in the following.
Rate of consumption of HMF (A):

$$-\frac{dC_{\mathrm{A}}}{dt} = \frac{k_1 K_{\mathrm{A}} C_{\mathrm{A}} \sqrt{K_{\mathrm{H_2}} p_{\mathrm{H_2}}} w}{[1 + K_{\mathrm{A}} C_{\mathrm{A}} + K_{\mathrm{B}} C_{\mathrm{B}} + K_{\mathrm{D}} C_{\mathrm{D}} + K_{\mathrm{E}} C_{\mathrm{E}}][1 + \sqrt{K_{\mathrm{H_2}} p_{\mathrm{H_2}}} + K_{\mathrm{W}} C_{\mathrm{W}}]} \tag{3.3}$$

Rate of consumption of BHMF (B):

$$\frac{dC_{\mathrm{B}}}{dt} = \frac{[k_1 K_{\mathrm{A}} C_{\mathrm{A}} - k_2 K_{\mathrm{B}} C_{\mathrm{B}}] \sqrt{K_{\mathrm{H_2}} p_{\mathrm{H_2}}} w}{[1 + K_{\mathrm{A}} C_{\mathrm{A}} + K_{\mathrm{B}} C_{\mathrm{B}} + K_{\mathrm{D}} C_{\mathrm{D}} + K_{\mathrm{E}} C_{\mathrm{E}}][1 + \sqrt{K_{\mathrm{H_2}} p_{\mathrm{H_2}}} + K_{\mathrm{W}} C_{\mathrm{W}}]} \tag{3.4}$$

Rate of production of 2,5DMF (D):

$$\frac{dC_{\mathrm{D}}}{dt} = \frac{[k_2 K_{\mathrm{B}} C_{\mathrm{B}} - k_3 K_{\mathrm{D}} C_{\mathrm{D}}] \sqrt{K_{\mathrm{H_2}} p_{\mathrm{H_2}}} w}{[1 + K_{\mathrm{A}} C_{\mathrm{A}} + K_{\mathrm{B}} C_{\mathrm{B}} + K_{\mathrm{D}} C_{\mathrm{D}} + K_{\mathrm{E}} C_{\mathrm{E}}][1 + \sqrt{K_{\mathrm{H_2}} p_{\mathrm{H_2}}} + K_{\mathrm{W}} C_{\mathrm{W}}]} \tag{3.5}$$

Rate of formation of DMTHF (E):

$$\frac{dC_{\mathrm{E}}}{dt} = \frac{k_3 K_{\mathrm{D}} C_{\mathrm{D}} \sqrt{K_{\mathrm{H_2}} p_{\mathrm{H_2}}} w}{[1 + K_{\mathrm{A}} C_{\mathrm{A}} + K_{\mathrm{B}} C_{\mathrm{B}} + K_{\mathrm{D}} C_{\mathrm{D}} + K_{\mathrm{E}} C_{\mathrm{E}}][1 + \sqrt{K_{\mathrm{H_2}} p_{\mathrm{H_2}}} + K_{\mathrm{W}} C_{\mathrm{W}}]} \tag{3.6}$$

Through the equations above, four set of parameters have been estimated by the authors for temperatures between 80 °C and 110 °C. Three levels of pressure have also been tested to investigate the effect of this variable on the system response. Notice eventually that parameter estimation statistics are not specified.

3.2.2 Gyngazova et al. (2017) kinetic model (M2)

Following the seminal work of Kong et al. (2014), Huang et al. (2014) and Yang et al. (2015), these authors studied the transformation of HMF to DMF over a carbon supported nickel catalyst (Ni/C) with the purpose of elucidating the reaction network and characterizing the key reaction intermediates. Thus, several Ni/C catalysts, containing different amounts of metal loading, were prepared by incipient-wetness impregnation. The experiments were then carried out in a 50 mL stainless

steel batch autoclave equipped with a sampling valve and a magnetic stirrer. The autoclave was loaded with the reactants, catalyst and 30 mL of THF: while different initial concentrations of HMF and catalyst loading were investigated, the hydrogen pressure was kept constant at 100 bar. For the collection of samples, the liquid was filtered through a 45 μm PTFE filter and then analysed off-line using a gas-chromatograph equipped with a FID detector and high polarity bonded wax column. Finally, to study the effect of mass transfer limitations, the Wagner criterion (3.1) was used. Since the catalyst particles were small enough, all experiments have been performed under the assumption of intrinsic kinetically controlled regime free of mass transfer limitations. The chosen impeller speed was 900 rpm.
Through the set-up discussed above, the authors derived a simple system of ordinary differential equations where the non-measurable parameters are the apparent kinetic constants of each reaction.

$$-\frac{d[\text{HMF}]}{dt} = k_{1,app} \cdot [\text{HMF}] \tag{3.7}$$

$$\frac{d[\text{BHMF}]}{dt} = k_{1,app} \cdot [\text{HMF}] - k_{2,app} \cdot [\text{BHMF}] - k_{5,app} \cdot [\text{BHMF}] \tag{3.8}$$

$$\frac{d[\text{MFA}]}{dt} = k_{2,app} \cdot [\text{BHMF}] - k_{3,app} \cdot [\text{MFA}] \tag{3.9}$$

$$\frac{d[\text{DMF}]}{dt} = k_{3,app} \cdot [\text{MFA}] - k_{4,app} \cdot [\text{DMF}] \tag{3.10}$$

$$\frac{d[\text{DMTHF}]}{dt} = k_{4,app} \cdot [\text{DMF}] \tag{3.11}$$

$$\frac{d[\text{DHMTHF}]}{dt} = k_{5,app} \cdot [\text{BHMF}] \tag{3.12}$$

The set of ordinary differential equations has been solved numerically by the authors and the parameters were estimated by least-squares fit of experimental data, using the Levenberg-Marquardt algorithm (Marquardt (1963)). The proposed estimates are told to describe the behaviour of the reactive system in a satisfactory way, although some slight deviations on the concentration profiles are present.

3.2.3 Jain and Vaidya (2016) kinetic model (M3)

The development of this kinetic model follows previous studies that were carried out on the kinetics of hydrogenation of biomass-derived compounds in aqueous solution over Ru/C catalyst (Bindwal and Vaidya (2013), Bindwal and Vaidya (2014)). The

kinetic data obtained in a wider range of temperatures, H_2 partial pressure, initial HMF concentration and catalyst loading, allowed to fit to a kinetic model the initial rates of HMF disappearance whose main assumptions are:

1. the surface reaction between non-dissociatively chemisorbed H_2 and HMF represents the rate determining step;
2. the reaction conditions are favourable for studying reaction kinetics.

While the Weisz criterion has been used to verify the intraparticle diffusion, the resistance to mass transfer of H_2 on the gas-side has been ignored due to its high diffusivity in the gas phase and low solubility in the liquid. The resistance of liquid-phase and liquid-solid mass transfer resistances was instead deemed negligible considering the stirring speed of 1200 rpm. Regarding the experimental set-up, the experiments were performed in a 100 mL high pressure reactor equipped with a four 45° pitched-blades turbine agitator (Bindwal and Vaidya (2013)), charged with 50 mL of aqueous solution and a fixed amount of fresh catalyst. N_2 was used to purge the gas after each cycle and ensure an inert atmosphere while the liquid samples were analysed by high pressure liquid chromatography (HPLC) supported by mass-spectrometry. Four different mechanisms have been proposed to contemplate as many model variants:

i. competitive adsorption of dissociatively chemisorbed hydrogen (M3.1);
ii. competitive adsorption of molecular chemisorbed hydrogen (M3.2);
iii. non-competitive adsorption of dissociatively chemisorbed hydrogen (M3.3)
iv. non-competitive adsorption of molecular chemisorbed hydrogen (M3.4)

The rates of reaction that can be used to derive the differential balances of each species are:

$$r^{\mathrm{i}} = \frac{k_1 K_{\mathrm{H_2}} K_{\mathrm{HMF}} C_{\mathrm{H_2}} C_{\mathrm{HMF}}}{(1 + K_{\mathrm{H_2}} C_{\mathrm{H_2}} + K_{\mathrm{HMF}} C_{\mathrm{HMF}})^2} \tag{3.13}$$

$$r^{\mathrm{ii}} = \frac{k_1 K_{\mathrm{H_2}} K_{\mathrm{HMF}} C_{\mathrm{H_2}} C_{\mathrm{HMF}}}{(1 + \sqrt{K_{\mathrm{H_2}} C_{\mathrm{H_2}}} + K_{\mathrm{HMF}} C_{\mathrm{HMF}})^3} \tag{3.14}$$

$$r^{\mathrm{iii}} = \frac{k_1 K_{\mathrm{H_2}} K_{\mathrm{HMF}} C_{\mathrm{H_2}} C_{\mathrm{HMF}}}{(1 + \sqrt{K_{\mathrm{H_2}} C_{\mathrm{H_2}}})^2 (1 + K_{\mathrm{HMF}} C_{\mathrm{HMF}})} \tag{3.15}$$

$$r^{\mathrm{iv}} = \frac{k_1 K_{\mathrm{H_2}} K_{\mathrm{HMF}} C_{\mathrm{H_2}} C_{\mathrm{HMF}}}{(1 + \sqrt{K_{\mathrm{H_2}} C_{\mathrm{H_2}}})(1 + K_{\mathrm{HMF}} C_{\mathrm{HMF}})} \tag{3.16}$$

Notice finally that the authors declare the last two alternatives did not provide a good fit of the data and they were hence rejected.

3.2.4 Luo et al. (2015) kinetic model (M4)

The objective of the study proposed by Luo et al. (2015) was to compare the three-phase hydrogenation of HMF and DMF over six different carbon-supported metal catalysts: Pt, Pd, Ir, Ru, Ni, Co. These catalysts are said by the authors to have stabilitites that follow the order Pt(most active)~Ir>Pd>Ni>Co>Ru(less active) and allow to speculate the possible deactivation mechanism: the deposition of humins (a class of organic compounds insoluble in water for all pH conditions) on the catalyst surface. Although other authors (Hu et al. (2014)) reported high yields to DMF using Ru/C catalysts in THF, in this study yields as high as 60% were obtained on a Pt/C catalyst and a tubular flow reactor with 1-propanol solvent under similar conditions of temperature and pressure. The tubular reactor was a 20-cm long, stainless-steel tube with an internal diameter of 4.6 mm. Furthermore, the liquid feed containing HMF and 100 mL of solvent was introduced into the reactor by an HPLC pump which could also vary the total pressure into the reactor. The reaction outlets were collected at room temperature and immediately injected into a gas-chromatograph mass-spectrometer equipped with an Innowax capillary column, for analysis where both liquid and gas phase products were examined.

The kinetic model arise from an attempt to quantify the differences between the metal catalysts. The HMF reaction was modeled as a series of first-order, sequential reactions. As usual, no mass transfer limitations are considered and the rate determining step is the conversion of HMF to BHMF. The system of 4 ordinary differential equations derived from these assumptions was:

$$-\frac{d[\text{HMF}]}{dt} = k_1 \cdot [\text{HMF}] \tag{3.17}$$

$$\frac{d[\text{BHMF}]}{dt} = k_1 \cdot [\text{HMF}] - k_2 \cdot [\text{BHMF}] \tag{3.18}$$

$$\frac{d[\text{DMF}]}{dt} = k_2 \cdot [\text{BHMF}] - k_3 \cdot [\text{DMF}] \tag{3.19}$$

$$\frac{d[\text{DMTHF}]}{dt} = k_3 \cdot [\text{DMF}] \tag{3.20}$$

Notice that this model is practically equal to M2, with a less complete reaction

pathway.

3.2.5 Grilc et al. (2014) kinetic model (M5)

The study proposed want to address the catalytic hydrocracking and hydrodeoxygenation (HDO) for four $NiMo/Al_2O_3$ bifunctional catalysts in oxide, reduced and sulphide form, and Pd/C. The conversion of the liquefied biomass was performed in a 300 mL cylindrical stainless steel reactor equipped with a magnetic turbine impeller located on the reactor bottom. Both gas and liquid phase products were analysed online by Fourier transform infrared (FTIR) spectroscopy. To propose a different approach on the kinetic modeling of the HMF hydrogenation process, instead of using the chemical species species concentration, the authors lumped together the contributions of similar chemical groups with analogous reactivity. In that way, the apparent rate for deoxygenation and dehydrogenation reactions was set to be dependent on the concentration of the main oxygenated functional groups. Furthermore, the external mass transfer resistance was told to have been eliminated by intensive stirring and high hydrogen pressure while internal mass transfer limitations have been implicitly incorporated in kinetic rate constant. The model is then represented by a set of ordinary differential equations for the mass balance for aldehyde, alcohol, ester groups and some specific molecules. Also in this case, the rate constants are considered as temperature dependent through the Arrhenius equation.

$$r_n = k_n y_i : \qquad y_i = \frac{C_i}{C_{\mathrm{OH}}}(t=0) \tag{3.21}$$

$$\frac{dy_{\mathrm{C=O},tot}}{dt} = k_2 y_{\mathrm{OH}} - k_3 y_{\mathrm{CHO}} - k_4 y_{\mathrm{CHO}} \tag{3.22}$$

$$\frac{dy_{\mathrm{CHO}}}{dt} = k_2 y_{\mathrm{OH}} - k_3 y_{\mathrm{CHO}} - k_4 y_{\mathrm{CHO}} \tag{3.23}$$

$$\frac{dy_{\mathrm{CO}}}{dt} = k_3 y_{\mathrm{CHO}} \tag{3.24}$$

$$\frac{dy_{\mathrm{CO_2}}}{dt} = k_4 y_{\mathrm{CHO}} \tag{3.25}$$

$$\frac{dy_{\mathrm{H_2O}}}{dt} = k_1 y_{\mathrm{OH}} \tag{3.26}$$

$$\frac{dy_{\mathrm{C=O},ester}}{dt} = 0 \tag{3.27}$$

$$y_{\mathrm{C=O},tot} = y_{\mathrm{CHO}} + y_{\mathrm{C=O},ester} \tag{3.28}$$

For the study conduced in this Thesis, the really specific equipment required makes the use of M5 too time and resource expensive. Even though the identifiability study would give a positive result, it would not be possible to validate the model with new data coming from lab experiments. Although it represents an interesting alternative to the more simple-structure versions proposed by other authors, it will not be further investigated in this context.

3.3 Kinetic models selection and summary of their features

Among the 5 kinetic models listed in the previous sections, some of them appear more suitable to be used for the analysis that have to be performed throughout this Thesis, rather then others. In particular, each model is compared with the others in terms of experimental conditions, parameters and state variables involved, to give an idea about the overall complexity which depends by:

1. number of parameters to be estimated;
2. number and type of state variables to be measured;
3. ease of validation, which is the ease of replicating the reaction framework.

As already specified, although M5 represents an interesting alternative to the other kinetic models, its validation could result very complex because of the equipment required. For this reason, only the first four kinetic models M1-M4 have been further investigated. Below, table 3.4 presents a summary of their most important features: it gives an idea about the range of applicability for each alternative proposed. Regardless to the catalyst or solvent used, there are indeed remarkable differences between the conditions which have been used to develop the different models. The explored values for the hydrogen pressure, for instance, goes from 5 atm for M1 up to 140 atm for M4. It could be interesting to study, once the identifiability has been verified, if the kinetic models are flexible enough to be validated through in silico data generated by other models. The purpose would be to understand if the wide differences in the experimental conditions used affect only the catalyst activity or the whole model behaviour.

Table 3.4: *Comparison of the most suitable models to be used for the study performed in this Thesis.*

	Temperature [K]	**P_{H_2} [atm]**	**C^0_{HMF} [M]**	**Catalyst**
M1	353 - 383	5 - 15	0.05 - 0.15	2Pd-20CsDTP/K-10
M2	423 - 463	100 - 140	0.143	Ni/C
M3	313 - 343	7 - 27	0.0198 - 0.0595	Ru/C (aq)
M4	523	33	N/A	(Pt, Pd, Ir, Ru, Ni, Co)/C
	Parameters			**Solvent**
M1	k_1, k_2, k_3, K_{HMF}, K_{BHMF}, K_{DMF}, K_{DMTHF}, K_{WATER}, K_{H_2}			THF
M2	k_1, k_2, k_3, k_4, k_5			THF
M3	k_1, K_{HMF}, K_{H_2}			Water
M4	k_1, k_2, k_3			1-propanol
	State variables			**Analysis technique**
M1	C_{HMF}, C_{BHMF}, C_{DMF}, C_{DMTHF}, C_{WATER}, P_{H_2}			GC-MS
M2	C_{HMF}, C_{MFA}, C_{BHMF}, C_{DMF}, C_{DMTHF}			GC
M3	C_{HMF}, P_{H_2}			HPLC-MS
M4	C_{HMF}, C_{BHMF}, C_{DMF}, C_{DMTHF}			GC

Among the other variables that can be used to determine the response of the system, hence to study the behaviour of the kinetic models proposed, some are more convenient to be used for design purposes rather than others. For instance, although the wide range of temperatures explored by different authors, it never appears explicitly in the models equations. In order to study the dependency of the temperature on the various kinetics, other equations have to be added and it would not be possible to use the temperature as a design variable without changing the structure of the model it-self. Among the possible alternatives, the design variables considered at the beginning of the study are:

1. hydrogen partial pressure, P_{H_2};
2. initial concentration of HMF, C^0_{HMF};
3. initial concentration of DMF, C^0_{DMF};
4. distribution of sampling points.

3.4 Structural uncertainties and limitations of the candidate kinetic models

In this section all the practical and theoretical uncertainties regarding the different models available are discussed. It represents a sort of preliminary analysis through which it is possible to identify in advance strengths and weaknesses of each proposed model. In this sense, it might result in a simplification of the identifiability analysis: being aware of the descriptive lacks and possible limitations or structural issues of a model allows a faster identification of alternatives that may be more phenomenologically reliable.

3.4.1 M1 inconsistencies and lacks

There are 3 main issues that come from the analysis of M1:

1. it is not clear whether the water concentration C_{WATER} has been considered as a constant or not;
2. the given units of measure for the kinetic constants $\left(\frac{L^2}{mol \cdot g \cdot s}\right)$ are not consistent;
3. the reactions considered do not satisfy the atomic balance between species.

About 2., the reactions used to develop the differential balances are reported to be the following:

$$A.S_1 + H.S_2 \xrightarrow{k_1} B.S_1 + S_2 \tag{3.29}$$

$$B.S_1 + H.S_2 \xrightarrow{k_2'} C.S_1 + W.S_2 \tag{3.30}$$

$$C.S_1 + H.S_2 \xrightarrow{k_2''} D.S_1 + W.S_2 \tag{3.31}$$

$$D.S_1 + H.S_2 \xrightarrow{k_3} E.S_1 + S_2 \tag{3.32}$$

where $I.S_j$ represents the adsorbed species to the two types of catalyst active sites. However, considering the conversion of C (MFA) into D (DMF) so fast that C (MFA) can barely be detected, the reaction (3.30) and (3.31) can be summed up to give:

$$B.S_1 + H.S_2 \xrightarrow{k_2} D.S_1 + W.S_2 \tag{3.33}$$

that does not fulfil the atomic balance between species. Actually, the overall reaction seems to be strange. For each step, indeed, an entire molecule of hydrogen is required but, on the reactions reported, only one atom of hydrogen seems to react. Although in this way the differential balances obtained are probably the most simple ones involving the LHHWs mechanism, a more precise stoichiometry would result in a greater reliability of the chemical relations used to represent the system. Furthermore, the unit of measure proposed for the kinetic constants is not fully clear. Let us consider the model equations (3.3)-(3.6): the dimensional analysis, using the units of measure provided by the authors, gives:

$$\left[\frac{mol}{s}\right] \neq \left[\frac{L^2}{mol \cdot g \cdot s} \cdot \frac{L}{mol} \cdot \frac{mol}{L} \cdot \frac{g}{L}\right] \tag{3.34}$$

3.4.2 M2 and M4 limitations

The limitations of M2 are mostly related to the identification of the highly reactive intermediate MFA. In particular, it is not sure whether the MFA can be reliably detected or not: if not, the identification of the kinetic constant related to its conversion appears tough and the model should be probably modified with a simplified version that relies on a different reaction pathway. On the other hand, the same authors who developed the model M4, warn that the model parameters proposed may not be really accurate since the system is a complex three-phase environment which would require further studies. However, notice that the structures of the two kinetic models are practically equal. Since the results of the various analysis are expected to be almost equivalent, the best choice for sake of conciseness is to study only the kinetic model M2.

3.4.3 M3 limitations

The main limitation of the kinetic model M3 is related to the fact that it has been developed through initial rate expressions that cause the model to be capable of representing in a reliable way the reaction beginning only. Since all the gathered kinetic models have to be treated in a general way to perform the analysis illustrated in the next Chapters, it is likely that this model will be rejected. In particular, by

setting a common reaction duration and a common sampling scheme, the behaviour of M3 is expected to be incompatible with the behaviour of the other models.

CHAPTER 4

RESULTS OF IDENTIFIABILITY ANALYSIS FOR THE HMF HYDROGENATION KINETIC MODELS

In this Chapter, the main results obtained from the analyses conducted on the kinetic models gathered in literature, are illustrated. After definition of the experimental design space, considering both technical and practical constraints, a general procedure for the models identification is employed. Throughout the Chapter, it is shown as the different analyses allow to confirm or discard the different kinetic models due to structural or practical identifiability issues. Furthermore, the design variables values are investigated aiming at ensuring a reliable estimation of the model parameters. The objectives are finding the most suitable kinetic models to describe the HMF hydrogenation process and, in parallel, conducing a ranking of the most informative regions of the design space.

4.1 Analysis procedure

The objective of this section is to guide the reader through the different analyses performed. Following the block diagram in Figure 4.1, it is firstly defined a design space common to all the kinetic models gathered in literature. The design variables choice, that considers also practical limitations, is addressed in details. Then, the correlation analysis results are reported with the objective of performing an initial discrimination of kinetic models and design variables. The information analysis results are then used to discriminate among the remaining design variables and to find the conditions that maximize the information available for a reliable parameter estimation. Finally, the covariance analysis allows to refine and confirm the infor-

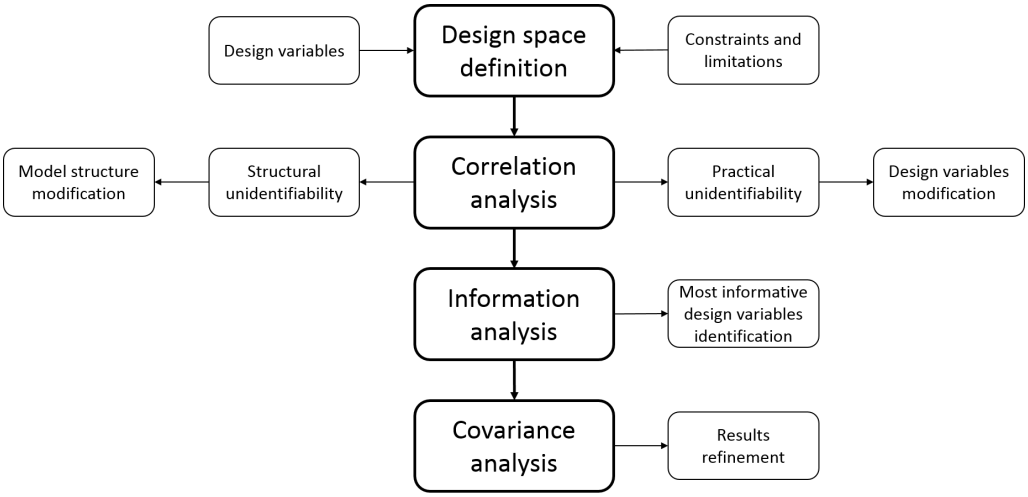

Figure 4.1: *Analysis procedure adopted throughout this Chapter to investigate the kinetic models available for the HMF hydrogenation process.*

mation analysis results. The final objective is to propose a set of kinetic models and experimental conditions that are expected to ensure the model identifiability and statistical reliability of the estimates.

4.2 Latin Hypercube Sampling

For sake of defining a general framework to perform the kinetic models analyses, an experimental design space (the region that encloses all the measurable variables meaningful to modify) must be firstly defined. However, since it is extremely time and computationally expensive to explore each value of that domain, appropriate techniques can be used to select few points that are still representative of the entire space. At the purpose, the Latin Hypercube Sampling (LHS) is a statistical method used to uniformly distribute a certain number of points into a multidimensional space. It comes from the generalization to an arbitrary number of dimensions of the Latin Square Sampling (LSS) that can only be applied to 2D domains (Montgomery and Douglas (2012)). The LHS is more efficient than a random sampling, where the sample points are generated without considering the previous ones, but simpler than the Orthogonal Sampling where the entire experimental domain is divided into a number of sub-spaces that ensure the resulting ensemble of measurements is a Latin Hypercube with the same density of samples for each sub-space. The main advantages of using a LHS are that:

1. a few number of samplings are capable of being representative of the entire domain under investigation;
2. the procedure does not require to increase the number of samples when the number of dimensions (variables) increases as well;
3. the selection of the points keeps memory of the previous choices allowing to take the samples one at a time.

In this work, in order to prevent the results from having a local reliability, the LHS is used to select the design variables values to be used for the various analyses.

4.3 Experimental design space

The experimental design space can be:

1. either mono-dimensional or multi-dimensional, as a function of the number of design variables that are contained in the model structure;
2. discontinuous, since some values cannot be experienced due to the existence of practical constraints;
3. with regions that allow to obtain higher amounts of information for the parameter estimation purposes.

In this work, some restriction based on the suggestions of the chemists in the University where the study has been conduced, are applied to the design space. These limitations are founded on:

1. practical constraints related to the equipment used;
2. specific regulations and security standards that applies to the experiments to be performed.

In particular, since the HMF hydrogenation process can be exploited at high temperatures and pressures, these two variables are considered as the critical ones and the restriction is applied to them only. However, other variables need to be defined too and in Table 4.1 all the values, or range of values, are reported.

Table 4.1: *Suggested design space taking into account the practical limitations and safety standards of the equipment that may be employed to carry out the process.*

T [K]	P_{H_2} [atm]	C^0_{HMF} [M]	C^0_{DMF} [M]	SPs distribution
353 ÷ 383	5 ÷ 7	0.0 ÷ 0.2	0.0 ÷ 0.2	S1, S2, S3

4.3.1 Temperature and pressure

The problems of considering temperature and pressure as design variables are essentially two:

1. none of the kinetic models gathered involve the direct reliance from the temperature;
2. not all the kinetic models available contain the dependency from the hydrogen pressure.

Although the Arrhenius equation could be used to explain the temperature effect, the price is that two parameters are added for each kinetic constant involved. To avoid that situation, it has been decided to consider the temperature as a discrete variable only for the kinetic model M1 that has been proposed by Gawade A.B. and coworkers (Gawade et al. (2016)) with four sets of estimated parameters according to as many temperature levels.
About the pressure, since the hydrogen is always assumed to be in excess, the lower pressure bound is set to 5 atm. However, since the pressure is not a common variable to all the kinetic models, it will be considered only for the model validation on the final set of kinetic models.

4.3.2 Initial concentrations

Being the HMF hydrogenation an equilibrium reaction, meaningful concentration profiles can be obtained by varying both the initial concentration of reactants and/or products. Furthermore, contrarily to temperature and pressure, the initial concentration is a continuous variable hence, to contains the computational expenditure, not all the values can be experienced. Instead, a campaign of 10 experiments is considered a good trade-off between resource expenditure and information that can

be collected. Thus, the LHS is used to generate the 10 combinations for the initial concentrations of HMF and DMF, reported in Table 4.2.

Table 4.2: *Sets of initial concentrations of HMF and DMF generated through the Latin Hypercube Sampling.*

Exp.	$\mathbf{C^0_{HMF}}$ [M]	$\mathbf{C^0_{DMF}}$ [M]
1	0.1556	0.0667
2	0.0667	0.0222
3	0.0000	0.0444
4	0.1333	0.0000
5	0.0889	0.0889
6	0.2000	0.2000
7	0.0222	0.1111
8	0.1778	0.1333
9	0.1111	0.1556
10	0.0444	0.1778

Although it is clear that some combinations are more meaningful – it is not likely that the third experiment will provide useful information – other experiments seem more promising. The analyses are then exploited for all the 10 experiments and the results are combined together to characterize the behaviour of the different kinetic models.

4.3.3 Sampling points distributions

For the sampling points (SPs), three distributions are arranged to allocate the various measurements along the entire experiment duration of 120 minutes. As for the number of experiments, 10 sampling points are assumed to be a sufficient amount of measures. The convenience of defining different sampling frameworks is that, since the reaction extent given by the expected kinetics of the various kinetic models may vary a lot, it is definitely interesting to assess the influence of the measurement procedure on the overall analysis results. For instance, the kinetic model M3 is characterized by an expected reaction duration of 5 minutes while, according to

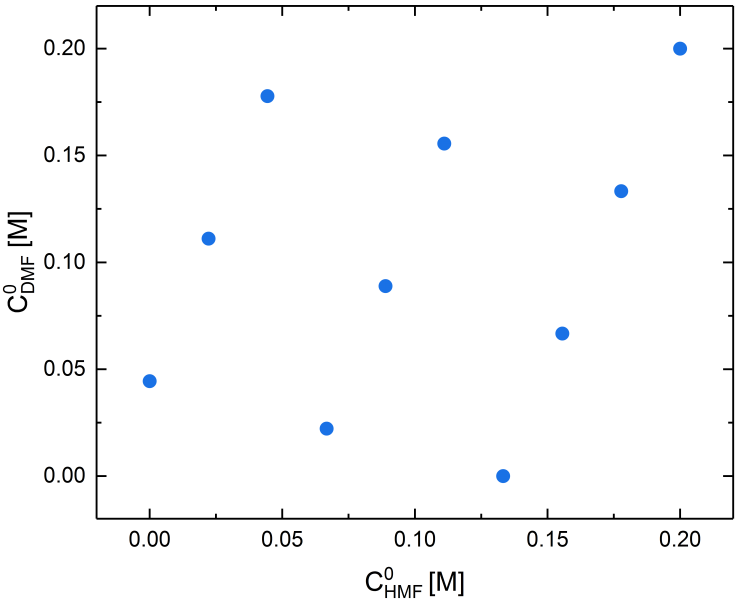

Figure 4.2: *Graphical representation of the 10 experiments listed in Table 4.2.*

M2, the reaction should require more than 2 hours to get the completion. Thus, it is clear how the sampling interval chosen – always respecting the physical constraints and limitations imposed by the reality of a chemical lab – causes a variation of the analyses results. The sampling points distributions, assuming 5 minutes as the minimum time between consecutive measurements, are reported geometrically in Figure 4.3 and listed below:

1. SPs concentrated at the beginning (S1);
2. SPs evenly spaced (S2);
3. SPs concentrated at the end (S3).

At this point, the experimental domain and all the values for the design variables have been defined. It is finally possible to proceed with further studies: first the correlation analysis has to be carried out.

4.4 Correlation analysis results

The study of the correlation based on the sensitivities, for different regions of the design space, allows to gather information on both the structural and the practical identifiability. On the one hand, if a model is unidentifiable for all the conditions

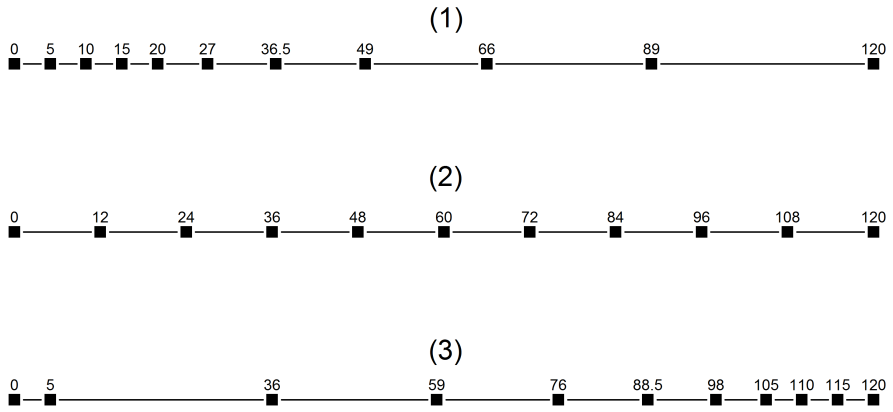

Figure 4.3: *Different distributions of 10 sampling points over an experiment duration of 120 minutes. Concentrated at the beginning (1), evenly spaced (2), concentrated at the end (3).*

investigated – established that these conditions are representative of the entire design space – it is possible to assume with a significant level of confidence that the problem of the model is structural. On the other hand, there could be regions of the experimental domain in which some parameters show correlation that in other regions does not exist. Then, it could happen that locally a model is not identifiable but it turns out to be identifiable globally.
Indeed, being the correlation analysis a function of the sensitivity through the estimability matrix $\mathbf{P_E}$, it is in particular affected by the sampling procedure adopted:

1. if the expected kinetics is really fast, the sensitivities of the model parameters are higher at the beginning and it is more likely that the distribution S1 can collect more useful information;

2. if the expected kinetics is slow, the sensitivities are almost null at the reaction beginning and more information is probably gathered through the distributions S2 or S3.

Although the parameters identification is, at least theoretically, always possible when the correlations r_{ij} are lower than 1, in practise the estimation could be extremely tough and resource expensive also when the correlation approach 1. In this study, the condition $r_{ij} > 0.9$ has been used to classify the so called *critical correlations*.

4.4.1 Correlation analysis on M1

A kinetic model like M1, characterized by a great number of parameters, is expected to show some identifiability problem because, in particular, the adsorption coefficients are known to be difficult to estimate precisely through concentration data. The objective is then to understand how the low sensitivities on that parameters reflect on the overall correlation.

From Tables 4.3 to 4.5 it is possible to appreciate the different correlation matrices computed for the three sampling points distributions. The results are obtained at 363 K but, for the other temperature levels, apart from slight variations the conclusions are exactly the same.

Table 4.3: *Correlation matrix for the kinetic model M1 based on $\boldsymbol{P}_E$ and built on a the campaign of 10 experiments with the sampling distribution S1: values and colormap.*

R	k_1	k_2	k_3	K_A	K_B	K_D	K_E	K_{H_2}	K_W
k_1	1.000								
k_2	0.703	1.000							
k_3	-0.020	-0.058	1.000						
K_A	**0.999***	0.687	-0.020	1.000					
K_B	0.700	**1.000***	-0.059	0.685	1.000				
K_D	-0.027	-0.070	**1.000***	-0.027	-0.071	1.000			
K_E	-0.679	-0.860	-0.008	-0.664	-0.858	0.003	1.000		
K_{H_2}	0.782	**0.991**	0.008	0.769	**0.990**	-0.004	-0.868	1.000	
K_W	-0.563	**-0.904**	-0.062	-0.553	**-0.904**	-0.049	0.841	-0.891	1.000
$\mathbf{r}_{crit}$	1	3	1	0	2	0	0	0	-

-1.00	-0.75	-0.50	-0.25	0	+0.25	+0.50	+0.75	+1.00

It appears clear that, for all the sampling distributions, the kinetic model M1 presents at least three total correlations and many other critical ones. The problem may be caused by the fact that in the model equations (3.3) - (3.6) the kinetic constants at the numerator are always multiplied by some adsorption coefficients. As already discussed in Chapter 2, these particular structures lead usually

Table 4.4: *Correlation matrix for the kinetic model M1 based on $\boldsymbol{P}_E$ and built on a the campaign of 10 experiments with the sampling distribution S2: values and colormap.*

R	k_1	k_2	k_3	K_A	K_B	K_D	K_E	K_{H_2}	K_W
k_1	1.000								
k_2	**0.926**	1.000							
k_3	-0.007	-0.040	1.000						
K_A	**1.000***	**0.927**	-0.007	1.000					
K_B	**0.925**	**1.000***	-0.040	**0.925**	1.000				
K_D	-0.012	-0.046	**1.000***	-0.012	-0.047	1.000			
K_E	-0.817	-0.862	-0.076	-0.812	-0.861	-0.069	1.000		
K_{H_2}	**0.938**	**0.992**	0.084	**0.938**	**0.991**	0.077	-0.870	1.000	
K_W	-0.746	**-0.903**	-0.185	-0.743	**-0.903**	-0.178	0.861	**-0.912**	1.000
$\mathbf{r}_{crit}$	4	4	1	2	2	0	0	1	-

-1.00	**-0.75**	**-0.50**	**-0.25**	**0**	**+0.25**	**+0.50**	**+0.75**	**+1.00**

to structural identifiability issues that has to be solved in order to proceed with further analyses. In this sense, the only solution could be represented by the re-parametrization of the kinetic model.

4.4.2 Correlation analysis on M2 and M4

The kinetic model M2 is the most simple but complete alternative available in literature. It does not involve adsorption coefficients but only kinetic constants. Furthermore, the reaction pathway considers all the most common intermediates and by-products so far identified. The model M4, instead, represents a sort of simplified version of M2: it does not consider the formation of MFA but the equations structure is totally the same. In order to avoid repetitions on the results presentation, from now on only the kinetic model M2 will be studied. However, M4 is not discarded: in case that critical identifiability issues would arise, it will be used as first alternative to M2.

The study of the correlation follows then the same procedure employed for M1 and,

Table 4.5: *Correlation matrix for the kinetic model M1 based on $\boldsymbol{P}_E$ and built on a the campaign of 10 experiments with the sampling distribution S3: values and colormap.*

R	k_1	k_2	k_3	K_A	K_B	K_D	K_E	K_{H_2}	K_W
k_1	1.000								
k_2	0.441	1.000							
k_3	0.009	-0.002	1.000						
K_A	**0.999***	0.409	0.009	1.000					
K_B	0.435	**1.000***	-0.003	0.403	1.000				
K_D	0.008	-0.004	**1.000***	0.008	-0.005	1.000			
K_E	-0.566	-0.808	-0.222	-0.540	-0.805	-0.220	1.000		
K_{H_2}	0.654	**0.931**	0.243	0.629	**0.929**	0.241	-0.870	1.000	
K_W	-0.217	-0.629	-0.512	-0.208	-0.631	-0.510	0.669	-0.695	1.000
$\mathbf{r}_{crit}$	1	2	0	0	1	0	0	0	-

-1.00	-0.75	-0.50	-0.25	0	+0.25	+0.50	+0.75	+1.00

from Tables 4.6 to 4.8, the correlation matrices obtained for the 3 different sampling distributions are reported. In this case, no critical correlations are highlight: it is reasonably to assume that no structural issues affect the kinetic model M2. Moreover, although the single values change for the different distributions – overall the correlation looks slightly higher with S3 – the discrimination of the best sampling procedure has to be refined on the basis of the information analysis.

4.4.3 Correlation analysis on M3

In the correlation study of the kinetic model M3, all the four variants proposed by the authors are considered. However, there are two characteristics of this kinetic model that are expected to affect strongly the analysis result:

1. the low number of measurable outputs;
2. the fact that initial-rate expressions are used.

In particular, since the practical limitations assumed for the sampling procedure do

Table 4.6: *Correlation matrix for the kinetic model M2 based on $\boldsymbol{P}_E$ and built on a the campaign of 10 experiments with the sampling distribution S1: values and colormap.*

R	$k_{1,app}$	$k_{2,app}$	$k_{3,app}$	$k_{4,app}$	$k_{5,app}$
$k_{1,app}$	1.000				
$k_{2,app}$	0.334	1.000			
$k_{3,app}$	0.299	0.419	1.000		
$k_{4,app}$	-0.246	-0.330	-0.160	1.000	
$k_{5,app}$	-0.271	-0.580	-0.176	0.376	1.000
$\mathbf{r}_{\text{crit}}$	0	0	0	0	-

-1.00	-0.75	-0.50	-0.25	0	+0.25	+0.50	+0.75	+1.00

Table 4.7: *Correlation matrix for the kinetic model M2 based on $\boldsymbol{P}_E$ and built on a the campaign of 10 experiments with the sampling distribution S2: values and colormap.*

R	$k_{1,app}$	$k_{2,app}$	$k_{3,app}$	$k_{4,app}$	$k_{5,app}$
$k_{1,app}$	1.000				
$k_{2,app}$	0.419	1.000			
$k_{3,app}$	0.340	0.428	1.000		
$k_{4,app}$	-0.284	-0.366	-0.157	1.000	
$k_{5,app}$	-0.307	-0.729	-0.204	0.390	1.000
$\mathbf{r}_{\text{crit}}$	0	0	0	0	-

-1.00	-0.75	-0.50	-0.25	0	+0.25	+0.50	+0.75	+1.00

not allow to collect high amounts of information at the beginning of the reaction, the initial-rate expression does not look to be suitable. As a demonstration of that, the correlation matrices for all the different cases are always equivalent to the identity matrix **I**. It is clear that the model cannot be identified: it is structurally unsuitable.

Table 4.8: *Correlation matrix for the kinetic model M2 based on $\boldsymbol{P}_E$ and built on a the campaign of 10 experiments with the sampling distribution S3: values and colormap.*

R	$k_{1,app}$	$k_{2,app}$	$k_{3,app}$	$k_{4,app}$	$k_{5,app}$
$k_{1,app}$	1.000				
$k_{2,app}$	0.460	1.000			
$k_{3,app}$	0.385	0.418	1.000		
$k_{4,app}$	-0.305	-0.392	-0.144	1.000	
$k_{5,app}$	-0.334	-0.865	-0.231	0.400	1.000
$\mathbf{r}_{\text{crit}}$	0	0	0	0	-

-1.00	-0.75	-0.50	-0.25	0	+0.25	+0.50	+0.75	+1.00

4.4.4 Correlation results summary

As expected, the different model structures led to peculiar results for the correlation analysis. Overall it has been highlighted that:

1. M1 has three couples of model parameters that are always totally correlated, plus several other couples critically correlated;

2. M2 does not show critical correlations, regardless to the conditions adopted;

3. M3 presents an unsuitable structure, independently on the design variables choice;

4. M4 shows an analogous behaviour to M2 and, since their structure is practically equivalent, M4 will not be investigated any more for sake of conciseness.

To conclude, while the correlation problem that affect M1 is likely to be solved through a re-parametrization of the model, the critical correlations that characterize M3 are different. The problem with this kinetic model is that its expected kinetics is extremely fast: after almost 5 minutes the hydrogenation is assumed to be complete and the concentration profiles become flat. The sensitivities after that

point are null and, as a numerical consequence, the model parameters always result totally correlated. Unfortunately, since the minimum time required to take a sample is 5 minutes, it is clear that regardless of the sampling distribution adopted, it is not possible to obtain a different correlation. Eventually, the conclusion is that the model structure of M3 is unsuitable for the type of investigation that has to be conduced in this work and, for the reasons aforementioned, it is not considered in the following sections.
Finally, about the sampling point distributions, no definitive conclusions can be drawn yet: for all the kinetic models investigated up to this point, the different distributions did not affect significantly the correlation results and they have to be further investigated – and discriminated – through the next analyses.

4.5 Re-parametrization of M1

The model re-parametrization is a technique that consists in changing the model structure, rearranging the terms of the various equations, keeping the model response invaried. It is strongly driven by the modelist experience because, often, the nonlinear structure of the models leads to non-trivial choices that are difficult to foresee. Recent studies tried to propose algorithms capable of modifying the kinetic models on the basis of certain statistics (Quaglio et al. (2019)) but the techniques require further improvement. In this study, a trial-and-error procedure based on the approach of Espie and Macchietto (1988), is instead used: starting from the observation of the critical correlations, new parameters are proposed, the sensitivity for the campaign of 10 experiments is calculated again and the correlation as well. If the changes are effective – in terms of correlation improvement – the new proposed modifications are hold, otherwise different alternative are formulated. With this rationale, several trials have been made trying to solve the critical correlation problems of M1. Eventually, the kinetic model has been modified introducing three new algebraic equations that represent as many lumped parameters. The new sys-

tem of DAEs is:

$$\mathrm{P}_1 = k_1 \mathrm{K_A} \sqrt{\mathrm{K}_{\mathrm{H_2}}} \tag{4.1}$$

$$\mathrm{P}_2 = k_2 \mathrm{K_B} \sqrt{\mathrm{K}_{\mathrm{H_2}}} \tag{4.2}$$

$$\mathrm{P}_3 = k_3 \mathrm{K_D} \sqrt{\mathrm{K}_{\mathrm{H_2}}} \tag{4.3}$$

$$-\frac{dC_\mathrm{A}}{dt} = \frac{\mathrm{P}_1 \cdot C_\mathrm{A} \sqrt{p_{\mathrm{H_2}}} w}{[1 + K_\mathrm{A} C_\mathrm{A} + K_\mathrm{B} C_\mathrm{B} + K_\mathrm{D} C_\mathrm{D} + K_\mathrm{E} C_\mathrm{E}][1 + \sqrt{K_{\mathrm{H_2}} p_{\mathrm{H_2}}} + K_\mathrm{W} C_\mathrm{W}]} \tag{4.4}$$

$$\frac{dC_\mathrm{B}}{dt} = \frac{[\mathrm{P}_1 \cdot C_\mathrm{A} - \mathrm{P}_2 \cdot C_\mathrm{B}] \sqrt{p_{\mathrm{H_2}}} w}{[1 + K_\mathrm{A} C_\mathrm{A} + K_\mathrm{B} C_\mathrm{B} + K_\mathrm{D} C_\mathrm{D} + K_\mathrm{E} C_\mathrm{E}][1 + \sqrt{K_{\mathrm{H_2}} p_{\mathrm{H_2}}} + K_\mathrm{W} C_\mathrm{W}]} \tag{4.5}$$

$$\frac{dC_\mathrm{D}}{dt} = \frac{[\mathrm{P}_2 \cdot C_\mathrm{B} - \mathrm{P}_3 \cdot C_\mathrm{D}] \sqrt{p_{\mathrm{H_2}}} w}{[1 + K_\mathrm{A} C_\mathrm{A} + K_\mathrm{B} C_\mathrm{B} + K_\mathrm{D} C_\mathrm{D} + K_\mathrm{E} C_\mathrm{E}][1 + \sqrt{K_{\mathrm{H_2}} p_{\mathrm{H_2}}} + K_\mathrm{W} C_\mathrm{W}]} \tag{4.6}$$

$$\frac{dC_\mathrm{E}}{dt} = \frac{\mathrm{P}_3 \cdot C_\mathrm{D} \sqrt{p_{\mathrm{H_2}}} w}{[1 + K_\mathrm{A} C_\mathrm{A} + K_\mathrm{B} C_\mathrm{B} + K_\mathrm{D} C_\mathrm{D} + K_\mathrm{E} C_\mathrm{E}][1 + \sqrt{K_{\mathrm{H_2}} p_{\mathrm{H_2}}} + K_\mathrm{W} C_\mathrm{W}]} \tag{4.7}$$

$$\frac{dC_\mathrm{W}}{dt} = \frac{\mathrm{P}_2 \cdot C_B \sqrt{p_{\mathrm{H_2}}} w}{[1 + K_\mathrm{A} C_\mathrm{A} + K_\mathrm{B} C_\mathrm{B} + K_\mathrm{D} C_\mathrm{D} + K_\mathrm{E} C_\mathrm{E}][1 + \sqrt{K_{\mathrm{H_2}} p_{\mathrm{H_2}}} + K_\mathrm{W} C_\mathrm{W}]} \tag{4.8}$$

The correlation matrix obtained with this new model structure is reported in Table 4.9 for the sampling distribution S3: overall, it leads to the lower correlation. However, even though the three total correlations previously identified have been now eliminated, the problem moved to parameters $\mathrm{K_D}$ and $\mathrm{K_W}$. Many trials have been made trying to tackle this issue but, eventually, the solution has not been achieved. According to the remarkably low sensitivity found for $\mathrm{K_W}$ and other adsorption coefficients, the new approach to address the correlation problem involves the investigation of whether some of the model parameters can be neglected or not.

4.6 Simplified version of M1 (M1.2)

The aim of studying a simplified version for the kinetic model M1, is to bypass the identifiability issues linked to the low sensitivities that characterize the adsorption coefficients. As underlined by the sensitivity analysis, they do not play a significant role on the determination of the model response, and it could be interesting to evaluate if they can be neglected from the model structure or not. In that case, the resulting model would be more simple and its parameters would be easier to estimate in a statistically reliable way. The new set of DAEs – with the same nomenclature

Table 4.9: *Correlation matrix for the re-parametrized kinetic model M1 based on $\boldsymbol{P}_E$ and built on a the campaign of 10 experiments with the sampling distribution S3: values and colormap.*

R	P_1	P_2	P_3	K_A	K_B	K_D	K_E	K_{H_2}	K_W
P_1	1.000								
P_2	0.441	1.000							
P_3	0.009	-0.002	1.000						
K_A	-0.728	-0.780	-0.011	1.000					
K_B	-0.712	-0.875	-0.045	**0.975**	1.000				
K_D	-0.215	-0.629	-0.510	0.281	0.466	1.000			
K_E	-0.566	-0.808	-0.222	0.781	0.858	0.667	1.000		
K_{H_2}	-0.655	**-0.932**	-0.243	0.842	**0.922**	0.695	0.870	1.000	
K_W	-0.218	-0.631	-0.509	0.284	0.469	**1.000***	0.669	0.697	1.000
$\mathbf{r}_{crit}$	0	1	0	1	1	0	0	0	-

-1.00	**-0.75**	**-0.50**	**-0.25**	**0**	**+0.25**	**+0.50**	**+0.75**	**+1.00**

used for the original model M1 – is:

$$-\frac{dC_A}{dt} = \frac{k_1\, C_A\, \sqrt{K_{H_2} p_{H_2}}\, w}{1+\sqrt{K_{H_2} p_{H_2}}} \tag{4.9}$$

$$\frac{dC_B}{dt} = \frac{[k_1\, C_A - k_2\, C_B]\sqrt{K_{H_2} p_{H_2}}\, w}{1+\sqrt{K_{H_2} p_{H_2}}} \tag{4.10}$$

$$\frac{dC_D}{dt} = \frac{[k_2\, C_B - k_3\, C_D]\sqrt{K_{H_2} p_{H_2}}\, w}{1+\sqrt{K_{H_2} p_{H_2}}} \tag{4.11}$$

$$\frac{dC_E}{dt} = \frac{k_3\, C_D\, \sqrt{K_{H_2} p_{H_2}}\, w}{1+\sqrt{K_{H_2} p_{H_2}}} \tag{4.12}$$

Notice that the new structure, does involve the adsorption coefficient of hydrogen because it is linked with the hydrogen partial pressure contribution. At this point, the comparison of the concentration profiles obtained from the original kinetic model M1 and its simplified version M1.2, allows to understand the "weight" of the approximations applied. In Figure 4.4, it is reported the comparison for one experiment randomly chosen among the set initially defined: the same results are anyway obtained also for all the other 9 experiments.

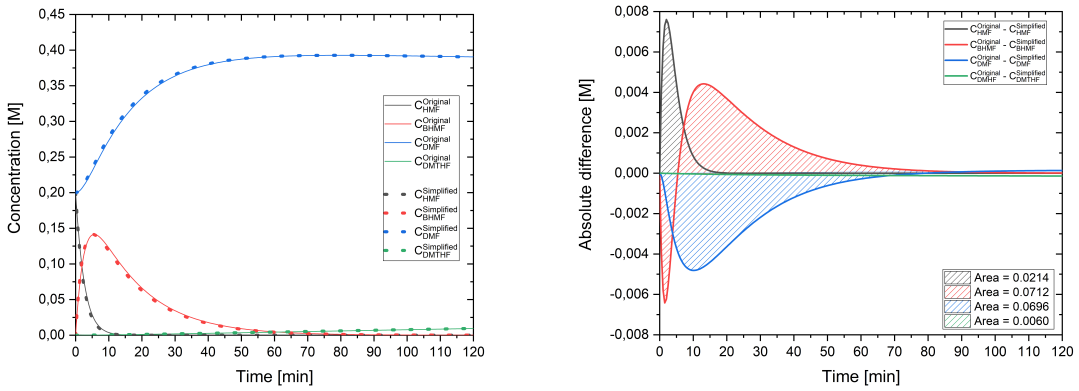

(a) *Concentration profiles comparison.* **(b)** *Absolute difference profiles comparison.*

Figure 4.4: *Response comparison between the original kinetic model M1 and the simplified version proposed M1.2: (a) comparison between the concentration profiles; (b) profiles of the difference between the responses. T = 363K,* C^0_{HMF} *= 0.20M,* C^0_{DMF} *= 0.20M.*

No substantial differences are present: the concentration profiles practically overlap and the average discrepancy for each species is in the order of ±0.01%. It is possible to say, with a high level of confidence, that the two models are equivalent. The subsequent analyses will be performed for only the simplified version M1.2. The conclusion is that, the high structural complexity and the high number of parameters involved in the original kinetic model M1, cause its structural unidentifiability. However, a simpler alternative, neglecting many of the unnecessary adsorption coefficients, has been found.

4.6.1 Correlation analysis on M1.2

Since the model structure has been modified, the correlation analysis is expected to give a different result as well. Thus, the correlation between parameters is assessed again for the three sampling distributions (see Appendix B) and, overall, it is possible to conclude that:

1. S1 cause the couple of parameters k_2-K_{H_2} to be critically correlated;
2. S2 has the same effect as S1, with a critical correlation for the same couple of parameter and high correlations – close to the critical conditions – also for other couples;

3. S3 leads to a situation in which no critical correlations are present.
4. different temperatures do not cause significant variations in the correlation between parameters hence do not affect the structural identifiability of the kinetic model.

According to the results obtained, the kinetic model M1.2 will be further investigated considering only the sampling distribution S3. Eventually, the information analysis is employed to further discriminate among the best temperature to be used.

4.7 Results from information analysis

Once a refined set of kinetic models without structural identifiability issues has been defined, it is possible to study the system information exploiting the FIM. In Chapter 2, all the details about the information analysis and the FIM derivation are discussed. In this section instead, the information analysis is used to perform a ranking of the design space regions that maximise the information required for the parameter estimation purposes.

4.7.1 Information analysis on M1.2

Since the authors who developed the kinetic model M1 proposed 4 sets of parameters according to 4 temperature levels, it is possible to study the effects of this variable on the information analysis. However, being a discrete variable, the temperature represents an "external" degree of freedom for the parameter estimation that cannot be managed by the optimizer but it can be set case by case from the user, as a function of the parameter that requires estimation. In Figure 4.5 the information analysis results are illustrated.

1. At the conditions of the third experiment, as expected, the information that can be collected is almost null for all the model parameters but k_3 that is related to the conversion of DMF, the only species present in the reactive system in this experiment.
2. Experiments 1, 8, 9 and 10 are, generally, the most informative.

3. The temperature at which the information is higher varies for each parameter. Overall, the two best alternatives are 353 K at which more information for k_1 and k_2 is provided, and 383 K at which both the total information and the information available for K_{H_2} are higher.
4. The information related to k_2 and k_3 is not significantly affected by the temperature.

Eventually, operate at 383 K represents the best choice for the estimation purposes. Looking at the information plots, indeed, it is clear that the hydrogen adsorption coefficient K_{H_2} is likely to be the most difficult parameter to estimate in a statistically reliable way. For that reason, the temperature of 383 K may ensures a less resource-expensive estimation without affecting heavily the statistics of the parameters. Notice finally that the condition number of the global FIM for that conditions is CN = $1.73 \cdot 10^{18}$ that is considerably high and denotes that the matrix inverse may not be reliable.

4.7.2 Information analysis on M2

Although for M1.2 is has already been figured out that the only suitable sampling points distribution is S3, the kinetic model M2 can be used to refine finding. At the purpose, the dependency of the information on the sampling distributions is assessed and, in Figure 4.6, the corresponding bar plots are reported.

1. The information provided by the third experiment is almost null, apart for the parameter $k_{4,app}$ related to the conversion of DMF;
2. Experiments 1,6 and 8 correspond to the most informative regions of the design space.
3. The samplings distributions S1 and S2 allow to maximise the information for the most critical parameter $k_{3,app}$ while S3 grants more information for $k_{4,app}$ and $k_{5,app}$.

Considering the results just listed, it is possible to conclude that the experiment 6 ($C^0_{\text{HMF}} = C^0_{\text{DMF}} = 0.20$M) and the sampling distribution S3 are the best alternatives to maximise the information for both M1.3 and M2 through a single experiment.

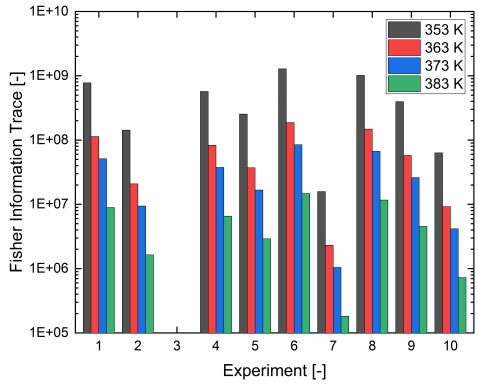

(a) *Information for* k_1

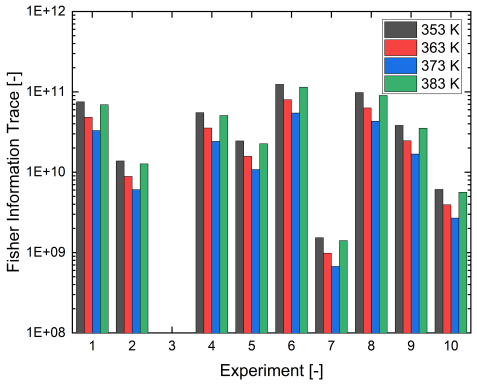

(b) *Information for* k_2

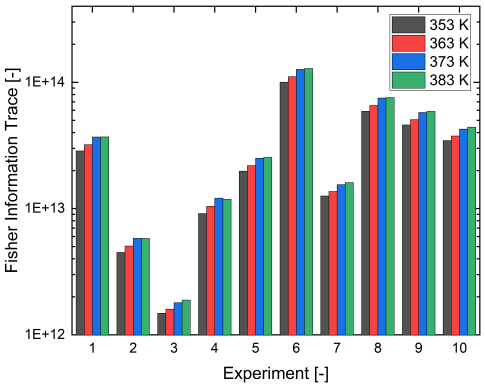

(c) *Information for* k_3

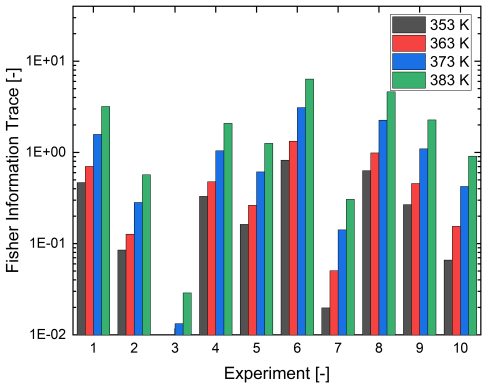

(d) *Information for* K_{H_2}

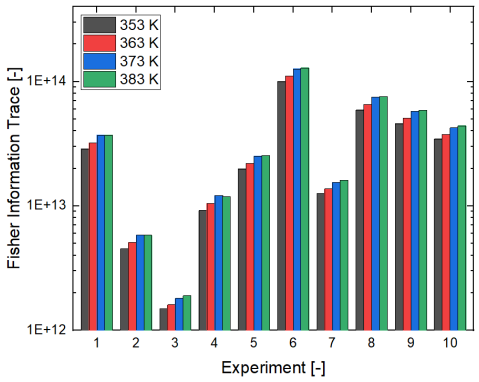

(e) *Total information*

Figure 4.5: *Bar plot comparing the information available for the parameters of the kinetic model M1.2 as a function of the experimental conditions (experiments) and temperature considered.*

At this point, to further refine the analysis just concluded, a covariance analysis has to be exploited. Through the covariance it is indeed possible to discriminate even better among the regions of the design space that allow to obtain the best statistics

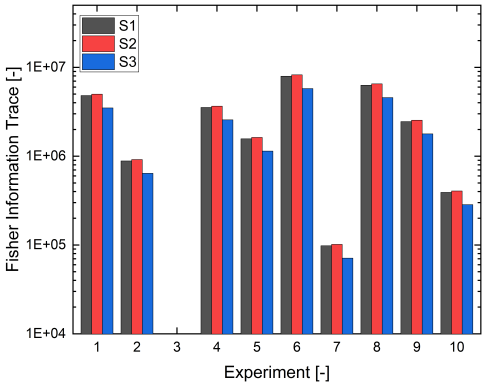

(a) *Information for* $k_{1,app}$

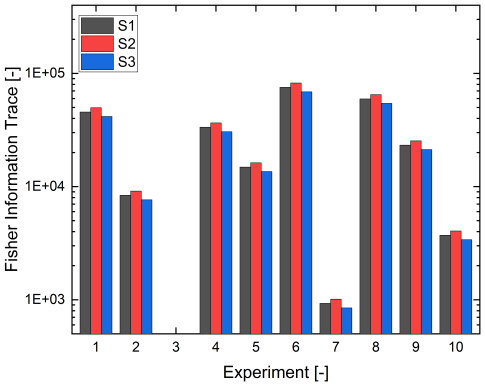

(b) *Information for* $k_{2,app}$

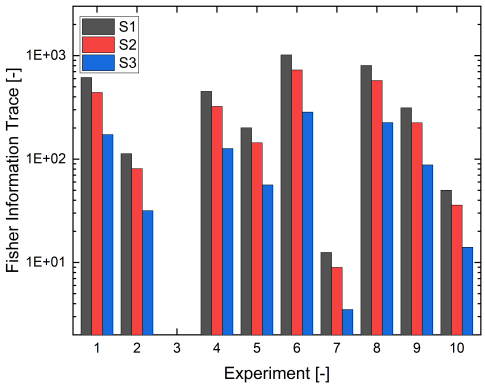

(c) *Information for* $k_{3,app}$

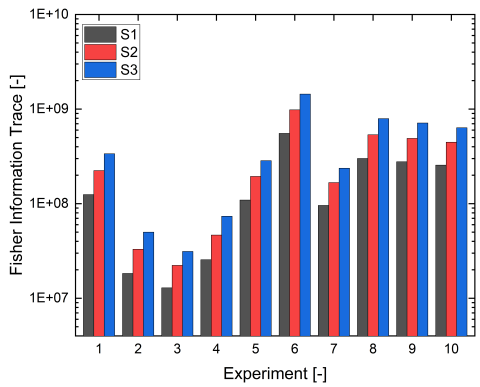

(d) *Information for* $k_{4,app}$

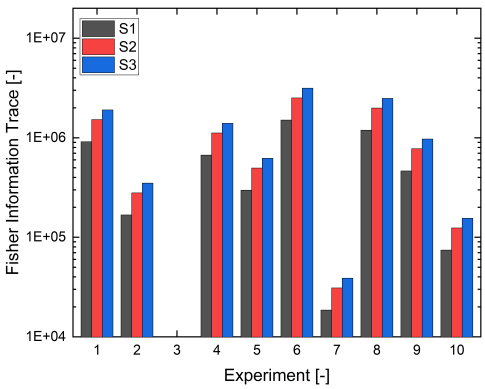

(e) *Information for* $k_{5,app}$

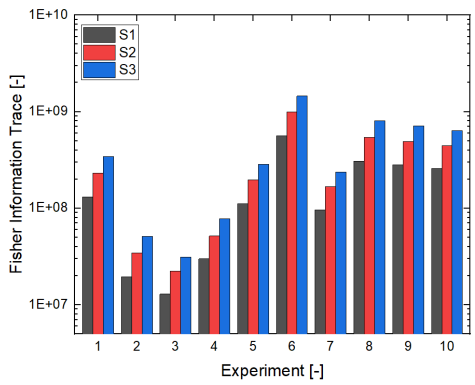

(f) *Total information*

Figure 4.6: *Bar plot comparing the information available for the parameters of the kinetic model M2 as a function of the experimental conditions (experiment) and temperature considered.*

for the parameters that require estimation.

4.8 Covariance analysis results

To study the covariance, the metrics used is the variance-covariance matrix. It allows to determine the most suitable experimental conditions to use, on the basis of both the information and the correlation analyses. Overall, the expected trend of the covariance is opposite in respect to the information one because, using (2.29), the lower the variance the higher the information. However, it could happen that the conditions that maximize the information are not exactly the same that minimise also the covariance: the divergence is due indeed to the correlation between parameters.

In Figure 4.7, the information and covariance profiles for the kinetic model M1.2 are reported. The abrupt increase in the covariance, for the second and third experiments, denotes the presence of a numerical error. As underlined in Section §2.7, the FIM inversion can lead to numerical problems if the matrix is not well-posed. In this case, the remarkably difference between sensitivity values of different parameters, cause the resulting FIM to be *sloppy* and singular: the inversion is only possible by using the SVD approximation that gives a pseudo-inverse of uncertain reliability.

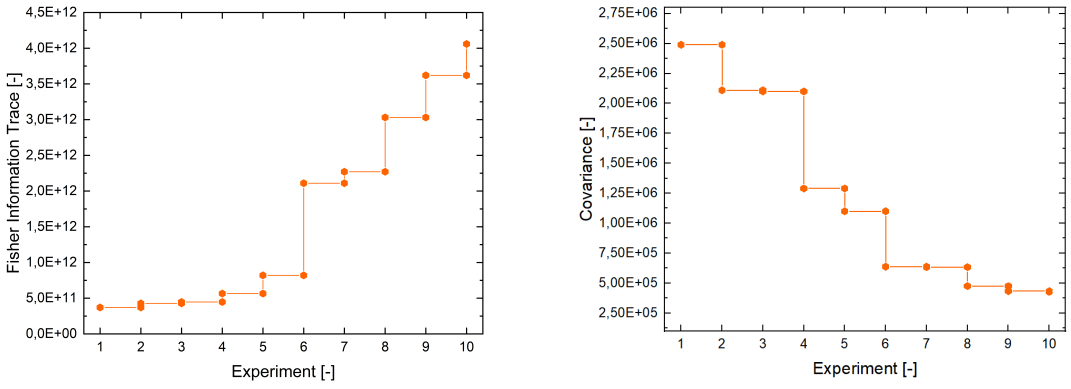

(a) *Total cumulative information profile.*

(b) *Total covariance profile.*

Figure 4.7: *Total Fisher information trace and covariance profiles for the kinetic model M1.2 with T = 383 K, P_{H_2} = 5 atm, S3 distribution.*

In Figure 4.8, the information and covariance profiles are reported for the kinetic model M2. In this case, the approximation of the variance-covariance matrix is not required because the FIM is well-posed and not singular.

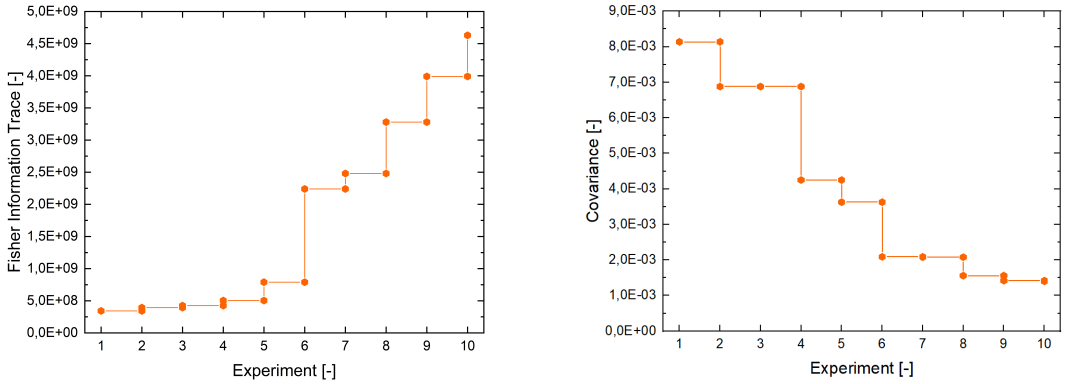

(a) *Total cumulative information profile.*

(b) *Total covariance profile.*

Figure 4.8: *Total Fisher information trace and covariance profiles for the kinetic model M2 with S3 distribution.*

Overall, what is possible to notice from the analysis of both kinetic models is that:

1. higher initial concentrations of DMF (e.g. experiments 6 and 8) allow to gather more information;

2. lower initial concentration of DMF (e.g. experiment 4 and 5) lead to a greater reduction of the covariance.

To conclude, although experiment 6 is characterized by high initial concentrations of both HMF and DMF, it appears a good trade-off between information maximisation and covariance reduction.

4.9 Results summary

The study carried out in this Chapter allowed to characterize, from an initial set of kinetic models gathered in literature, the ones not affected by identifiability issues: both structural and practical identifiability analysis have been carried out. Furthermore, to pursue the analyses, an ad-hoc design space has been defined by restriction of a larger domain: practical limitations related to the equipment to be employed and to safety standards to be respected, have been considered.
Firstly, the critical correlations identified for M1 brought to the definition of M1.2: a simplified version which structure is capable of solving all the correlation issues when the sampling distribution S3 is adopted. Instead, for M2 no particular problems have been detected: the model parameters are not correlated regardless to the

sampling distribution employed. Subsequently, the results for the kinetic model M3 highlighted that its structure is completely unsuitable for the type of study carried out in this work, it has been discarded. Finally, the kinetic model M4 has been considered as a simplified version of M2, meaningful to be further investigated only whether some issues in using M2 would arise.
Secondly, the information analysis has been performed taking into account the effect of temperature for M1.2, and the effect of sampling points distributions for M2. The conclusion are that:

1. at high initial concentrations of HMF and DMF the expected information available for the parameter estimation is higher;
2. the temperature of 383 K is the best choice in order to maximize both the global and, specifically, the information available for the most critical parameters;
3. the best sampling distribution is S3 because it maximise the global information and, although other distributions are even valid, it is the only one suitable for both kinetic models.

To conclude, the covariance analysis based on the variance-covariance matrix has been performed to consider both information and correlation for each model parameter. It demonstrated that the experimental conditions for which the information is higher do not always correspond to the conditions that minimise also the covariance. Eventually, the initial concentration of experiment 6 (Table 4.2) and the sampling point distribution S3, are considered as the best design variables to avoid structural and practical identifiability issues and to maximise the quality of the parameter estimation for the selected kinetic models M1.2 and M2.

CHAPTER 5

VALIDATION OF KINETIC MODELS AND OPTIMISATION OF DISCRIMINATING POWER

WHEN a refined set of kinetic models is available, the study proceeds with the validation and the identification of the design space regions that maximise the difference in predictions between candidate models. Firstly, a sensitivity analysis is carried out to ensure the reliability of the previously obtained results to significant variations of the model parameters value. Then, in absence of data from real experiments, the kinetic models validation has to be performed with in-silico data. Finally, the discriminating power optimization leads to identify the range of application for each kinetic model: the conditions conditions allowing a clear distinction between model predictions.

5.1 Effect of parametric uncertainty on parameter correlation and information

By definition, the sensitivity analysis depends on the local value of the model parameter. It is then required to verify whether the analyses results change significantly when the estimated parameters vary from the original value proposed. This verification ensures that the findings described throughout Chapter 4 and Chapter 5 are valid globally, although the analyses used to obtain them are based on the local sensitivities. It could happen, indeed, that even slight variations in the value of the model parameters lead to:

1. changes in the parameters correlation;
2. changes in the information profiles.

To assess this kind of sensitivity, random variations of ±15% and ±30% are applied to the model parameters of both M1.2 and M2: the results of correlation and information analysis are then compared with the nominal cases already illustrated in Chapter 4. To provide an example, the correlation matrices in Tables 5.1 and 5.2 and the information profiles in Figure 5.1, are reported for the kinetic model M2.

Table 5.1: *Correlation matrix for the kinetic model M2 based on $\boldsymbol{P}_E$ and built on a campaign of 10 experiments with sampling distribution S3, after a random parameter variation of ±15%: values and colormap.*

R	k_1	k_2	k_3	k_4	k_5
k_1	1.000				
k_2	0.472	1.000			
k_3	0.397	0.419	1.000		
k_4	-0.270	-0.361	-0.100	1.000	
k_5	-0.333	-0.840	-0.201	0.398	1.000
r_{crit}	0	0	0	0	0

-1.00	-0.75	-0.50	-0.25	0	+0.25	+0.50	+0.75	+1.00

Besides some minor variations, the overall behaviour of M2 does not change: as for the nominal case, no correlation issues characterizes the kinetic model. Therefore, the findings coming from the several analyses performed can be treated in a general way.

Furthermore, although for some experiments the information content diverge from the nominal case, the overall trend is respected: the design space regions that are more informative remain so. Notice that the conclusions illustrated here for M2 have been obtained also for the kinetic model M1.2 but they have not been reported for sake of conciseness.

5.2 Kinetic models validation

Once a final set of identifiable kinetic models for the process of interest has been defined, the subsequent step consists in the application of validation techniques

Table 5.2: *Correlation matrix for the kinetic model M2 based on $\boldsymbol{P}_E$ and built on a campaign of 10 experiments with sampling distribution S3, after a random parameter variation of ±30%: values and colormap.*

R	k_1	k_2	k_3	k_4	k_5
k_1	1.000				
k_2	0.489	1.000			
k_3	0.380	0.479	1.000		
k_4	-0.345	-0.378	-0.197	1.000	
k_5	-0.387	-0.802	-0.277	0.389	1.000
$\mathbf{r}_{\text{crit}}$	0	0	0	0	0

-1.00	-0.75	-0.50	-0.25	0	+0.25	+0.50	+0.75	+1.00

that lead to a further discrimination and understanding of the remaining models. At the purpose, the model validation can be carried out exploiting:

1. reliable data already available;
2. data coming from direct experiments (better if designed);
3. in-silico data generated from another kinetic model.

Through the model validation procedure it is possible to verify whether the kinetic models under investigation can accurately fit the data and give reliable predictions in a wide range of experimental conditions. The final objective is to find a kinetic model – if possible – capable of being representative of the reality even when the experimental conditions adopted are significantly different from those employed to develop it.

5.2.1 Response comparison between M1.2 and M2

When a set of kinetic models is collected, it is expected that their structures have been obtained by different theories, assumptions and balances. For that reason, the model discrimination techniques are used to determine exactly which model

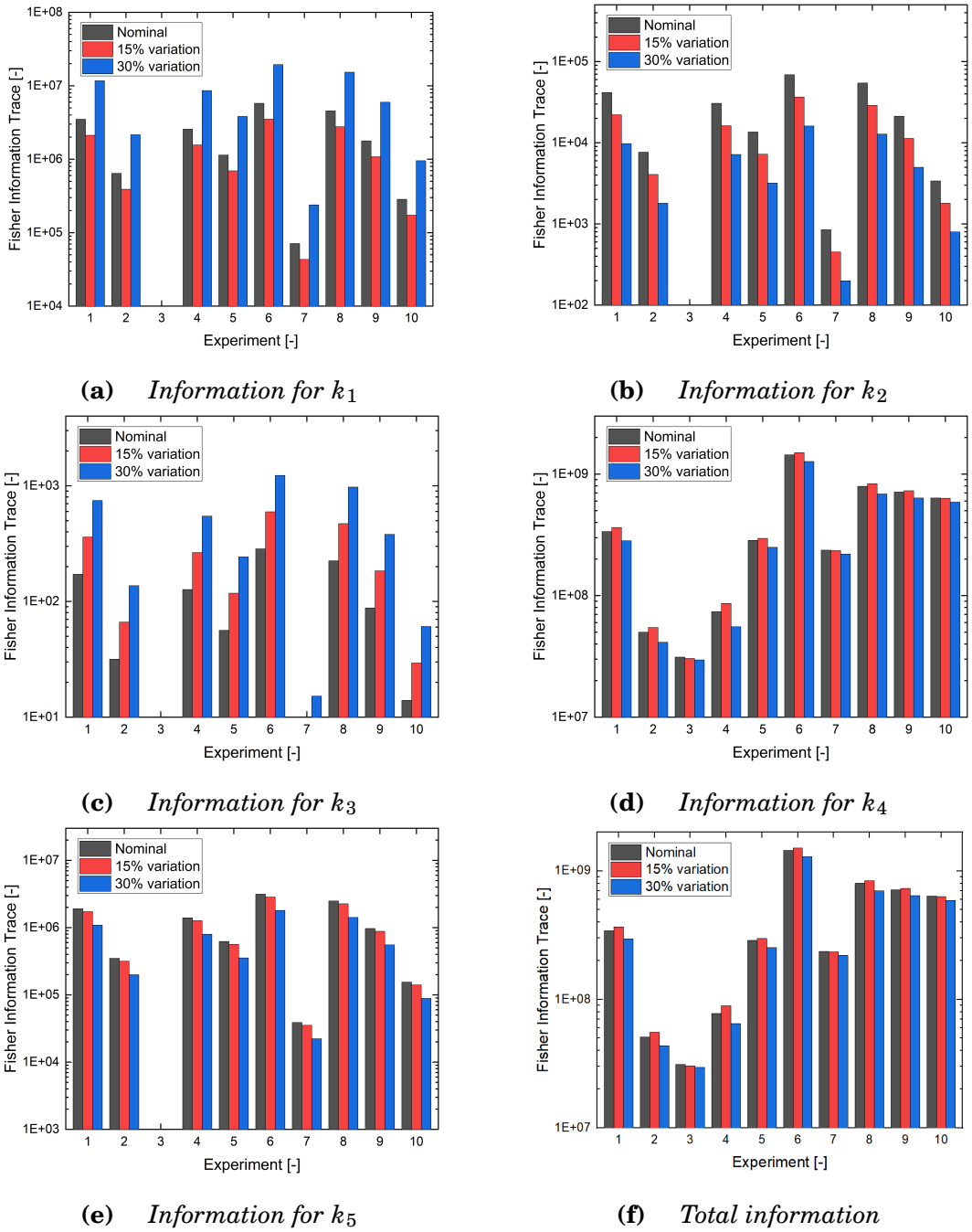

(a) *Information for* k_1 **(b)** *Information for* k_2

(c) *Information for* k_3 **(d)** *Information for* k_4

(e) *Information for* k_5 **(f)** *Total information*

Figure 5.1: *Bar plot comparing the information available for the parameters of the kinetic model M2 as a function of the experimental conditions (experiment) for the nominal case, ±15% parameters variation and ±30% parameters variation.*

structure is more appropriate in order to represent the system under investigation. Thus, it is important to assess firstly the difference between the concentration profiles obtained from the kinetic models M1.2 and M2, using the experimental conditions and the parameters proposed by the authors who developed the models (see Table 5.3).

From the comparison in Figure 5.2, the concentration profiles for the species in common are shifted toward shorter times for the left case (M1.2), and longer times for the right one (M2). The two kinetics have indeed different velocities, suggesting that a change on the M2 kinetic constants – supposedly an increment – could make the profiles considerably alike. Instead, no speculations can be made for M1.2 since it contains also an adsorption coefficient which effect on the reaction velocity is not easy to determine as for the kinetic constants.

Table 5.3: *Set of parameters and experimental conditions employed to obtain the concentration profiles that allow to compare the two kinetic models M1.2 and M2.*

Experimental conditions					
	T [K]	P [atm]	C^0_{HMF} [M]	C^0_{DMF} [M]	
M1.2	363	5	0.0667	0.0222	
M2	443	100	0.0667	0.0222	
Parameters					
M1.2	k_1 = 1.8E-3	k_2 = 0.6E-3	k_3 = 0.43E-4	K_{H_2} = 8.6	
M2	k_1 = 0.13247	k_2 = 0.55482	k_3 = 2.26789	k_4 = 0.00332	k_5 = 0.07100

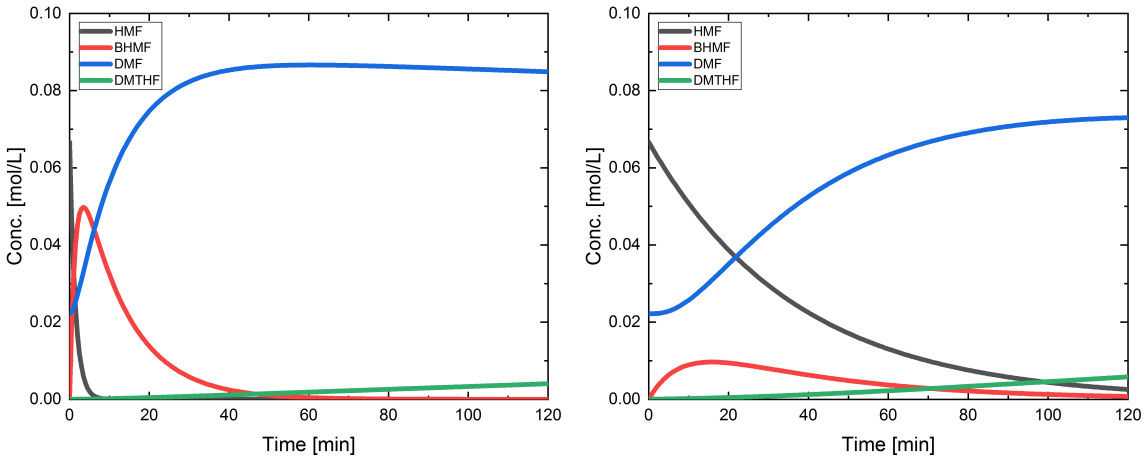

(a) *Concentration profiles for M1.2.* **(b)** *Concentration profiles for M2.*

Figure 5.2: *Comparison between concentration profiles for the species in common to M1.2 (left) and M2 (right) obtained using the set of experimental conditions and parameters listed in Table 5.3.*

5.2.2 Validation of kinetic model M2 results

As anticipated previously, since the kinetic model M2 showed a more flexible behaviour and less critical correlations, the idea is to use the data generated from M1.2 to determine if statistically reliable estimates can be obtained for M2. First of all, it is important to modify the data from simulated profile adding a Gaussian white noise with SDV σ = 0.003M, consistent to the variance model chosen for the estimation, that simulates the measurement errors always present when the data are collected through real experiments. Without the noise, the statistics obtained would be exceedingly good.

The estimation is then carried out considering to perform only a single experiment, then 5 and finally 10 experiments: from Tables 5.4 to 5.6, it is possible to appreciate the improvement of the various statistics. Notice that some model parameters cannot be estimated from the data generated: if a kinetic model cannot generate information related to a specific reactant, product or intermediate, it is not possible to estimate the kinetic constant related to that species. In particular, since M1.2 does not consider the production of DHMTHF, the kinetic constant in M2 related to its production cannot be estimated and its statistics are not reported.

Table 5.4: *Parameters statistics, t-test and χ^2-test for the validation of the kinetic model M2. Constant variance of σ = 3·10^{-3}, T = 363K , P= 5atm, 1 experiments randomly chosen among the 10 of the experimental campaign.*

Par.	Value	95% Conf. Interval	95% t-value	Standard Deviation
$k_{1,app}$	$1.142 \cdot 10^{-2}$	$3.917 \cdot 10^{-3}$	2.916	$1.931 \cdot 10^{-3}$
$k_{2,app}$	$1.400 \cdot 10^{-3}$	$1.794 \cdot 10^{-4}$	7.802	$8.845 \cdot 10^{-5}$
$k_{3,app}$	$2.311 \cdot 10^{-1}$	$3.091 \cdot 10^{+0}$	**0.075***	$1.524 \cdot 10^{+0}$
$k_{4,app}$	$6.994 \cdot 10^{-6}$	$1.324 \cdot 10^{-6}$	5.283	$6.527 \cdot 10^{-7}$
Ref. t-value: 1.688				
Weighted Residual: 0.0558			χ^2**-Value (95%)**: 51.0	

In Figure 5.3 are reported the predicted values against the data points used for the validation: the results for only one temperature are illustrated but, however, all the other cases are characterized by exactly the same peculiarities (see Appendix B).

Table 5.5: *Parameters statistics, t-test and χ^2-test for the validation of the kinetic model M2. Constant variance of σ = 3·10^{-3}, T = 363K , P= 5atm, 5 experiment randomly chosen among the 10 of the experimental campaign.*

Par.	Value	95% Conf. Interval	95% t-value	Standard Deviation
$k_{1,app}$	$2.350 \cdot 10^{-2}$	$2.458 \cdot 10^{-2}$	**0.956***	$1.245 \cdot 10^{-2}$
$k_{2,app}$	$1.288 \cdot 10^{-3}$	$1.142 \cdot 10^{-4}$	9.075	$7.188 \cdot 10^{-5}$
$k_{3,app}$	$2.362 \cdot 10^{-1}$	$2.331 \cdot 10^{+0}$	**0.101***	$1.180 \cdot 10^{+0}$
$k_{4,app}$	$6.945 \cdot 10^{-6}$	$8.787 \cdot 10^{-7}$	7.903	$4.449 \cdot 10^{-7}$
Ref. t-value: 1.649				
Weighted Residual: 11.799			χ^2**-Value (95%)**: 186.1	

Table 5.6: *Parameters statistics, t-test and χ^2-test for the validation of the kinetic model M2. Constant variance of σ = 3·10^{-3}, T = 363K , P= 5atm, 10 experiments.*

Par.	Value	95% Conf. Interval	95% t-value	Standard Deviation
$k_{1,app}$	$1.158 \cdot 10^{-2}$	$1.667 \cdot 10^{-3}$	6.950	$8.473 \cdot 10^{-4}$
$k_{2,app}$	$1.500 \cdot 10^{-3}$	$8.006 \cdot 10^{-5}$	18.74	$4.072 \cdot 10^{-5}$
$k_{3,app}$	$4.939 \cdot 10^{-2}$	$5.399 \cdot 10^{-2}$	**0.915***	$2.746 \cdot 10^{-2}$
$k_{4,app}$	$6.996 \cdot 10^{-6}$	$3.901 \cdot 10^{-7}$	17.93	$1.984 \cdot 10^{-7}$
Ref. t-value: 1.645				
Weighted Residual: 7.743			χ^2**-Value (95%)**: 401.0	

Overall, what is possible to highlight is that:

1. the χ^2-test is successful as to indicate a good fitting of the data;
2. the t-values for the estimated $k_{1,app}$, $k_{2,app}$ and $k_{4,app}$ are significantly good while the same does not hold for $k_{3,app}$, related to the MFA consumption, that is not satisfactory;
3. the absolute value of the estimated $k_{3,app}$ is, as expected, large to justify the high reactivity of the species (MFA) at which it is related to.

At this point, the goodness of statistics and fitting stimulates the idea that, maybe, the two kinetic models could be actually equivalent. Eventually, the low t-value of the estimated $k_{3,app}$ would be justified by the fact that it is the only parameter that

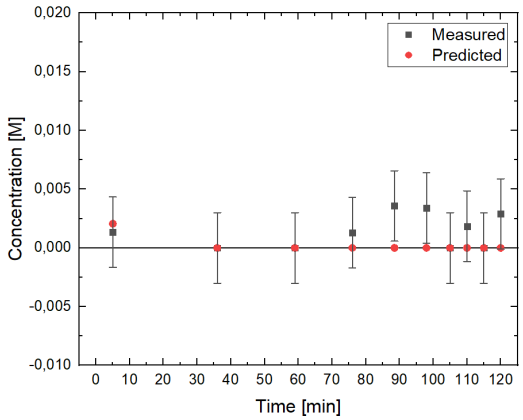

(a) *Fitting of HMF concentration profile.*

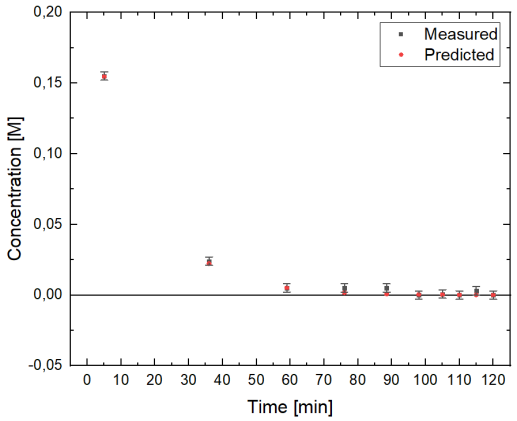

(b) *Fitting of BHMF concentration profile.*

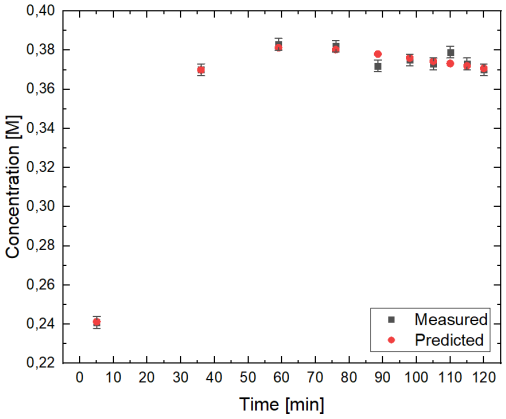

(c) *Fitting of DMF concentration profile.*

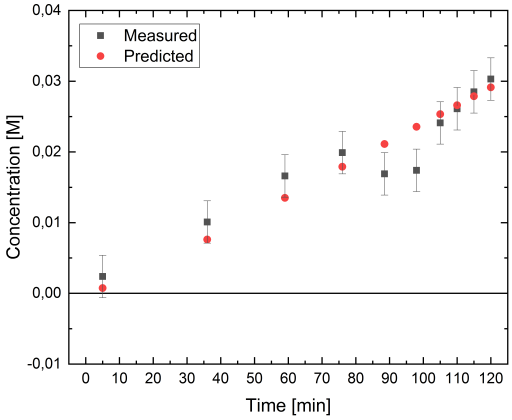

(d) *Fitting of DMTHF concentration profile.*

Figure 5.3: *Fitting results of the concentration profiles predicted from the kinetic model M2 against the data points generated from M1.2 at which Gaussian noise with σ = 0.003M has been added.*

is not in common between the two models and the data generated from M1.2 do not contain information through which it can be estimated in a statistically reliable way. At the purpose, the comparison of the concentration profiles is reported in Figure 5.4.

The negligible differences between the concentration profiles denote that the responses are practically equal. Moreover, since the analysis has been repeated for all the 10 experiments previously defined, and the results showed the same behaviour, it is possible to conclude that the two kinetic models are equivalent in the design space previously defined.

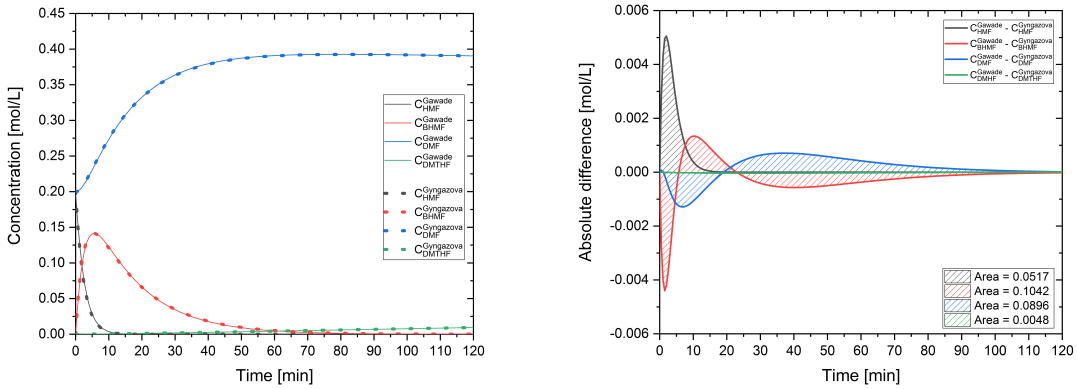

(a) *Concentration profiles comparison.* **(b)** *Absolute difference profiles comparison.*

Figure 5.4: *Response comparison between the kinetic models M1.2 and M2: (a) comparison between the concentration profiles; (b) profiles of the difference between the responses. T = 383K, C^0_{HMF} = 0.20M, C^0_{DMF} = 0.20M.*

5.2.3 Validation of kinetic model M1.2 results

Following the same analysis framework described on the previous section, also the validation of the kinetic model M1.2, exploiting the data same data generated before, is performed. The objective of this section is to understand whether it would be possible to estimate all the non-measurable parameters of the kinetic model M1.2, in particular K_{H_2}, in a statistically reliable way: the information available for its estimation has been previously found to be extremely low on the entire design space. The results are illustrated in Table 5.7.

Table 5.7: *Parameters statistics, t-test and χ^2-test for the validation of the kinetic model M1.2. Constant variance of $\sigma = 3{\cdot}10^{-3}$, T = 383K, P= 5atm, 10 experiments.*

Par.	Value	95% Conf. Interval	95% t-value	Standard Deviation
$k_{1,app}$	8.624E-04	3.554E-01	**2.426E-03***	1.809E-01
$k_{2,app}$	1.091E-04	4.495E-02	**2.426E-03***	2.287E-02
$k_{3,app}$	1.601E-06	7.939E-04	**2.017E-03***	4.040E-04
K_{H_2}	8.625E+00	1.566E+04	**5.507E-04***	7.969E+03
Ref. t-value: 1.648				
Weighted Residual: 327.502			χ^2**-Value (95%)**: 496.236	

Unfortunately, these results are affected by numerical issues. Although no critical correlations are present, the high determinant of the FIM cause that heavy numerical errors occur. Eventually, the resulting pseudo variance-covariance matrix, coming from the SVD approximation, cannot be trusted and, since the t-test is based on this matrix, it turns out to be not predictable too. Unfortunately, there are no specific techniques to solve this kind of problems. The only possible solution is to assign a fixed value to K_{H_2}, the parameter supposedly responsible of this problem, and assess the behaviour of the model again. The new results are shown in Table 5.8.

Table 5.8: *Parameters statistics, t-test and χ^2-test for the validation of the kinetic model M1.2. Constant variance of $\sigma = 3 \cdot 10^{-3}$, T = 383K, P= 5atm, 10 experiments.*

Par.	Value	95% Conf. Interval	95% t-value	Standard Deviation
$k_{1,app}$	8.623E-04	6.230E-05	1.384E+01	3.170E-05
$k_{2,app}$	1.092E-04	3.532E-06	3.092E+01	1.797E-06
$k_{3,app}$	1.600E-06	1.058E-07	1.512E+01	5.384E-08
K_{H_2}	8.600E+00	Value fixed by user		
Ref. t-value: 1.648				
Weighted Residual: 327.502			χ^2**-Value (95%)**: 496.236	

As expected, by removing the parameter for which the information was significantly lower in respect to the others, the overall parameter statistics improve remarkably. At the light of the just obtained findings, K_{H_2} should be then identified exploiting ad-hoc adsorption experiments that ensure its reliable estimation.

5.3 Optimisation of discriminating power

The objective of this section is to find the design space regions that maximise the difference between the kinetic models M1.2 and M2. The rationale is that, after having found that the two models are equivalent under certain experimental conditions, it is definitely interesting to assess when they are significantly different and to find the conditions for which each kinetic model is more suitable to be used. Supposedly, the hydrogen partial pressure plays an important role on the discriminating power

because it is the only measurable variable that is not in common to the two models. However, also the effect of the initial concentrations of the chemical species – some of which have never been accounted before – is now studied. In Tables from 5.9 to 5.11 it is possible to appreciate the results of three different studies, considering as optimization variables: only the pressure, only the initial concentrations or both. The results are obtained exploiting the Hunter-Reiner criterion (Hunter and Reiner (1965)) in (5.1):

$$\min\left(\sum_{i=1}^{N_m}\int_{t_0}^{t_{reac}}\left|C_i^{\mathrm{M1.2}}(t)-C_i^{\mathrm{M2}}(t)\right|dt\right) \tag{5.1}$$

Table 5.9: *Result of the discriminating power optimisation by varying the hydrogen pressure.*

Variable	**Final value**	**Initial guess**	**Lower bound**	**Uper bound**
P_{H_2}	1.0	4.0	1.0	20.0
Obj. function: 4.022				

Table 5.10: *Result of the discriminating power optimisation by varying the initial concentrations of the species in common to M1.2 and M2 kinetic models.*

Variable	**Final value**	**Initial guess**	**Lower bound**	**Uper bound**
C_{HMF}	0.2	0.1	0.0	0.2
C_{BHMF}	0.2	0.0	0.0	0.2
C_{DMF}	0.2	0.1	0.0	0.2
C_{DMTHF}	0.2	0.0	0.0	0.2
Obj. function: 0.366				

It is clear that the initial concentrations do not contribute significantly to the discriminating power maximisation. Even tough the difference in the concentration profiles tends to increase when the initial concentrations increase as well, the effect of the hydrogen partial pressure is much more remarkable. However, even tough theoretically it would be better to set the pressure as low as possible, this is not practically achievable because one of the basic assumptions of the kinetic models is that, in the reactive system, the hydrogen must be in excess. For this reason, it is not possible to decrease the hydrogen pressure too much: in such that case it

Table 5.11: *Result of the discriminating power optimisation by varying both the initial concentrations of the species in common to M1.2 and M2 kinetic models and the hydrogen pressure.*

Variable	Final value	Initial guess	Lower bound	Uper bound
P_{H_2}	1.0	4.0	1.0	20.0
C_{HMF}	0.2	0.1	0.0	0.2
C_{BHMF}	0.2	0.0	0.0	0.2
C_{DMF}	0.2	0.1	0.0	0.2
C_{DMTHF}	0.2	0.0	0.0	0.2
Obj. function: 7.601				

should be required to modify the models in order to consider also the hydrogen rate of change by adding a specific differential equation. Since the minimum pressure has to be 5 atm, the other alternative is to increase it as much as possible: above 20 atm the effect on the discriminating power starts to be remarkably.

5.4 Results summary

To conclude this Chapter, a brief summary of the main results attained is presented. First of all, the study of the analyses sensitivity to the local values of the model parameters demonstrated that the kinetic models behaviour remains the same also after significant variations of the parameter values. This result introduced the possibility of using in-silico data, generated from the kinetic model M1.2 and equivalent to M1, to validate M2 and M1.2 itself. The validation allowed to underline if, at specific experimental conditions, the kinetic models were still capable of representing the system accurately. It emerged that:

1. the quality of the fitting provided by both kinetic models is good, as highlighted by the χ^2-test;
2. both M1.2 and M2 show exactly the same behaviour inside the design space defined in this Thesis, hence they can be considered as equivalent for those experimental conditions;

3. a reliable estimation for M1.2 is not possible when K_{H_2} is considered as a model parameter due to the presence of numerical errors that affect the calculation of the statistics used to assess the parameters quality. In particular, when the parameters vector θ contains both kinetic constants and adsorption coefficients, the difference in the sensitivities order of magnitude cause the resulting FIM to be sloppy and non-invertible.
4. for M2, a reliable estimation of the kinetic parameters is possible. However, since the campaign of 10 experiment considered to performed the analysis was simply generated through the LHS, to cover the entire design space without distinction between more or less informative regions, the quality of the presented statistics could be further improved by applying proper DoE techniques.

At this point, considering that the two remaining kinetic models are identifiable and equivalent inside the defined design space, the attention moved on finding the conditions that maximise instead the discriminating power. The kinetic models responses have been compared by changing specific variables and calculating the integral of the absolute difference between concentration profiles in respect to the time. Thus, it emerged that the optimisation of the discriminating power is enhanced by:

1. very low hydrogen pressure (below 1 atm), solution that has been marked as infeasible since one of the main assumption common to all the kinetic model gathered in literature, is that the hydrogen has to be in excess;
2. very high hydrogen pressure (above 20 atm), solution that leads to higher process costs and increasing safety issues and it has been considered as suitable only using specific equipment and safety standards.

In general, notice that the most remarkable finding is that the two kinetic models, involving different structures and considering different phenomena, turned out to be exactly equivalent inside the design space considered. The study proceeded by setting a constant value for the hydrogen pressure and by allowing to change only the initial concentrations of the species in common. It emerged that these variables give only a minor contribution on the discriminating power optimisation. Indeed,

even though by increasing the initial concentration as much as possible the two model responses start to diverge, this difference is significantly smaller – one order of magnitude on the objective function value – in respect to the divergence obtained by changing the pressure. However, a greater improvement is obtained by varying both initial concentrations and hydrogen pressure: by increasing the pressure, the effect of the initial concentrations on the discriminating power is enhanced as well. Thus, finally, the higher the hydrogen pressure and the greater the effect of the initial concentration on the discriminating power.

In any case, the validation technique underlined as the two kinetic models can be used to describe the process in a wide range of experimental conditions. Virtually:

1. M1.2 is more appropriate when the process is conducted at high hydrogen pressure, and when it is possible to estimate the hydrogen adsorption coefficient through ad-hoc adsorption experiments that ensure its reliability;
2. M2 is more suitable when the process is carried out at relatively low pressure. However, although its apparent kinetic constants can be reliably estimated through simple concentration data, particular attention must be employed in the measurement of the very reactive intermediate MFA which profile ensure a reliable estimation of $k_{3,app}$.

Conclusions

The work presented in this Thesis involved the analysis of different kinetic models, gathered in literature, for the HMF hydrogenation process. The objective was to recognize structural and practical identifiability issues and define, finally, a set of identifiable kinetic models which parameters can be estimated in a statistically reliable way. The kinetic models used for the analyses and the process description were based on:

1. dual-site Langmuir-Hinshelwood-Hougen-Watson ;
2. power law;
3. initial-rate expressions.

The theories and the assumptions used to develop the models, as well as their mathematical structures, have been first analysed to verify the presence of limitations and uncertainties that could have affected the identifiability analysis. The kinetic model developed by Grilc et al. (2014) has been excluded because its characteristics were different from all the other kinetic models and a comparison was not possible. To assess the structural identifiability – the possibility of estimating all the model parameters as a function of the model equations structure – an identifiability test based on a local sensitivity analysis has been exploited. The results have been rearranged to perform:

1. correlation analysis;
2. information and covariance analysis.

The possibility of using the sensitivities to built the so called estimability matrix, allowed to analyse the behaviour of each kinetic model under specific conditions. Through the analysis of the correlation matrix and its evolution for different values of the design variables, it has been possible to detect and classify the presence of

identifiability issues for the kinetic models. Sometimes they turned to be structural, hence related to the shape of the differential balances used to describe the system, in other cases they have been found to be practical, hence related to the regions of the design space defined. Furthermore, for the kinetic model of Gawade et al. (2016), the results stimulated the application of re-parametrization techniques with the objective of solving the critical correlations. Although the trial-and-error procedure adopted has been finally unable of solving the correlation problem, it allowed to underline the limited utility of some adsorption coefficients. These have been discarded from the kinetic model in order to propose a simplified version not affected by critical correlations.
Subsequently, the study of the Fisher Information Matrix (FIM) quantified the expected information content of experiments used to estimate the model parameters. Eventually, by merging the results of correlation and information analyses, it has been possible to define the region of the design space capable of ensuring the kinetic models identifiability and a reliable estimation of the parameters.

The last part of the project involved the validation of the simplified version of the kinetic model proposed by Gawade et al. (2016) and the one proposed by Gyngazova et al. (2017). At the purpose, in-silico data have been generated and the procedure led to establish that:

1. through concentration data only it is not possible to reliably estimate adsorption coefficients;
2. the kinetic model proposed by Gyngazova et al. (2017), and based on the power law theory, is considerably flexible and can easily adapt to kinetics obtained for experimental conditions significantly different from the ones at which is has been originally developed.

Eventually, the validation techniques highlighted that the two selected models – the simplified version of the model proposed by Gawade et al. (2016) and the original model proposed by Gyngazova et al. (2017) – were equivalent within the design space explored in this Thesis. The study then aimed at assessing how to modify the design variable values to maximise the discriminating power. The conclusion is that for a very high hydrogen pressure, above 20 atm, it should be preferred the

use of the simplified version of the kinetic model proposed by Gawade et al. (2016), although a reliable estimation of the hydrogen adsorption coefficient cannot be obtained.

To conclude, the work presented in this Thesis represents a first step toward the identification of a more complete kinetic model that contemplate the explicit dependency of reaction rates on both temperature and pressure. Furthermore, it highlights that to obtain reliable predictions on concentration, an extremely complex representation of the chemistry at the basis of the process is not required. Indeed, kinetic models with many parameters are likely to be unidentifiable and not suitable to be validated through simple kinetic experiments.

APPENDIX A

THE Appendix contains the mathematical derivation of the condition number introduced in Chapter 2 (§2.7.1) as a function of the matrix eigenvalues. The condition number has been used for the analyses described throughout this Thesis to assess whether the FIM was reliably invertible or not.

A.1 Condition number calculation using the matrix norm-2

The study of the condition number allows to assess the entity of the numerical errors that may arise in solving linear equations. For the development strategy of the condition number through the matrix norm-2, it is required to consider first the linear equation below:

$$\mathbf{A}\vec{x} = \vec{b} \tag{A.1}$$

The problems occur when small changes in $\vec{b}$, due to measurements or computational errors, lead to large variations of $\vec{x}$. Thus, assuming to perturb $\vec{b}$ with a small error vector $\vec{\epsilon}$ such that $\vec{b} \rightarrow \vec{b}+\vec{\epsilon}$, the aim is to measure the variation of $\vec{x}$ that results to be $\vec{x} \rightarrow \vec{x}+\vec{\delta}$. In other words, the addition of $\vec{\epsilon}$ causes $\vec{x}$ to be perturbed by $\vec{\delta}$:

$$\mathbf{A}(\vec{x}+\vec{\delta}) = \vec{b}+\vec{\epsilon} \tag{A.2}$$

$$\mathbf{A}\vec{x}+\mathbf{A}\vec{\delta} = \vec{b}+\vec{\epsilon} \tag{A.3}$$

Considering (A.1), (A.3) finally becomes:

$$\mathbf{A}\vec{\delta} = \vec{\epsilon} \tag{A.4}$$

To have an indication about the matrix condition it is now interesting to assess how different are the norms of the two perturbation vectors just introduced. It is

required to assess:

$$||\vec{\epsilon}|| \text{ vs } ||\vec{\delta}|| \tag{A.5}$$

However, it is better to normalize these two quantities in order to exclude any scaling effect that does not affect the solution of (A.1) but, instead, affects the values of $\vec{\epsilon}$ and $\vec{\delta}$. Thus, rather that looking directly at the two perturbations vectors, it is better to compare the normalized values such that (A.5) becomes:

$$\frac{||\vec{\epsilon}||}{||\vec{b}||} \text{ vs } \frac{||\vec{\delta}||}{||\vec{x}||} \tag{A.6}$$

where $||\vec{b}||$ and $||\vec{x}||$ at the denominator are called *normalizing factors*.

The problem with the matrix condition is when the first term of (A.6) is small compared with the second term. Then, in order to find a more compact index, the ratio of the two normalized perturbation vectors can be introduced:

$$\frac{||\vec{\delta}|| \,/\, ||\vec{x}||}{||\vec{\epsilon}|| \,/\, ||\vec{b}||} \tag{A.7}$$

When this ratio is small, either the smaller is $\vec{\delta}$ or the bigger is $\vec{\epsilon}$, the matrix condition is better. Furthermore, if the matrix $\mathbf{A}$ is diagonalizable, its eigenvalues λ_i are real and there must be matrix eigenvectors that satisfy:

$$\mathbf{A}v_i = \lambda_i v_i \tag{A.8}$$

Substituting (A.1) inside (A.8), it is possible to end up with:

$$\frac{||\vec{b}||}{||\vec{x}||} = |\lambda_i| \tag{A.9}$$

Since there are several eigenvalues – which value is not strictly required to be known – it is possible to state that the ratio on the left-hand side of (A.9) must be equal or lower than the maximum eigenvalue:

$$\frac{||\vec{b}||}{||\vec{x}||} \leq |\lambda_{max}| \tag{A.10}$$

Repeating exactly the same considerations from (A.8) to (A.10), the following must hold too:

$$\frac{||\vec{\epsilon}||}{||\vec{\delta}||} \leq |\lambda_{max}| \tag{A.11}$$

Eventually, the ratio of the ratios in (A.10) and (A.11) gives almost (A.7). Thus, in order to make it consistent with this equation, it is possible to consider:

$$\frac{||\vec{\epsilon}||}{||\vec{\delta}||} \geq |\lambda_{min}| \tag{A.12}$$

which is based on the same concept of using the maximum eigenvalue.
Finally, taking its inverse, (A.12) turns to be:

$$\frac{||\vec{\delta}||}{||\vec{\epsilon}||} \leq \frac{1}{|\lambda_{min}|} \tag{A.13}$$

It has been previously states as this ratio was wanted to be small. Considering (A.11) and (A.13), the equation (A.7) has now an upper bound such that:

$$\frac{||\vec{\delta}|| \,/\, ||\vec{x}||}{||\vec{\epsilon}|| \,/\, ||\vec{b}||} = \frac{||\vec{\delta}||}{||\vec{\epsilon}||} \cdot \frac{||\vec{b}||}{||\vec{x}||} \leq \frac{1}{|\lambda_{min}|} \cdot |\lambda_{max}| \tag{A.14}$$

Clearly, the maximum and the minimum size of the eigenvalues represent the key to assess the condition number (CN) of a matrix. The conclusion is that, given a symmetric matrix, the condition number is:

$$\text{CN} = \frac{|\lambda_{max}|}{|\lambda_{min}|} \tag{A.15}$$

It represents a measure of how good is the condition of a matrix: it is called *well-conditioned* if this number is small, *ill-conditioned* if the number is large.

APPENDIX B

THIS Appendix contains all the tables derived from the various analyses performed on the kinetic models and not reported in Chapter 4 to avoid repetitions. Here, it is possible to find the results of the structural identifiability assessment for various temperatures and sampling points distributions for the kinetic model M1.2. Moreover, the tables containing the difference, in terms of integral value between the kinetic model M1, M1.2 and M2, are reported.

B.1 Correlation matrices of the kinetic model M1.2

Below, the correlation matrices for the kinetic model M1.2, related to all the sampling points distributions and all the temperature levels, are reported.

Table B.1: *Correlation matrix for the kinetic model M1.2 based on $\boldsymbol{P}_E$ and built on a the campaign of 10 experiments with the sampling distribution S1 and T = 353 K.*

R	k_1	k_2	k_3	K_{H_2}
k_1	1.000	0.499	-0.038	0.684
k_2	0.499	1.000	-0.105	0.970
k_3	-0.038	-0.105	1.000	-0.179
K_{H_2}	0.684	0.970	-0.179	1.000
$\mathbf{r}_{crit}$	0	1	0	-

Table B.2: *Correlation matrix for the kinetic model M1.2 based on $\boldsymbol{P}_E$ and built on a the campaign of 10 experiments with the sampling distribution S1 and T = 363 K.*

R	k_1	k_2	k_3	K_{H_2}
k_1	1.000	0.631	-0.036	0.723
k_2	0.631	1.000	-0.088	0.983
k_3	-0.036	-0.088	1.000	-0.211
K_{H_2}	0.723	0.983	-0.211	1.000
$\mathbf{r}_{crit}$	0	1	0	-

Table B.3: *Correlation matrix for the kinetic model M1.2 based on $\boldsymbol{P}_E$ and built on a the campaign of 10 experiments with the sampling distribution S1 and T = 373 K.*

R	k_1	k_2	k_3	K_{H_2}
k_1	1.000	0.700	-0.033	0.762
k_2	0.700	1.000	-0.077	0.982
k_3	-0.033	-0.077	1.000	-0.229
K_{H_2}	0.762	0.982	-0.229	1.000
$\mathbf{r}_{crit}$	0	1	0	-

Table B.4: *Correlation matrix for the kinetic model M1.2 based on $\boldsymbol{P}_E$ and built on a the campaign of 10 experiments with the sampling distribution S1 and T = 383 K.*

R	k_1	k_2	k_3	K_{H_2}
k_1	1.000	0.773	-0.040	0.792
k_2	0.773	1.000	-0.097	0.984
k_3	-0.040	-0.097	1.000	-0.263
K_{H_2}	0.792	0.984	-0.263	1.000
$\mathbf{r}_{crit}$	0	1	0	-

B.2 Difference between kinetic models

In the tables below it is possible to find the values for the integral of the absolute difference between the responses of different kinetic models. The values are re-

Table B.5: *Correlation matrix for the kinetic model M1.2 based on $\boldsymbol{P}_E$ and built on a the campaign of 10 experiments with the sampling distribution S2 and T = 353 K.*

R	k_1	k_2	k_3	K_{H_2}
k_1	1.000	0.882	-0.040	0.898
k_2	0.882	1.000	-0.091	0.988
k_3	-0.040	-0.091	1.000	-0.228
K_{H_2}	0.898	0.988	-0.228	1.000
$\mathbf{r}_{crit}$	0	1	0	-

Table B.6: *Correlation matrix for the kinetic model M1.2 based on $\boldsymbol{P}_E$ and built on a the campaign of 10 experiments with the sampling distribution S2 and T = 363 K.*

R	k_1	k_2	k_3	K_{H_2}
k_1	1.000	0.910	-0.024	0.894
k_2	0.910	1.000	-0.067	0.972
k_3	-0.024	-0.067	1.000	-0.293
K_{H_2}	0.894	0.972	-0.293	1.000
$\mathbf{r}_{crit}$	1	1	0	-

Table B.7: *Correlation matrix for the kinetic model M1.2 based on $\boldsymbol{P}_E$ and built on a the campaign of 10 experiments with the sampling distribution S2 and T = 373 K.*

R	k_1	k_2	k_3	K_{H_2}
k_1	1.000	0.922	-0.013	0.888
k_2	0.922	1.000	-0.051	0.958
k_3	-0.013	-0.051	1.000	-0.333
K_{H_2}	0.888	0.958	-0.333	1.000
$\mathbf{r}_{crit}$	1	1	0	-

ported for all the components in common. The total difference, to assess how much the two models actually diverge, is also present.

Table B.8: *Correlation matrix for the kinetic model M1.2 based on $\boldsymbol{P}_E$ and built on a the campaign of 10 experiments with the sampling distribution S2 and T = 383 K.*

R	k_1	k_2	k_3	K_{H_2}
k_1	1.000	0.890	-0.017	0.848
k_2	0.890	1.000	-0.075	0.956
k_3	-0.017	-0.075	1.000	-0.364
K_{H_2}	0.848	0.956	-0.364	1.000
$\mathbf{r}_{crit}$	0	1	0	-

Table B.9: *Correlation matrix for the kinetic model M1.2 based on $\boldsymbol{P}_E$ and built on a the campaign of 10 experiments with the sampling distribution S3 and T = 353 K.*

R	k_1	k_2	k_3	K_{H_2}
k_1	1.000	0.085	-0.004	0.559
k_2	0.085	1.000	-0.069	0.821
k_3	-0.004	-0.069	1.000	-0.348
K_{H_2}	0.559	0.821	-0.348	1.000
$\mathbf{r}_{crit}$	0	0	0	-

Table B.10: *Correlation matrix for the kinetic model M1.2 based on $\boldsymbol{P}_E$ and built on a the campaign of 10 experiments with the sampling distribution S3 and T = 363 K.*

R	k_1	k_2	k_3	K_{H_2}
k_1	1.000	0.273	0.002	0.503
k_2	0.273	1.000	-0.032	0.843
k_3	0.002	-0.032	1.000	-0.480
K_{H_2}	0.503	0.843	-0.480	1.000
$\mathbf{r}_{crit}$	0	0	0	-

Table B.11: *Correlation matrix for the kinetic model M1.2 based on $\boldsymbol{P}_E$ and built on a the campaign of 10 experiments with the sampling distribution S3 and T = 373 K.*

R	k_1	k_2	k_3	K_{H_2}
k_1	1.000	0.430	0.008	0.544
k_2	0.430	1.000	-0.006	0.820
k_3	0.008	-0.006	1.000	-0.534
K_{H_2}	0.544	0.820	-0.534	1.000
$\mathbf{r}_{crit}$	0	0	0	-

Table B.12: *Correlation matrix for the kinetic model M1.2 based on $\boldsymbol{P}_E$ and built on a the campaign of 10 experiments with the sampling distribution S3 and T = 383 K.*

R	k_1	k_2	k_3	K_{H_2}
k_1	1.000	0.539	0.012	0.524
k_2	0.539	1.000	-0.030	0.838
k_3	0.012	-0.030	1.000	-0.561
K_{H_2}	0.524	0.838	-0.561	1.000
$\mathbf{r}_{crit}$	0	0	0	-

Table B.13: *Difference between models responses, kinetic model M1 and M1.2 at T = 353K.*

M1 vs M1.2					
EXP.	**HMF**	**BHMF**	**DMF**	**DMTHF**	**TOTAL**
1	2.54E-02	8.28E-02	8.12E-02	4.65E-03	1.94E-01
2	4.66E-03	1.52E-02	1.49E-02	7.85E-04	3.55E-02
3	0.00E+00	0.00E+00	4.51E-05	4.51E-05	9.01E-05
4	1.84E-02	5.89E-02	5.81E-02	2.17E-03	1.37E-01
5	8.46E-03	2.82E-02	2.75E-02	2.37E-03	6.66E-02
6	4.29E-02	1.42E-01	1.39E-01	1.19E-02	3.36E-01
7	6.01E-04	2.29E-03	2.30E-03	7.25E-04	5.92E-03
8	3.36E-02	1.11E-01	1.08E-01	7.91E-03	2.60E-01
9	1.34E-02	4.53E-02	4.42E-02	4.73E-03	1.08E-01
10	2.32E-03	8.58E-03	8.51E-03	2.18E-03	2.16E-02

Table B.14: *Difference between models responses, kinetic model M2 and M1 at T = 353K.*

M2 vs M1					
EXP.	**HMF**	**BHMF**	**DMF**	**DMTHF**	**TOTAL**
1	1.22E-02	4.40E-02	4.22E-02	1.60E-03	1.00E-01
2	1.26E-03	3.17E-02	3.68E-02	1.61E-03	7.13E-02
3	0.00E+00	0.00E+00	7.97E-04	7.97E-04	1.59E-03
4	7.18E-03	4.37E-02	4.56E-02	1.77E-03	9.82E-02
5	1.78E-03	3.63E-02	4.12E-02	2.00E-03	8.13E-02
6	2.59E-02	5.21E-02	4.48E-02	2.38E-03	1.25E-01
7	1.30E-03	1.32E-02	1.48E-02	2.04E-03	3.13E-02
8	1.85E-02	4.63E-02	4.15E-02	1.54E-03	1.08E-01
9	4.16E-03	3.80E-02	4.20E-02	1.89E-03	8.61E-02
10	1.47E-03	2.24E-02	2.58E-02	2.52E-03	5.22E-02

Table B.15: *Difference between models responses, kinetic model M2 and M1.2 at T = 353K.*

M2 vs M1.2					
EXP.	**HMF**	**BHMF**	**DMF**	**DMTHF**	**TOTAL**
1	1.32E-02	1.09E-01	1.20E-01	5.85E-03	2.48E-01
2	5.67E-03	4.66E-02	5.15E-02	2.39E-03	1.06E-01
3	0.00E+00	0.00E+00	8.42E-04	8.42E-04	1.68E-03
4	1.13E-02	9.31E-02	1.03E-01	3.93E-03	2.12E-01
5	7.56E-03	6.21E-02	6.82E-02	4.31E-03	1.42E-01
6	1.70E-02	1.40E-01	1.54E-01	9.69E-03	3.20E-01
7	1.89E-03	1.55E-02	1.70E-02	2.76E-03	3.71E-02
8	1.51E-02	1.24E-01	1.37E-01	7.77E-03	2.84E-01
9	9.45E-03	7.76E-02	8.51E-02	6.23E-03	1.78E-01
10	3.78E-03	3.10E-02	3.39E-02	4.68E-03	7.33E-02

Table B.16: *Difference between models responses, kinetic model M1 and M1.2 at T = 363K.*

M1 vs M1.2					
EXP.	**HMF**	**BHMF**	**DMF**	**DMTHF**	**TOTAL**
1	1.37E-02	5.52E-02	5.35E-02	5.67E-03	1.28E-01
2	2.50E-03	1.01E-02	9.78E-03	9.61E-04	2.34E-02
3	0.00E+00	0.00E+00	7.19E-05	7.19E-05	1.44E-04
4	9.88E-03	3.91E-02	3.78E-02	2.62E-03	8.93E-02
5	4.56E-03	1.89E-02	1.85E-02	2.93E-03	4.49E-02
6	2.31E-02	9.55E-02	9.33E-02	1.47E-02	2.27E-01
7	3.30E-04	1.58E-03	1.87E-03	9.63E-04	4.75E-03
8	1.81E-02	7.40E-02	7.20E-02	9.69E-03	1.74E-01
9	7.22E-03	3.05E-02	3.01E-02	5.89E-03	7.37E-02
10	1.26E-03	5.89E-03	6.53E-03	2.84E-03	1.65E-02

Table B.17: *Difference between models responses, kinetic model M2 and M1 at T = 363K.*

M2 vs M1					
EXP.	**HMF**	**BHMF**	**DMF**	**DMTHF**	**TOTAL**
1	2.45E-03	3.54E-02	5.16E-02	4.00E-03	9.34E-02
2	3.45E-03	2.74E-02	3.40E-02	3.14E-04	6.52E-02
3	0.00E+00	0.00E+00	5.09E-04	5.09E-04	1.02E-03
4	2.40E-03	3.68E-02	4.95E-02	6.51E-04	8.93E-02
5	3.37E-03	3.11E-02	4.21E-02	2.48E-03	7.91E-02
6	5.96E-03	3.32E-02	5.04E-02	1.37E-02	1.03E-01
7	1.66E-03	1.09E-02	1.47E-02	1.72E-03	2.90E-02
8	3.63E-03	3.37E-02	5.19E-02	8.34E-03	9.76E-02
9	2.68E-03	3.23E-02	4.85E-02	5.76E-03	8.92E-02
10	2.70E-03	1.91E-02	2.72E-02	3.93E-03	5.29E-02

Table B.18: *Difference between models responses, kinetic model M2 and M1.2 at T = 363K.*

M2 vs M1.2					
EXP.	**HMF**	**BHMF**	**DMF**	**DMTHF**	**TOTAL**
1	1.38E-02	8.73E-02	1.00E-01	1.67E-03	2.03E-01
2	5.93E-03	3.74E-02	4.29E-02	7.80E-04	8.70E-02
3	0.00E+00	0.00E+00	4.37E-04	4.37E-04	8.75E-04
4	1.18E-02	7.48E-02	8.54E-02	2.00E-03	1.74E-01
5	7.90E-03	4.99E-02	5.78E-02	5.97E-04	1.16E-01
6	1.78E-02	1.12E-01	1.30E-01	1.34E-03	2.61E-01
7	1.97E-03	1.25E-02	1.53E-02	7.62E-04	3.05E-02
8	1.58E-02	9.98E-02	1.15E-01	1.40E-03	2.32E-01
9	9.87E-03	6.23E-02	7.26E-02	7.40E-04	1.46E-01
10	3.94E-03	2.49E-02	3.02E-02	1.09E-03	6.01E-02

Table B.19: *Difference between models responses, kinetic model M1 and M1.2 at T = 373K.*

M1 vs M1.2					
EXP.	**HMF**	**BHMF**	**DMF**	**DMTHF**	**TOTAL**
1	9.35E-03	3.82E-02	3.76E-02	5.68E-03	9.09E-02
2	1.72E-03	7.03E-03	6.89E-03	9.58E-04	1.66E-02
3	0.00E+00	0.00E+00	7.42E-05	7.42E-05	1.48E-04
4	6.76E-03	2.71E-02	2.63E-02	2.61E-03	6.27E-02
5	3.12E-03	1.31E-02	1.33E-02	2.95E-03	3.25E-02
6	1.58E-02	6.62E-02	6.67E-02	1.48E-02	1.63E-01
7	2.29E-04	1.11E-03	1.54E-03	9.87E-04	3.87E-03
8	1.24E-02	5.13E-02	5.11E-02	9.74E-03	1.24E-01
9	4.94E-03	2.12E-02	2.18E-02	5.95E-03	5.39E-02
10	8.68E-04	4.12E-03	5.20E-03	2.92E-03	1.31E-02

Table B.20: *Difference between models responses, kinetic model M2 and M1 at T = 373K.*

M2 vs M1					
EXP.	**HMF**	**BHMF**	**DMF**	**DMTHF**	**TOTAL**
1	1.47E-02	4.32E-02	3.99E-02	2.37E-03	1.00E-01
2	3.98E-03	2.54E-02	2.44E-02	4.89E-04	5.43E-02
3	0.00E+00	0.00E+00	1.30E-04	1.30E-04	2.60E-04
4	1.13E-02	4.14E-02	3.67E-02	3.69E-04	8.98E-02
5	6.14E-03	3.10E-02	3.06E-02	1.12E-03	6.88E-02
6	2.26E-02	4.67E-02	4.82E-02	1.07E-02	1.28E-01
7	9.77E-04	9.31E-03	1.01E-02	6.44E-04	2.11E-02
8	1.84E-02	4.45E-02	4.37E-02	6.04E-03	1.13E-01
9	8.72E-03	3.51E-02	3.59E-02	3.73E-03	8.34E-02
10	2.37E-03	1.72E-02	1.93E-02	2.17E-03	4.10E-02

Table B.21: *Difference between models responses, kinetic model M2 and M1.2 at T = 373K.*

M2 vs M1.2					
EXP.	**HMF**	**BHMF**	**DMF**	**DMTHF**	**TOTAL**
1	5.34E-03	7.13E-02	7.19E-02	3.30E-03	1.52E-01
2	2.29E-03	3.06E-02	3.08E-02	1.42E-03	6.51E-02
3	0.00E+00	0.00E+00	5.58E-05	5.58E-05	1.12E-04
4	4.57E-03	6.11E-02	6.16E-02	2.90E-03	1.30E-01
5	3.05E-03	4.08E-02	4.11E-02	1.82E-03	8.67E-02
6	6.86E-03	9.17E-02	9.24E-02	4.10E-03	1.95E-01
7	7.61E-04	1.02E-02	1.03E-02	3.52E-04	2.16E-02
8	6.10E-03	8.15E-02	8.21E-02	3.70E-03	1.73E-01
9	3.81E-03	5.09E-02	5.13E-02	2.22E-03	1.08E-01
10	1.52E-03	2.04E-02	2.05E-02	7.47E-04	4.32E-02

Table B.22: *Difference between models responses, kinetic model M1 and M1.2 at T = 383K.*

M1 vs M1.2					
EXP.	**HMF**	**BHMF**	**DMF**	**DMTHF**	**TOTAL**
1	5.35E-03	3.13E-02	2.86E-02	5.60E-03	7.08E-02
2	9.87E-04	5.71E-03	5.19E-03	9.41E-04	1.28E-02
3	0.00E+00	0.00E+00	6.23E-05	6.23E-05	1.25E-04
4	3.87E-03	2.21E-02	2.01E-02	2.58E-03	4.86E-02
5	1.78E-03	1.08E-02	9.97E-03	2.88E-03	2.54E-02
6	9.01E-03	5.44E-02	5.05E-02	1.45E-02	1.28E-01
7	1.32E-04	9.09E-04	1.15E-03	9.24E-04	3.12E-03
8	7.06E-03	4.21E-02	3.87E-02	9.58E-03	9.74E-02
9	2.82E-03	1.74E-02	1.64E-02	5.79E-03	4.24E-02
10	4.96E-04	3.39E-03	3.92E-03	2.76E-03	1.06E-02

Table B.23: *Difference between models responses, kinetic model M2 and M1 at T = 383K.*

M2 vs M1					
EXP.	**HMF**	**BHMF**	**DMF**	**DMTHF**	**TOTAL**
1	7.70E-03	3.99E-02	1.72E-02	3.02E-03	6.78E-02
2	1.98E-03	9.42E-03	4.03E-03	1.39E-04	1.56E-02
3	0.00E+00	0.00E+00	3.14E-04	3.14E-04	6.28E-04
4	5.88E-03	2.94E-02	1.18E-02	8.62E-04	4.80E-02
5	3.12E-03	1.57E-02	5.70E-03	9.72E-04	2.55E-02
6	1.20E-02	6.54E-02	3.33E-02	1.02E-02	1.21E-01
7	4.60E-04	2.15E-03	1.84E-03	3.17E-04	4.77E-03
8	9.75E-03	5.19E-02	2.44E-02	6.15E-03	9.22E-02
9	4.49E-03	2.35E-02	9.13E-03	3.03E-03	4.02E-02
10	1.16E-03	5.86E-03	2.55E-03	6.80E-04	1.03E-02

Table B.24: *Difference between models responses, kinetic model M2 and M1.2 at T = 383K.*

M2 vs M1.2					
EXP.	**HMF**	**BHMF**	**DMF**	**DMTHF**	**TOTAL**
1	2.38E-03	8.76E-03	1.60E-02	2.58E-03	2.97E-02
2	1.02E-03	3.75E-03	6.81E-03	1.05E-03	1.26E-02
3	0.00E+00	0.00E+00	3.76E-04	3.76E-04	7.53E-04
4	2.04E-03	7.50E-03	1.33E-02	1.73E-03	2.46E-02
5	1.36E-03	5.00E-03	9.44E-03	1.91E-03	1.77E-02
6	3.06E-03	1.13E-02	2.12E-02	4.29E-03	3.98E-02
7	3.39E-04	1.25E-03	2.94E-03	1.23E-03	5.76E-03
8	2.72E-03	1.00E-02	1.86E-02	3.44E-03	3.48E-02
9	1.70E-03	6.25E-03	1.21E-02	2.76E-03	2.28E-02
10	6.79E-04	2.50E-03	5.58E-03	2.08E-03	1.08E-02

References

Asprey, S. P. and S. Macchietto

2000. Statistical tools for optimal dynamic model building. *Computers & Chemical Engineering*, 24(2):1261–1267.

Atkinson, A. C. and V. V. Fedorov

1975. Optimal Design: Experiments for Discriminating between Several Models. *Biometrika*, 62(2):289–303.

Augustine, R. L. and P. Techasauvapak

1994. Heterogeneous catalysis in organic synthesis. Part 9. Specific site solvent effects in catalytic hydrogenations. *Journal of Molecular Catalysis*, 87(1):95–105.

Bard, Y.

1974. *Nonlinear Parameter Estimation*.

Bindwal, A. B. and P. D. Vaidya

2013. Kinetics of Aqueous-Phase Hydrogenation of Levoglucosan over Ru/C Catalyst. *Industrial & Engineering Chemistry Research*, 52(50):17781–17789.

Bindwal, A. B. and P. D. Vaidya

2014. Reaction Kinetics of Vanillin Hydrogenation in Aqueous Solutions Using a Ru/C Catalyst. *Energy & Fuels*, 28(5):3357–3362.

Blau, G., M. Lasinski, and S. Orcun

2008. High fidelity mathematical model building with experimental data: A Bayesian approach. *Computers & Chemical Engineering*, 32(4):971–989.

Box, G. E. P. and H. L. Lucas

1959. Design of Experiments in Non-Linear Situations. *Biometrika*, 46(1/2):77–90.

Box, G. E. P. and K. B. Wilson

1992. On the Experimental Attainment of Optimum Conditions. In *Breakthroughs in Statistics*, Springer Series in Statistics, Pp. 270–310. Springer, New York, NY.

Burke, J.

1984. Solubility Parameters: Theory and Application.

Buzzi-Ferraris, G. and P. Forzatti

1983. A new sequential experimental design procedure for discriminating among rival models. *Chemical Engineering Science*, 38(2):225–232.

Buzzi-Ferraris, G., P. Forzatti, and C. Paolo

1990. An improved version of a sequential design criterion for discriminating among rival multiresponse models. *Chemical Engineering Science*, 45(2):477–481.

Charnes, A., E. L. Frome, and P. Yu

1976. The Equivalence of Generalized Least Squares and Maximum Likelihood Estimates in the Exponential Family. *Journal of The American Statistical Association*, 71:169–171.

Chatterjee, M., T. Ishizaka, and H. Kawanami

2014. Hydrogenation of 5-hydroxymethylfurfural in supercritical carbon dioxide–water: a tunable approach to dimethylfuran selectivity. *Green Chemistry*, 16(3):1543–1551.

Chen, S. Bermingham, and S. P. Asprey

2004. On the Design of Optimally Informative Experiments for Dynamic Crystallization Process Modeling.

Chum, H. L. and R. P. Overend

2001. Biomass and renewable fuels. *Fuel Processing Technology*, 71(1):187–195.

Crezee, E., B. W. Hoffer, and R. J. Berger

2003. Three-phase hydrogenation of d-glucose over a carbon supported ruthe-

nium catalyst: mass transfer and kinetics. *Applied Catalysis A: General*, 251(1):1–17.

Davies, O. L. and F. J. van Dun En

1955. Design and analysis of industrial experiments. *Statistica Neerlandica*, 9(4):189–207.

Demirbas, A.

2010. Fuels from Biomass. In *Biorefineries*, Green Energy and Technology, Pp. 33–73. Springer, London.

Dereniowski, D. and M. Kubale

2004. Cholesky Factorization of Matrices in Parallel and Ranking of Graphs. In *Parallel Processing and Applied Mathematics*, Lecture Notes in Computer Science, Pp. 985–992. Springer Berlin Heidelberg.

Donckels, B., D. J.W. De Pauw, and P. Vanrolleghem

2009. A kernel-based method to determine optimal sampling times for the simultaneous estimation of the parameters of rival mathematical models. *Journal of computational chemistry*, 30:2064–77.

Emery, A. F.

2001. Using the Concept of Information to Optimally Design Experiments With Uncertain Parameters. *Journal of Heat Transfer*, 123(3):593–600.

Espie, D. M. and S. Macchietto

1988. Nonlinear transformations for parameter estimation. *Industrial & Engineering Chemistry Research*, 27(11):2175–2179.

Espie, D. M. and S. Macchietto

1989. The optimal design of dynamic experiments. *AIChE Journal*, 35(2):223–229.

Fisher, R. A.

1935. *The design of experiments*. Oxford, England: Oliver & Boyd.

Franceschini, G. and S. Macchietto

2008. Model-based design of experiments for parameter precision: State of the art. *Chemical Engineering Science*, 63(19):4846–4872.

Galvanin, F., A. Boschiero, M. Barolo, and F. Bezzo

2011. Model-Based Design of Experiments in the Presence of Continuous Measurement Systems. *Industrial & Engineering Chemistry Research*, 50(4):2167–2175.

Galvanin, F., S. Macchietto, and F. Bezzo

2007. Model-Based Design of Parallel Experiments. *Industrial & Engineering Chemistry Research*, 46(3):871–882.

Gawade, A. B., M. S. Tiwari, and G. D. Yadav

2016. Biobased Green Process: Selective Hydrogenation of 5-hydroxymethylfurfural to 2,5-dimethylfuran under Mild Conditions Using Pd-Cs2.5h0.5pw12o40/K-10 Clay. *Acs Sustainable Chemistry & Engineering*, 4(8):4113–4123.

Grilc, M., B. Likozar, and J. Levec

2014. Hydrodeoxygenation and hydrocracking of solvolysed lignocellulosic biomass by oxide, reduced and sulphide form of NiMo, Ni, Mo and Pd catalysts. *Applied Catalysis B: Environmental*, 150-151:275–287.

Gyngazova, M. S., L. Negahdar, L. C. Blumenthal, and R. Palkovits

2017. Experimental and kinetic analysis of the liquid phase hydrodeoxygenation of 5-hydroxymethylfurfural to 2,5-dimethylfuran over carbon-supported nickel catalysts. *Chemical Engineering Science*, 173:455–464.

Hu, L., X. Tang, J. Xu, Z. Wu, L. Lin, and S. Liu

2014. Selective Transformation of 5-Hydroxymethylfurfural into the Liquid Fuel 2,5-Dimethylfuran over Carbon-Supported Ruthenium. *Industrial & Engineering Chemistry Research*, 53(8):3056–3064.

Huang, Y. B., M.-Y. Chen, L. Yan, Q.-X. Guo, and Y. Fu

2014. Nickel–Tungsten Carbide Catalysts for the Production of 2,5-

dimethylfuran from Biomass-Derived Molecules. *ChemSusChem*, 7(4):1068–1072.

Hunter, W. G. and A. M. Reiner

1965. Designs for Discriminating between Two Rival Models. *Technometrics*, 7(3):307–323.

Jain, A. B. and P. D. Vaidya

2016. Kinetics of Catalytic Hydrogenation of 5-Hydroxymethylfurfural to 2,5-bis-hydroxymethylfuran in Aqueous Solution over Ru/C. *International Journal of Chemical Kinetics*, 48(6):318–328.

Kiefer, J.

1959. Optimum Experimental Designs. *Journal of the Royal Statistical Society. Series B (Methodological)*, 21(2):272–319.

Kong, X., Y. Zhu, H. Zheng, and F. Dong

2014. Switchable synthesis of 2,5-dimethylfuran and 2,5-dihydroxymethyl-tetrahydrofuran from 5-hydroxymethylfurfural over Raney Ni catalyst. *RSC Advances*, 4(105):60467–60472.

Kreutz, C. and J. Timmer

2009. Systems biology: experimental design. *The FEBS journal*, 276(4):923–942.

Lamia, K. Z., L. Negadi, I. Mokbel, N. Msakni, and J. Jose

2012. Liquid–vapor equilibria of binary systems containing alcohols (1-butanol, or 2-butanol or 1-hexanol) present in the production by chemical process of 2,5-dimethyl furan from biomass. *Fuel*, 95:438–445.

Liang, Y. Z., K. T. Fang, and Q. S. Xu

2001. Uniform design and its applications in chemistry and chemical engineering. *Chemometrics and Intelligent Laboratory Systems*, 58(1):43–57.

Ljung, L.

1999. System Identification: Theory For The User. In *1981 Tutorial Workshop on Syst Identif*.

Luo, J., L. Arroyo-Ramirez, J. Wei, and H. Yun

2015. Comparison of HMF hydrodeoxygenation over different metal catalysts in a continuous flow reactor. *Applied Catalysis a-General*, 508:86–93.

Margaria, G., E. Riccomagno, M. J. Chappell, and H. P. Wynn

2001. Differential algebra methods for the study of the structural identifiability of rational function state-space models in the biosciences. *Mathematical Biosciences*, 174(1):1–26.

Marquardt, D. W.

1963. An Algorithm for Least-Squares Estimation of Nonlinear Parameters. *Journal of the Society for Industrial and Applied Mathematics*, 11(2):431–441.

Montgomery and C. Douglas

2012. *Design and Analysis of Experiments*, 8th edition. Wiley.

Nauman, E. B.

2008. *Chemical Reactor Design, Optimization, and Scaleup*. John Wiley & Sons.

Negahdar, L., J. U. Oltmanns, S. Palkovits, and R. Palkovits

2014. Kinetic investigation of the catalytic conversion of cellobiose to sorbitol. *Applied Catalysis B: Environmental*, 147:677–683.

Neyman, J. and E. Pearson

1933. On the Problem of the Most Efficient Tests of Statistical Hypotheses. *Philosophical Transactions of the Royal Society, A*, 231:289–337.

Nocedal, J. and S. J. Wright

1999. *Numerical optimization*, Springer series in operations research. New York: Springer.

Parikka, M.

2004. Global biomass fuel resources. *Biomass and Bioenergy*, 27(6):613–620.

Pintar, A., G. Berčič, and J. Levec

1998. Catalytic liquid-phase nitrite reduction: Kinetics and catalyst deactivation. *AIChE Journal*, 44(10):2280–2292.

Pohjanpalo, H.

1978. System identifiability based on the power series expansion of the solution. *Mathematical Biosciences*, 41(1):21–33.

Puhl, H.

1991. Solubility of Gases in Liquids. *Chemie Ingenieur Technik*, 63(12):1272–1272.

Quaglio, M., C. Waldron, A. Pankajakshan, and A. Gavriilidis

2019. On the use of online reparametrization in automated platforms for kinetic model identification. *Chemie Ingenieur Technik*.

Ragauskas, A. J., C. K. Williams, and B. H. Davison

2006. The path forward for biofuels and biomaterials. *Science*, 311(5760):484–489.

Roman-Leshkov, Y., C. J Barrett, Z. Y Liu, and J. A Dumesic

2007. Production of Dimethylfuran for Liquid Fuels from Biomass-Derived Carbohydrates. *Nature*, 447:982–5.

Rosatella, A. A., S. P. Simeonov, and R. F. M. Frade

2011. 5-Hydroxymethylfurfural (HMF) as a building block platform: Biological properties, synthesis and synthetic applications. *Green Chemistry*, 13(4):754–793.

Saccomani P., M., S. Audoly, and L. D'Angiò

2003. Parameter identifiability of nonlinear systems: the role of initial conditions. *Automatica*, 39(4):619–632.

Salmi, T., D. Y. Murzin, and J. P. Mikkola

2004. Advanced Kinetic Concepts and Experimental Methods for Catalytic Three-Phase Processes. *Industrial & Engineering Chemistry Research*, 43(16):4540–4550.

Saltelli, A.

2002. Sensitivity Analysis for Importance Assessment. *Risk Analysis*, 22(3):579–590.

Schöneberger, J. C., H. Arellano-Garcia, and G. Wozny

2009. Model-Based Experimental Analysis of a Fixed-Bed Reactor for Catalytic SO2 Oxidation. *Industrial & Engineering Chemistry Research*, 48(11):5165–5176.

Thananatthanachon, T. and T. Rauchfuss

2010. Efficient Production of the Liquid Fuel 2,5-Dimethylfuran from Fructose Using Formic Acid as a Reagent. *Angewandte Chemie (International ed. in English)*, 49:6616–8.

Toukoniitty, E., P. Mäki-Arvela, and J. Kuusisto

2003. Solvent effects in enantioselective hydrogenation of 1-phenyl-1,2-propanedione. *Journal of Molecular Catalysis A: Chemical*, 192(1):135–151.

Trucco, E. and A. Verri

1998. *Introductory Techniques for 3-D Computer Vision*. Prentice Hall.

van Putten, R., J. C. Waal, and E. de Jong

2013. Hydroxymethylfurfural, A Versatile Platform Chemical Made from Renewable Resources. *Chemical reviews*, 113.

Walter, E. and L. Pronzato

1996. On the identifiability and distinguishability of nonlinear parametric models. *Mathematics and Computers in Simulation*, 42(2):125–134.

Yang, P., Q. Cui, and Y. Zu

2015. Catalytic production of 2,5-dimethylfuran from 5-hydroxymethylfurfural over Ni/Co3o4 catalyst. *Catalysis Communications*, 66.

Zhang, J., L. Lin, and S. Liu

2012. Efficient Production of Furan Derivatives from a Sugar Mixture by Catalytic Process. *Energy & Fuels*, 26(7):4560–4567.

ACKNOWLEDGEMENTS

I would like to thank all the people who supported me throughout the realisation of this Thesis. Their guidance and support has been essential to me. Prof. Fabrizio Bezzo of the Department of Chemical Engineering at the University of Padua for the patience, support and the wonderful opportunity he offered to me, Prof. Federico Galvanin of the Department of Chemical Engineering at the University College London for his precious guidance and supervision of the project.

Ed infine desidero ringraziare tutte le persone che mi hanno sostenuto e motivato durante il mio percorso universitario. Non riesco a credere che questi anni siano già trascorsi, mi sembra davvero ieri quando per la prima volta ho preso il treno verso Padova con un misto di curiosità e timore per l'avventura che si prospettava davanti a me. Le persone a me vicine lo sanno, il tempo è un aspetto della vita che mai riuscirò a comprendere fino in fondo: mi stupisce e mi spaventa. Si pensa sempre di averlo sotto controllo, di essere consapevoli del suo trascorrere, ma in realtà, quando guardiamo indietro, restiamo sempre annichiliti dalla velocità con cui ci sfugge di mano.

Grazie a papà Paolo e mamma Monica, che mi hanno permesso di diventare la persona che sono ora.

Grazie a Luca, che resterà sempre il mio fratellino nonostante sia ormai più alto di me. Posso solo augurarti il meglio per il futuro. Rimani ambizioso, credi negli obiettivi che ti sei prefissato e non permettere che le insicurezze degli altri diventino le tue. Fai sempre ciò che pensi possa essere meglio per te, confrontati con tutti ma non paragonarti a nessuno: ognuno ha i propri pregi, difetti e capacità. Se anche la vita ci porterà ad essere lontani, spero tu possa sempre considerarmi come una sicurezza che, se mai dovessi avere bisogno, sarà lì per sostenerti.

Grazie di cuore a zia Silvia e nonna Maria, le due persone che mai finiranno di dimostrarmi quanto mi vogliono bene. Siete sempre state e siete tuttora un punto di riferimento senza il quale mi sentirei perso.
Grazie a Sara, che mi è sempre stata vicina con amore e pazienza. Sei il mio amore, la mia "tata", la mia "plantigrada tuberalis" (solo per veri intenditori). Abbiamo un rapporto di cui sono orgoglioso perché in pochi possono vantarlo, grazie per questo e per esserci sempre.
Grazie a Filippo. La nostra amicizia è esplosa in questi ultimi due anni ma non sai quanto desidererei di averti conosciuto prima. Le giornate a giocare coi Pokémon, i viaggi in treno, le lezioni trascorse assieme, le focacce, le pizze e gli hamburger: sei una persona che mi ha permesso di crescere e migliorare.
Grazie a Fabrizio e Federico che mi hanno accolto nei loro team di ricerca e mi hanno guidato, assistito e consigliato nell'ultima parte di questo importante percorso.
Grazie a tutti i ragazzi con cui ho avuto il piacere di collaborare a Londra, in particolare Marco, Arun e Chunbing che hanno reso la mia permanenza all'estero veramente speciale.
Grazie infine a tutte le persone che non ho nominato ma che mi sono vicine e che comunque porto dentro di me. A voi, che siete parte della mia vita e ci avete lasciato un segno, un ricordo, la mia più profonda gratitudine.